GEOLOGICA ULTRAIECTINA

Mededelingen van het
Instituut voor Aardwetenschappen der
Rijksuniversiteit te Utrecht

No. 62

THERMAL AND MECHANICAL MODELLING OF CONVERGENT PLATE MARGINS

JILLES VAN DEN BEUKEL

GEOLOGICA ULTRAIECTINA

Mededelingen van het
Instituut voor Aardwetenschappen der
Rijksuniversiteit te Utrecht

No. 62

THERMAL AND MECHANICAL MODELLING OF CONVERGENT PLATE MARGINS

JILLES VAN DEN BEUKEL

THERMAL AND MECHANICAL MODELLING OF CONVERGENT PLATE MARGINS

THERMISCH EN MECHANISCH MODELLEREN

VAN CONVERGENTE PLAATGRENZEN

(met een samenvatting in het Nederlands)

PROEFSCHRIFT

TER VERKRIJGING VAN DE GRAAD VAN DOCTOR
AAN DE RIJKSUNIVERSITEIT TE UTRECHT
OP GEZAG VAN DE RECTOR MAGNIFICUS, PROF. DR. J.A. VAN GINKEL
INGEVOLGE BESLUIT VAN HET COLLEGE VAN DECANEN
IN HET OPENBAAR TE VERDEDIGEN
OP WOENSDAG 14 FEBRUARI 1990 DES NAMIDDAGS TE 2.30 UUR

DOOR

PIETER JILLES VAN DEN BEUKEL

GEBOREN OP 11 SEPTEMBER 1958 TE SCHIEDAM

PROMOTOREN: PROF. DR. M.J.R. WORTEL
PROF. DR. N.J. VLAAR

Aan mijn ouders

The research described in this thesis was carried out at the:

Department of Theoretical Geophysics
Institute of Earth Sciences
University of Utrecht
Budapestlaan 4
3584 CD Utrecht
The Netherlands

ISBN 90-71577-15-5

Contents

Chapter 1
Introduction and summary 9
References 13

Chapter 2
Temperatures and shear stresses in the upper part of a subduction zone 15
2.1 Introduction 16
2.2 Description of the model 17
2.3 Constraints on temperatures and shear stresses 20
2.4 Model calculations 24
2.5 High-pressure metamorphism 30
2.6 Discussion 33
2.7 Conclusions 34
References 35

Chapter 3
Thermal modelling of the Cascadia subduction zone: A case study for the subduction of young oceanic lithosphere 41
3.1 Introduction 41
3.2 Model description 42
3.3 Results 46
3.4 Discussion 50
References 51

Chapter 4
Break-up of young oceanic lithosphere in the upper part of a subduction zone: Implications for the emplacement of ophiolites 53
4.1 Introduction 54
4.2 Thermal modelling 55
4.3 Finite element modelling 62
4.3.1 Model description 62
4.3.2 Modelling results: set A 65
4.3.3 Modelling results: set B 72
4.3.4 An alternative approach: a condition for detachment 76
4.4 Implications of modelling results for the emplacement of ophiolites 80
4.4.1 Tectonic setting of the detached sheet 80
4.4.2 Recent ridge-trench interactions 83

4.4.3 Observed properties of ophiolites: Comparison with modelling results 84
4.5 Summary 88
References 88

Chapter 5
Some thermo-mechanical aspects of the subduction of continental lithosphere 93
5.1 Introduction 94
5.2 Thermal modelling 95
5.3 Mechanical modelling 103
5.4 Discussion 114
References 119

Samenvatting 123

Acknowledgements 125

Curriculum vitae 126

Chapter 1

Introduction and summary

The essential feature of the plate tectonic model (e.g., Le Pichon, 1968; Morgan, 1968) is that the outermost part of the earth - to which we will refer as the lithosphere - is seen as a mosaic of rigid plates that move with respect to one another. Material within these plates is of lower temperature, and hence of greater strength, than material within the underlying upper mantle. In addition, the upper part of these plates, i.e. the crust, has a composition and physical properties quite distinct from mantle material. The thickness of the lithosphere is of an order of magnitude of 100 km; the thickness of the crust is about 7 km for oceanic lithosphere and generally about 25 - 40 km for continental lithosphere.

Most of the tectonic and magmatic activity on earth takes place at the plate boundaries. Key roles are played by the divergent plate boundaries, where new oceanic lithosphere is created, and by the convergent plate boundaries, where oceanic lithosphere is subducted into the mantle. Not only are convergent plate margins the site of the destruction of oceanic lithosphere, but they are also the site of the creation or reworking of continental crust. Subduction of oceanic lithosphere is generally associated with a linear belt of volcanoes, situated where the subducting plate has reached a depth of about 100 - 150 km. Creation of new continental crust at these volcanic belts is due to melting of the crustal part of the subducting oceanic plate and/or to melting of overlying mantle material (e.g., Gill, 1981; Wyllie, 1988). In addition, the growth of continental crust at convergent plate margins may be caused by the transfer of material from the subducting plate to the overriding plate. This process refers either to the more or less continuous transfer of sedimentary material on top of the subducting plate (which may be metamorphosed to a high-pressure, low-temperature metamorphic facies), or to the transfer of crystalline

material, originating from the subducting plate itself. The North American Cordillera provides a prime example of continental growth due to subduction related processes. Subduction of oceanic lithosphere over a period of time of several hundreds of Myr has here resulted in a collage of oceanic terranes (sediments, slivers of oceanic lithosphere, seamounts) and volcanic arcs (e.g., Coney et al., 1980; Suppe, 1985).

The much less frequent arrival of continental lithosphere at a subduction zone leads to the formation of an orogenic belt. A present-day example is provided by the India-Eurasia collision that has resulted in the formation of the Himalayas. During this process, continental crust is subducted to a depth of a few tens of km and will thus be subjected to pervasive metamorphism, if not to (partial) melting. Although Archean (> 2.5 Gyr old) continental crust has been preserved in several places, it is likely that much of the continental crust that has been formed in Archean times has been unrecognizably changed during later orogenic phases (Windley, 1984; Taylor and McLennan, 1985). Much of western Europe, for instance, consists of older continental crust that has been extensively reworked during the Caledonian, Hercynian and Alpine orogenic phases.

The plate tectonic model in its simplest form (rigid plates, all deformation concentrated at narrow plate boundaries) runs into problems at convergent plate margins. Near the Himalayas, the colliding Indian and Eurasian continents do no longer behave as coherent plates. Rather, the collision has lead to the break-up[1] of Indian continental lithosphere at more and more southward situated major thrust faults (Molnar, 1984; Mattauer, 1986), and to the formation of a diffuse zone of deformation, several hundreds of km wide, in Eurasian continental lithosphere to the North of the suture zone (e.g., Tapponier et al., 1986). It is unclear, what mechanisms can account for the break-up of young oceanic lithosphere and their subsequent incorporation in mountain ranges, leading to belts of ophiolites such as that near the Indus-Tsangpo suture zone for the Himalayas (e.g., Moores, 1982).

Processes such as metamorphism or melting of material at convergent plate margins, or the break-up of a plate during the early phase of its subduction, are of course closely related to the thermal and mechanical structure of convergent plate margins. Thermo-mechanical models of subduction zones (see Wortel and Vlaar, 1988, and references

1. The term break-up here denotes that a plate breaks up over at least a substantial fraction of its entire thickness, leading to the formation of a new plate contact within or at the base of the plate. For the Himalayas, break-up of Indian continental lithosphere has only involved its crustal part, and has thus only lead to the detachment and transfer of crustal material to the upper Eurasian plate. On the other hand, the break-up of oceanic lithosphere that has resulted in ophiolite emplacement, has involved an entire section of (be it relatively young and thin) oceanic lithosphere.

therein) have generally focused on the subduction process in general, thus including the entire slab up to depths of about 700 km. These models are less well suited for a detailed investigation of processes within the shallow part of a subduction zone. Thus, the thermal structure of the shallow part of a subduction zone is relatively poorly known, and it is unclear what factors determine the conditions during high-pressure, low-temperature metamorphism within accretionary wedges. That most of the deformation within the outer shell of the earth is situated at relatively narrow plate boundaries, indicates that the strength of material at these boundaries must be much lower than the strength of material within the plates. For subduction shear zones, the subduction of sediments and fluids (leading to relatively high pore fluid pressures) provides a mechanism to establish relatively low strengths of material at the plate contact, at depths of a few tens of km. Detailed information on the magnitude of shear stresses at subduction shear zones (e.g., as a function of depth) is still lacking, however.

In this thesis, the thermal and mechanical structure of convergent plate margins will be investigated by means of numerical modelling. In addition, we will discuss the implications of modelling results for geological processes such as metamorphism or the break-up of a plate at a convergent plate margin. Both the thermal models (chapters 2 and 3) and the mechanical models (chapters 4 and 5) focus on the more shallow part of a subduction zone, where the downgoing plate is still in contact with the upper plate and has not yet been subducted into the mantle. This enables us to make a more detailed investigation of the thermo-mechanical structure of the upper part of a subduction zone. Throughout this thesis, numerical modelling techniques such as finite difference methods (for the thermal models) and finite element methods (for the mechanical models) have been used.

Vlaar and Wortel have demonstrated the prime importance of the age of a subducting oceanic plate on subduction zone temperatures and on the subduction process in general (Vlaar, 1975; Vlaar and Wortel, 1976; Wortel, 1980). Following these authors, much emphasis has here been emplaced on the influence of various parameters (in particular the age of a subducting oceanic plate) on the thermal and mechanical structure of the more shallow part of a subduction zone.

The use of pressure and temperature dependent rheologies, which (apart from elastic deformation) incorporate both brittle failure at lower temperatures and ductile deformation at higher temperatures, has been a major step forward in modelling deformation and stress within plates under various loading conditions (e.g., Goetze and Evans, 1979; Cloetingh, 1982; see also Cloetingh et al., 1982). In this thesis, such rheologies have been used in a finite element analysis of the mechanical structure of a subducting plate. Different rheologies have been used to model the strength of material within a subducting plate and at the plate contact.

During the mechanical modelling, we have first focused on the subduction of medium-age or older oceanic lithosphere (which was found not to break up), next on the subduction of young oceanic lithosphere (which was found to break up only under relatively rare circumstances) and finally on the subduction of continental lithosphere (which was found to break up frequently; if not as a rule).

The subduction of oceanic lithosphere and of continental lithosphere has been modelled in a similar way. These two sorts of subduction processes should not be seen as being fundamentally different. Rather, the differences in the compositional structure between these two types of lithosphere seem to be responsible for the different response of continental lithosphere to the subduction process, compared to that of oceanic lithosphere.

Chapter 2 of this thesis presents the results of finite difference modelling of the thermal structure of the shallow part of a subduction zone during the subduction of oceanic lithosphere. Heat flow data, in combination with rheological arguments and the distribution of interplate thrust earthquakes at the plate contact, are used to constrain the thermal structure of this region and the magnitude of shear stresses acting on the plate contact. It is shown that temperatures are primarily determined by the downward movement of relatively cold material and by frictional heating. Except for the subduction of young oceanic lithosphere (less than 30 Myr old), temperatures at the plate contact and within the upper plate are found to be essentially independent of the age of the subducting plate and the convergence velocity between the two plates. For models that satisfy the constraints, temperatures are shown to be in good agreement with pressure-temperature conditions during high-pressure metamorphism, inferred from mineral assemblages in the Franciscan Complex of California.

Chapter 3 focuses in more detail on the thermal consequences of the subduction of young oceanic lithosphere. A case study is carried out for the Cascadia subduction zone of southwestern Canada. For this subduction zone, there is both an extensive heat flow data set (Lewis et al, 1988), as well as several seismic reflection and refraction profiles, which constrain the geometry of the subducting plate (e.g., Clowes et al., 1987). In addition, plate motion studies (e.g., Engebretson et al., 1985) provide detailed information on the age of the subducting plate and the convergence velocity between the two plates, as a function of time. It is found that the prolonged subduction of very young oceanic lithosphere (less than 10 Myr old) can still lead to very low temperatures at the plate contact and within the upper plate. The models indicate that the small age of the subducting plate in itself does not preclude the existence of significant shear stresses at the plate contact.

In chapter 4 it is investigated, by means of finite element modelling, whether oceanic lithosphere may break up, just prior to or during the early phase of its subduction. In general, this is found not to be the case, except during the interaction between a relatively fast spreading ridge and a subduction zone. Break-up is caused by the relatively slow

decrease of resistive forces (due to buoyancy of the oceanic crust and primarily to friction at the plate contact) and the relatively fast decrease of the strength of the subducting plate, during the subduction of gradually younger oceanic lithosphere. If break-up occurs, some young oceanic lithosphere that has descended to a depth up to a few tens of km, as well as the oceanic plate between the ridge and the trench, will be detached from the other parts of the subducting plate. The geometry of the detached sheet will depend upon the spreading rate and the length of the ridge segment that interacts with the trench. Instead of being subducted into the mantle, the detached sheet of thin oceanic lithosphere (which has a maximum thickness of about 10 - 20 km) may be incorporated into the forearc region. Our modelling thus provides a mechanism to incorporate thin sheets of oceanic lithosphere into an arc-trench region and eventually, upon closure of the ocean basin, into an orogenic belt. It is proposed that ophiolites with a harzburgite-dominated mantle section (see e.g., Boudier and Nicolas, 1985) have experienced an emplacement history in which the break-up of young oceanic lithosphere in the upper part of a subduction zone is the first phase.

Chapter 5 focuses on both thermal and mechanical consequences of the subduction of continental lithosphere. It is found that, contrary to oceanic lithosphere, continental lithosphere as a rule breaks up during the early phase of its subduction. In addition, it is shown that the break-up of continental lithosphere only leads to the transfer of crustal material to the upper plate. The more frequent break-up of continental lithosphere in the shallow part of a subduction zone is in part due to greater resistive forces, due to the buoyancy of continental crust, but primarily to the lower strength of subducting continental lithosphere (and in particular the existence of zones with very low strength in the middle or lower crust). Finally, it is shown that the arrival of a a cool continental shield at a subduction zone, or alternatively of continental lithosphere with a relatively small crustal thickness, may lead to the subduction of both upper and lower crust to mantle depths.

References

Boudier, F., and A. Nicolas, Harzburgite and lherzolite subtypes in ophiolitic and oceanic environments, *Earth Planet. Sci. Lett., 76,* 84-92, 1985.

Cloetingh, S. A. P. L., Evolution of passive continental margins and initiation of subduction zones, Ph. D. Thesis, 111 pp., Univ. of Utrecht, Utrecht, 1982.

Cloetingh, S. A. P. L., M. J. R. Wortel, and N. J. Vlaar, Evolution of passive continental margins and initiation of subduction zones., *Nature, 297,* 139-142, 1982.

Clowes, R. M., M. T. Brandon, A. G. Green, C. J. Yorath, A. Sutherland Brown, E. R. Kanasewich, and C. Spencer, LITHOPROBE-southern Vancouver Island: Cenozoic subduction complex imaged by deep seismic reflections, *Can. J. Earth Sci., 24,* 31-51, 1987.

Coney, P. J., D. L. Jones, and J. W. H. Monger, Cordilleran suspect terranes, *Nature, 288,* 329-333, 1980.

Engebretson, D. C., A. Cox, and R. G. Gordon, Relative motions between oceanic plates of the Pacific Basin, *Geol. Soc. Am. Spec. Paper, 206,* 59 pp., 1985.

Gill, J., *Orogenic andesites and plate tectonics,* 390 pp., Springer, Berlin, 1981.

Goetze, C., and B. Evans, Stress and temperature in the bending lithosphere as constrained by experimental rock mechanics, *Geophys. J. R. Astron. Soc., 59,* 463-478, 1979.

Le Pichon, X., Sea floor spreading and continental drift, *J. Geophys. Res., 73,* 3661-3697, 1968.

Lewis, T. J., W. H. Bentkowski, E. E. Davis, R. D. Hyndman, J. G. Souther, and J. A. Wright, Subduction of the Juan de Fuca plate: Thermal consequences, *J. Geophys. Res., 93,* 15207-15225, 1988.

Mattauer, M., Intracrustal subduction, crust-mantle decollement and crustal-stacking wedge in the Himalayas and other collision belts, in *Collision tectonics, Geol. Soc. London, Spec. Publ., 19,* edited by M. P. Coward and A. C. Ries, pp. 37-50, Oxford, 1986.

Molnar, P., Structure and tectonics of the Himalaya, *Ann. Rev. Earth Planet. Sci., 12,* 489-518, 1984.

Moores, E. M., Origin and emplacement of ophiolites, *Rev. Geophys. Space Phys., 20,* 735-760, 1982.

Morgan, W. J., Rises, trenches, great faults, and crustal blocks, *J. Geophys. Res., 73,* 1959-1982, 1968.

Suppe, J., *Principles of structural geology,* 537 pp., Prentice-Hall, Englewood Cliffs, 1985.

Taylor, S. R., and S. M. McLennan, *The continental crust: its composition and evolution,* 312 pp., Blackwell, Oxford, 1985.

Tapponier, P., G. Peltzer, and R. Armijo, On the mechanics of the collision between India and Asia, in *Collision tectonics, Geol. Soc. London, Spec. Publ., 19,* edited by M. P. Coward and A. C. Ries, pp. 115-157, Oxford, 1986.

Vlaar, N. J., The driving mechanism of plate tectonics, in *Progress in geodynamics,* edited by G. R. Borradaille, A. R. Ritsema, H. E. Rondeel and O. J. Simon, pp. 234-245, Amsterdam, 1975.

Vlaar, N. J., and M. J. R. Wortel, Lithospheric aging, instability and subduction, *Tectonophysics, 32,* 331-351, 1976.

Windley, B. F., *The evolving continents,* 399 pp., Wiley, Chichester, 1984.

Wortel, M. J. R., Age-dependent subduction of oceanic lithosphere, Ph. D. Thesis, 147 pp., Univ. of Utrecht, Utrecht, 1980.

Wortel, M. J. R., and N. J. Vlaar, Subduction zone seismicity and the thermo-mechanical evolution of downgoing lithosphere, *Pure Appl. Geophys., 128,* 625-659, 1988.

Wyllie, P. J., Magma genesis, plate tectonics, and chemical differentiation of the earth, *Rev. Geophys., 26,* 370-404, 1988.

Chapter 2

Temperatures and shear stresses in the upper part of a subduction zone

J. van den Beukel and R. Wortel

Abstract. The thermal structure of the shallow part of a subduction zone, i.e. the region between the trench and the volcanic line, has been calculated with a finite difference method. Published heat flow measurements, in combination with rheological arguments and the distribution of interplate thrust earthquakes, are used to constrain the thermal structure of this region and the magnitude of shear stresses acting on the plate contact. A pressure and temperature dependent rheology is used to model shear stresses. From our thermo-mechanical modelling it follows that temperatures at the plate contact and within the upper plate are determined by the subduction of cold material and by frictional heating. For models that satisfy the constraints the average shear stress at the plate contact (between the trench and the volcanic line) varies from about 10 to about 40 MPa and shear stresses during brittle deformation range from 2.5 to 7.5 % of the lithostatic pressure. For a wide range of convergence velocities (4 - 12 cm/yr) and ages of the subducting oceanic lithosphere (30 - 150 Myr), shear stresses and temperatures at and above the plate contact are essentially independent of these parameters. Temperatures at the upper surface of the slab for the preferred thermal models are in good agreement with pressure-temperature

This chapter has been published as:

van den Beukel, J., and R. Wortel, Thermo-mechanical modelling of arc-trench regions, *Tectonophysics, 154,* 177-193, 1988.

conditions during high-pressure metamorphism inferred from mineral assemblages in the Franciscan Complex of California. Frictional heating has a large influence on the conditions for high-pressure metamorphism.

2.1 Introduction

Processes at convergent plate margins, associated with the subduction of oceanic lithosphere, are important for the evolution of continental crust. High-pressure metamorphic belts are formed in the region near the trench (Oxburgh and Turcotte, 1971; Ernst, 1977). Subduction related volcanism results in the formation of new continental crust (Gill, 1981). It is obvious that the thermal structure of the upper part of a subduction zone has a large influence on these processes.

Here, we present a thermal model for the region between the trench and the volcanic line (arc-trench region; see Fig. 2.1). Arc-trench regions are characterized by a small, gradually increasing dip of the slab and, as can be inferred from heat flow data, by the absence of an asthenospheric wedge between the slab and the surface. Temperatures are relatively low as a consequence of the subduction process. The depth of the upper surface of the slab in this region is less than about 100 km.

Several authors have studied the thermal structure of a subduction zone (e.g. Minear and Toksöz, 1970; Andrews and Sleep, 1974; Anderson et al., 1978, 1980; Hsui and Toksöz, 1979; Honda and Uyeda, 1983; Honda, 1985). These models, which encompass both the subducting and the overriding plate, exhibit large differences in temperature for the arc-trench region which are primarily caused by differences in heat production by friction at the upper surface of the subducting slab. Shear stresses at the plate contact vary from zero MPa (e.g. Honda and Uyeda, 1983) to values over 100 MPa (e.g. Anderson et al., 1978). Constraints on either temperatures or shear stresses are thus essential for the thermal modelling of an arc-trench region. In addition, the dip of the slab in these models is constant and approximately equal to the dip of the slab at great depth, whereas in reality the dip gradually increases until the slab has reached a depth of about 100 - 200 km. The geometry of the slab in these models is not suitable for a detailed investigation of the thermal structure of an arc-trench region.

In this study we use published heat flow data, in combination with rheological arguments and the depth distribution of interplate thrust earthquakes, to infer the thermal structure of an arc-trench region and the magnitude of shear stresses acting on the plate contact. A constant curvature, rather than a constant dip, has been employed to model the geometry of the slab, giving a much better approximation of its actual geometry in an arc-

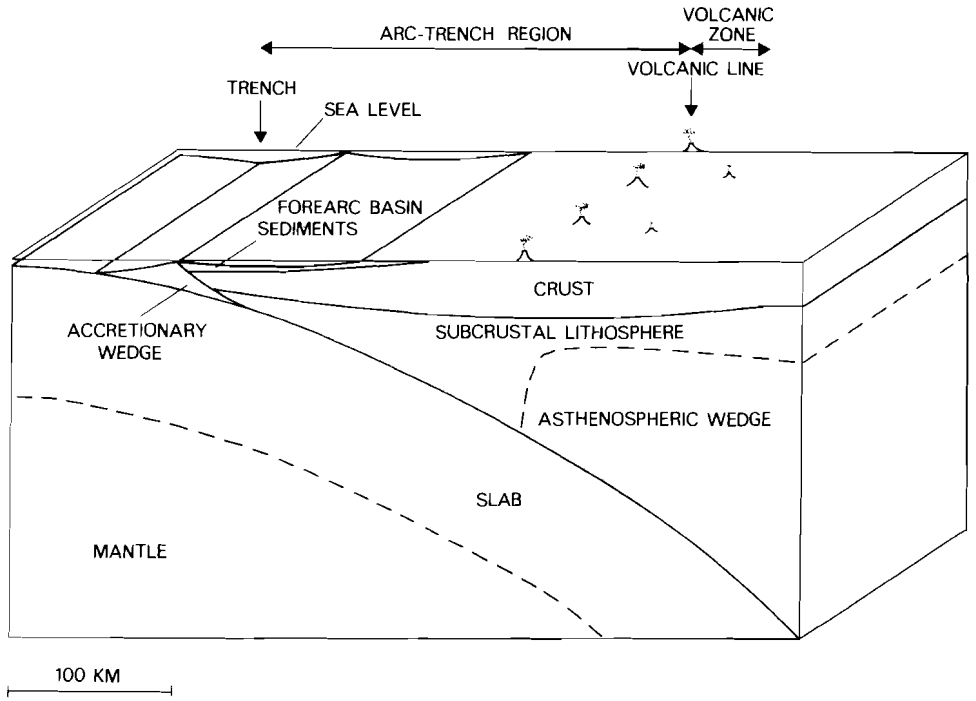

Figure 2.1. The shallow part of a subduction zone. Dashed lines indicate the base of the lithosphere, which can only be given schematically. No vertical exaggeration.

trench region.

2.2 Description of the model

Isacks and Barazangi (1977) give the geometry of the upper surface of the descending slab, as inferred from seismicity, for a number of subduction zones. Differences in the geometry of the slab at depths less than 100 km are small compared to differences at greater depths. The distance between the trench and the volcanic line is typically 175 - 275 km; the depth of the upper surface of the slab below the volcanic line is typically 90 - 110 km.

The geometry of the model is given in Fig. 2.2. The upper surface of the slab is part of a circle, which gives a reasonable approximation of the actual geometry of the slab in an arc-trench region (Isacks and Barazangi, 1977; Furlong et al., 1982). In the model the dip below the trench is 7° and the dip below the volcanic line is slightly over 30°. The total distance between the trench and the volcanic line is about 250 km; the depth of the upper

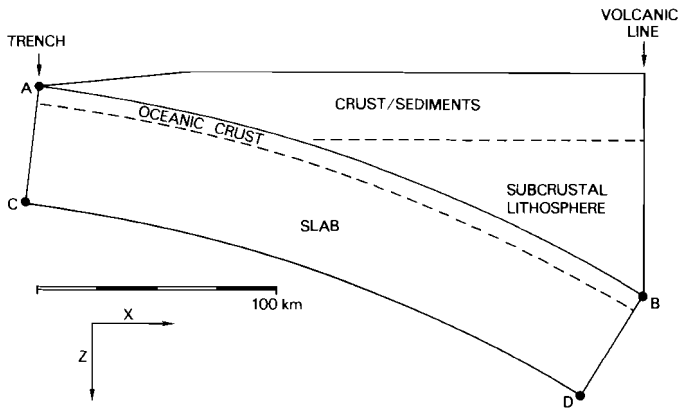

Figure 2.2. Geometry of the model.

surface of the slab below the volcanic line is about 95 km. The geometry of the model is particularly close to that of the subduction zone near N.E. Honshu, Japan (Yoshii, 1979). The thickness of the crustal and sedimentary part of the upper plate is 25 km and the thickness of the crust of the slab is 7.5 km. Since we focus here on temperatures at and above the upper surface of the slab, it is sufficient to incorporate only the upper 50 km of the slab in the model. Within an arc-trench region heating of the slab takes place only in the upper 20 - 30 km of the slab.

The time dependent two-dimensional temperature distribution T(x,z,t) (where z is the depth, x the horizontal distance from the trench and $\vec{v}$ the velocity; T in °C) is calculated from:

$$\frac{\partial T}{\partial t} + \vec{v}.\nabla T = \frac{1}{\rho c_p}(\nabla.(k\nabla T) + A) \qquad (1)$$

For crustal material the density ρ is taken to be 2.7×10^3 kg m^{-3} and the thermal conductivity k is 2.5 W m^{-1} °C^{-1}. For subcrustal lithosphere the density is 3.3×10^3 kg m^{-3} and a temperature dependent thermal conductivity for olivine, from Schatz and Simmons (1972), is used. A value of 1.05×10^3 J kg^{-1} °C^{-1} has been adopted for the specific heat c_p. It can be inferred from heat flow data (see below) that the asthenospheric wedge does not extend significantly into the arc-trench region. We have assumed that velocities are zero for material above the slab, thereby neglecting internal deformation in the accretionary wedge (see also below). For the slab itself velocities are equal to the convergence velocity v_c between the two plates, except for a small effect due to downbending of the slab. Velocities along circular arcs within the slab (e.g. lines AB and CD in Fig. 2.2) are constant. A is the heat production rate per unit volume due to friction and the decay of radioactive elements. For the slab adiabatic compression gives also a small contribution to A (see Minear and

Toksöz, 1970).

Finite difference methods are used to solve eqn. (1) numerically. The system of ordinary differential equations which results from the discretization of space variables in the partial differential eqn. (1), is solved with a class of explicit three-step Runge Kutta methods (van der Houwen, 1977; Verwer, 1977). Gridpoints are located at segments of a circle (e.g. lines AB and CD in Fig. 2.2) and at straight lines perpendicular to these segments (e.g. lines AC and BD). The distance between gridpoints at these straight lines is 5 km. In order to check the results, calculations have also been made for models with smaller distances between gridpoints. The amount of frictional heat Q_f, generated at the upper surface of the descending slab is (per unit time and unit surface of plate contact):

$$Q_f = v\,\tau \tag{2a}$$

where v is the velocity of the upper surface of the slab, relative to the upper plate, and τ the shear stress. Shear stresses have been modelled with a pressure and temperature dependent rheology (see below). For gridpoints at the upper surface of the slab the heat production rate by friction A_f (per unit volume) is:

$$A_f = \frac{v\,\tau}{z_g} \tag{2b}$$

where z_g is the distance between gridpoints at a straight line perpendicular to the plate contact, taken to be equal to the thickness of the shear zone.

Temperatures at the top of the model are assumed to be 0 °C. Temperatures for the downbending oceanic lithosphere below the trench depend on the age of the subducting oceanic lithosphere and are calculated for a boundary layer model (Crough, 1975) with a temperature of 1325 °C at the base of the lithosphere. At a depth of 50 km within the slab (line CD in Fig. 2.2) a constant heat flow, perpendicular to the line CD and equal to the calculated heat flow at point C, has been assumed. Temperatures below the volcanic line, at depths less than 80 km, are those of a geotherm with a surface heat flow of 80 mW m^{-2}. Such a high heat flow is common for the volcanic zone and the back-arc region (see also Fig. 2.3). High temperatures below the volcanic zone can also be inferred from the composition of magmas (Tatsumi et al., 1983) and are likely to be caused by processes within the asthenospheric wedge below the volcanic zone and the back-arc region. Migration of the volcanic line, if any, is slow (Dickinson, 1973) and a high temperature boundary condition, as defined above, thus seems reasonable. At the start of the model calculations temperatures are those of a geotherm with a surface heat flow of 55 mW m^{-2} and subduction starts instantaneously. Here, we do not focus on the thermal structure of an arc-trench region during the early stages of subduction, but rather on the steady state thermal structure, which has been reached in many subduction zones (see below). A discussion of the mechanisms for the initiation of subduction is given by Cloetingh et al. (1982). During model calculations the geometry of the slab is assumed to be constant.

A substantial part of the heat flow at the surface will be caused by the decay of

radioactive elements, concentrated in sediments and crustal material. Thus radiogenic heat production must be incorporated in the thermal models, in order to be able to use heat flow data as a constraint. Generally the following sequence exists in the direction from the trench to the volcanic arc: accretionary wedge - oceanic crust and forearc sediments - arc crust and/or continental crust (Dickinson and Seely, 1979). The heat production rate in crust of oceanic origin is about 0.5 $\mu W\ m^{-3}$ (Pollack and Chapman, 1977). Crust formed by subduction related volcanism (arc crust) has a low heat production rate of 0.25 - 0.50 $\mu W\ m^{-3}$ (Gill, 1981, p. 45). Sediments in the forearc basin, which are derived from arc crust (Dickinson, 1974), are thus also expected to have a low radiogenic heat production. Radiogenic heat production in continental crust, however, is higher: estimates for the average radiogenic heat production rate in continental crust, as given by Weaver and Tarney (1984), range from 0.73 - 0.95 $\mu W\ m^{-3}$. During the thermal modelling the radiogenic heat production rate in the upper 25 km of the overriding plate has been varied between a low estimate of 0.4 $\mu W\ m^{-3}$ (typical for arc crust and oceanic crust) and a high estimate of 0.9 $\mu W\ m^{-3}$ (typical for continental crust). Note that the radiogenic heat production rate for offscraped deep-sea sediments, which may form a part of the accretionary wedge, is uncertain and may fall outside of the range 0.4 - 0.9 $\mu W\ m^{-3}$. For the crust of the slab a radiogenic heat production rate has been assumed of 0.5 $\mu W\ m^{-3}$.

2.3 Constraints on temperatures and shear stresses

Heat flow

Heat flow measurements (from Anderson, 1980; Nakamura and Wakita, 1982 and Yoshii, 1983) for the subduction zone near the Japan trench (N.E. Honshu) are given in Fig. 2.3. Heat flow is low in the entire arc-trench region; most data are lower than 40 $mW\ m^{-2}$. The volcanic line is associated with an increase in heat flow to 75 - 100 $mW\ m^{-2}$ over a relatively short distance. The large spread in the heat flow data is attributed to errors in the data and not to real differences in heat flow as a function of distance in the direction parallel to the trench axis. Heat flow data for small segments of this subduction zone, given by Yoshii (1983), show a similar spread. The error for heat flow measurements in arc-trench regions, using ocean probe techniques, is estimated to be about 12 $mW\ m^{-2}$ (Hyndman, 1976).

Other subduction zones show a similar pattern; low heat flow ($< 40\ mW\ m^{-2}$) in the arc-trench region and high heat flow in the volcanic zone and the back-arc region (e.g. Watanabe et al., 1977). The increase in heat flow near the volcanic line may be somewhat more gradual than is suggested by the data given in Fig. 2.3. The low heat flow in the arc-trench region points to temperatures above the slab that are considerably below mantle temperatures. Subduction induced flow of mantle material in the arc-trench region can thus be ruled out. Average values for heat flow data in the central part of the arc-trench region

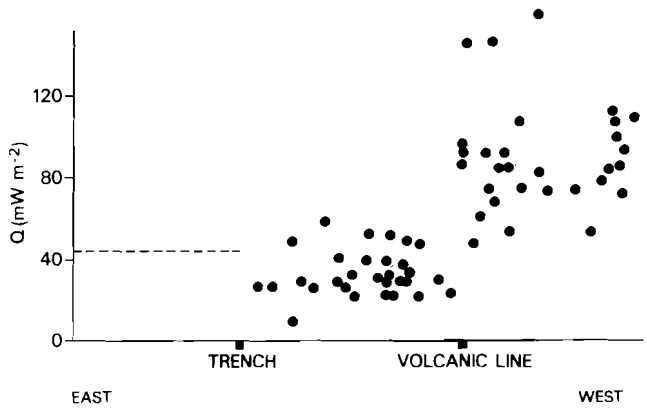

Figure 2.3. Heat flow for the subduction zone near the Japan trench (N.E. Honshu). Heat flow data from Anderson (1980); Nakamura and Wakita (1982) and Yoshii (1983). The dashed line is the theoretical heat flow (for a boundary layer model from Crough (1975)) for oceanic lithosphere with an age of 120 Ma. This is the age of the descending Pacific plate at the Japan trench. The distance between the trench and the volcanic line is about 260 km.

are given in table 2.1. The central part of the arc-trench region is defined as the region, where the distance to the trench and the distance to the volcanic line are both greater than $X_{AT}/3$ (where X_{AT} is the distance between the trench and the volcanic line). The heat flow in this part of the arc-trench region will not be influenced by the high temperatures below the volcanic zone (via horizontal conduction) or by processes within the accretionary wedge. Subduction zones with a very large accretionary wedge (Sumatra, Aleutians) may be an exception to this. These subduction zones do not conform to the adopted geometry (Fig. 2.2) and are not included in this study. The number of heat flow measurements that have been used to calculate the average values, given in table 2.1, ranges from 9 (South America) to 15 (N.E. Honshu). For an error of 12 mW m^{-2} (which is likely to be a high estimate for many of the heat flow data for the Cascades and South America which are inferred from drill hole measurements) these average values are expected to have an error of about 3 - 4 mW m^{-2} only.

An average value higher than 40 mW m^{-2} is only obtained for the S.W. Honshu subduction zone. The time passed since the initiation of subduction is relatively short for this subduction zone (see table 2.1). This may explain the higher heat flow, since it will take time for the lithosphere above the slab to cool, after the initiation of subduction. The other subduction zones have all been active for more than 50 Myr. Such a duration of subduction is sufficient for the upper plate to reach a steady state thermal structure (see below). Average values of heat flow data in the central part of the arc-trench region for these subduction zones range from 31 to 35 mW m^{-2}. Heat flow profiles and maps for the Central America (Blackwell et al., 1977) and Kuriles (Smirnov and Sugrobov, 1982)

Subduction zone	Heat flow[(a)] ($mW\ m^{-2}$)	Duration[(b)] (Myr)
N.E. Honshu	34	> 50
S.W. Honshu	54	± 15
Cascades	35	> 50
South America	31	> 50

a) Average values for heat flow data at distances greater than 0.33 x X_{AT} from the trench and the volcanic line (where X_{AT} is the total distance between the trench and the volcanic line). Heat flow data from Anderson, 1980 (N.E. Honshu); Blackwell et al., 1982 (Cascades); Henry, 1981 (South America); Hyndman, 1976 (Cascades); Nakamura & Wakita, 1982 (N.E. Honshu); Uyeda & Watanabe, 1982 (South America); Watanabe et al., 1977 (S.W. Honshu)
b) Duration since the initiation of subduction, taken or inferred from Coney and Reynolds, 1978 (Cascades); Hilde et al., 1977 (N.E. Honshu); Kobayashi, 1983 (S.W. Honshu); Palacios, 1984 (South America).

Table 2.1. Average values of heat flow data in the central part of the arc-trench region. Also given is the time since the initiation of subduction.

subduction zones exhibit a heat flow of about 30 $mW\ m^{-2}$ in the central part of the arc-trench region. These subduction zones have also been active for more than 50 Myr (Hilde et al., 1977; Karig et al., 1978). For our modelling we have required that, once that a steady state thermal structure has been reached, average heat flow in the central part of the arc-trench region should fall between 30 and 35 $mW\ m^{-2}$.

Rheology

As follows from rock mechanics experiments the strength of material is determined by pressure, temperature, pore fluid pressure, rock type and strain rate (Kirby, 1983; Tsenn and Carter, 1987). Brittle deformation takes place at lower temperatures whereas plastic deformation dominates at higher temperatures. For brittle deformation the shear stress τ required to cause sliding on a pre-existing fault is given by:

$$\tau = \mu\sigma_n^* \tag{3}$$

where μ is the coefficient of friction and σ_n^* the effective normal stress, acting on the fault surface:

$$\sigma_n^* = \sigma_n - P_f \tag{4}$$

where σ_n is the normal stress and P_f the pore fluid pressure. For a wide variety of rocks it follows from experimental data that, for σ_n^* less than 200 MPa, μ is approximately equal to

0.85 (Byerlee, 1978). Clays, however, have a much lower coefficient of friction (Bird, 1984). For an arc-trench region the underthrusting of fluid-rich sediments will lead to high pore fluid pressures near the shear zone up to substantial depths (von Huene, 1984). The exact magnitude of these pore fluid pressures, however, is uncertain. During modelling it has been assumed that, for brittle deformation near the upper surface of the slab, the average shear stress during fault motion increases linearly with the lithostatic pressure P:

$$\tau = \gamma P \tag{5}$$

Flow laws for plastic deformation that is caused by steady state power law creep have the form (Kirby, 1983):

$$\dot{\varepsilon} = A_o(\sigma_1 - \sigma_3)^n \exp(-Q/RT) \tag{6}$$

where $\dot{\varepsilon}$ is the strain rate, T the absolute temperature, R the gas constant and σ_1 and σ_3 the maximum and minimum principal stress. Q, A_o and n are material constants. The flow law that should be used to model plastic deformation near the upper surface of a descending slab is that of the weakest material near the shear zone. This may be either sedimentary material or oceanic crust (see also Yuen et al., 1978). We have taken a relatively weak limestone rheology as a lower limit for the strength, during plastic deformation, of material at a subduction shear zone. Furthermore, calculations have been made using flow laws for quartzite and diorite (under wet conditions) which are appropriate for material where respectively quartz and feldspar are the dominant minerals, controlling plastic flow. An upper limit for the strength of crustal material, during plastic deformation, at a subduction shear zone is taken to be given by a flow law for diabase (under dry conditions). Material constants for flow laws that are used during model calculations are given in table 2.2. Note that these laboratory derived flow laws should be regarded as giving an upper bound for the strength of the material under natural conditions.

Flow law	A_o ($Kbar^{-n}\ s^{-1}$)	n	Q (Kcal/mole)	Reference
Limestone	4.9×10^7	2.05	50.4	Schmid (1976)
Quartzite (wet)	4.36	2.44	38.2	Koch et al. (1980)
Diorite (wet)	80	2.4	52.3	Hansen and Carter (1982)
Diabase	5.2×10^8	3.0	85	Caristan (1982)

Table 2.2. Flow law parameters

By using several flow laws (and also including a model without any frictional heating), we are able to cope with the difficulties that arise from the uncertainty as to what material determines the strength during ductile deformation at the shear zone and the uncertainty in

the extrapolation of laboratory flow laws to geologic strain rates. We do not want to exclude the possibility that a relatively weak limestone or quartzite flow law gives a better approximation of the strength of oceanic crust, during ductile deformation at geologic strain rates, than a diorite or diabase flow law. From our modelling we infer the magnitude of shear stresses at the plate contact, rather than the type of material that determines the strength at the shear zone during ductile deformation.

In order to calculate τ (= $(\sigma_1-\sigma_3)/2$) from eqn. (6), an estimate of $\dot{\varepsilon}$ is needed. Yuen et al. (1978) have modelled deformation at shear zones for a number of different rheologies. A typical strain rate that can be inferred from their models is 10^{-12} s^{-1}. Here, $\dot{\varepsilon}$ is taken to be (v_c/v_{ref}) x 10^{-12} s^{-1} (v_c in cm/yr). v_{ref} is a reference velocity of 8 cm/yr. During modelling, shear stresses for a certain place at the plate contact are calculated both for brittle deformation (eqn. (5)) and for plastic deformation (eqn. (6)). The lowest of these two values is used to model heat production by friction (eqn. (2b)).

Seismicity

Near the upper surface of the slab a zone of thrust earthquakes extends from a depth of about 15 - 20 km to a depth of about 40 km, occasionally to depths of 60 - 70 km (Isacks and Molnar, 1971; McCann et al., 1979). Great thrust earthquakes do not rupture the interface between the two plates below a depth of about 40 km (McCann et al., 1979; Ruff and Kanamori, 1983). At the same depth Sykes and Quittmeyer (1981) locate the transition from principally seismic to principally aseismic motion at the plate contact. This is confirmed by studies of the seismicity for several subduction zones (e.g. Davies and House (1979) for the Aleutians; Isacks et al. (1981) for the New Hebrides; LeFevre and McNally (1985) for Middle America).

For continental fault zones Meissner and Strehlau (1982) have shown that below the seismogenic zone the strength of material is low as a consequence of thermally activated creep. For oceanic lithosphere the absence of intraplate earthquakes below the 700 °C - 800 °C isotherm is consistent with rapid weakening for olivine rheologies at these temperatures (Wiens and Stein, 1983). Reduced strength, due to thermally activated creep, also seems the most likely explanation for principally aseismic motion at a subduction shear zone for depths greater than about 40 km. For our models we have required that the brittle-ductile transition at the plate contact takes place at a depth between 30 and 50 km.

2.4 Model calculations

Parameters for all models are given in table 2.3. As a starting point calculations have been made for five models (TA1, TLIM1, TQUA1, TDIO1 and TDIA1). The age of the subducting oceanic lithosphere in these models is 70 Myr and the convergence velocity is 8

Model	γ	Flow law	$T_{sl}^{(a)}$ (Myr)	$v_c^{(b)}$ (cm/yr)	$A_r^{(c)}$ ($\mu W\ m^{-3}$)
TA1	0.		70	8	.7
TA2	0.		70	8	.9
TLIM1	0.03	Limestone	70	8	.7
TLIM2	0.03	Limestone	70	8	.9
TLIM3	0.025	Limestone	70	8	.9
TQUA1	0.05	Quartzite	70	8	.7
TQUA2	0.05	Quartzite	70	4	.7
TQUA3	0.05	Quartzite	70	12	.7
TQUA4	0.05	Quartzite	30	8	.7
TQUA5	0.05	Quartzite	150	8	.7
TDIO1	0.09	Diorite	70	8	.7
TDIO2	0.09	Diorite	70	8	.4
TDIO3	0.075	Diorite	70	8	.4
TDIA1	0.11	Diabase	70	8	.7
TDIA2	0.11	Diabase	70	8	.4

a) Age of the oceanic lithosphere at the trench.
b) Convergence velocity between the two plates.
c) Radiogenic heat production rate in the upper 25 km of the upper plate.

Table 2.3. Input parameters for model calculations.

cm/yr. These values are close to the average values of these parameters for present-day subduction zones (Wortel, 1982). The models have a radiogenic heat production rate A_r within the crustal and sedimentary part of the upper plate of 0.7 $\mu W\ m^{-3}$. Model TA1 is a model without heat production by friction. Shear stresses for plastic deformation for the other models are determined by flow laws for limestone, quartzite, diorite and diabase. For these models values for γ, which determines the shear stress (and thus heat production by friction) for brittle deformation, are chosen in such a way that the transition from brittle to plastic deformation at the shear zone takes place at a depth of approximately 40 km (thus satisfying the depth constraint for the brittle-ductile transition at the plate contact).

At a time 50 Myr after the initiation of subduction a steady state thermal structure has been reached completely (see Fig. 2.4a). All results of model calculations will be given for a steady state situation 50 Myr after the initiation of subduction. The heat flow for the models TA1 - TDIA1, 50 Myr after the initiation of subduction, is given in Fig. 2.4b. The models exhibit a low heat flow in the arc-trench region, which is the result of the advection of cold material. It is clear that frictional heating at the plate contact has a large influence on the magnitude of this low. Average heat flow in the central part of the arc-trench region varies from less than 20 $mW\ m^{-2}$ for model TA1 to about 45 $mW\ m^{-2}$ for model TDIA1. Only the model with a flow law for quartzite has an average heat flow in the central part of

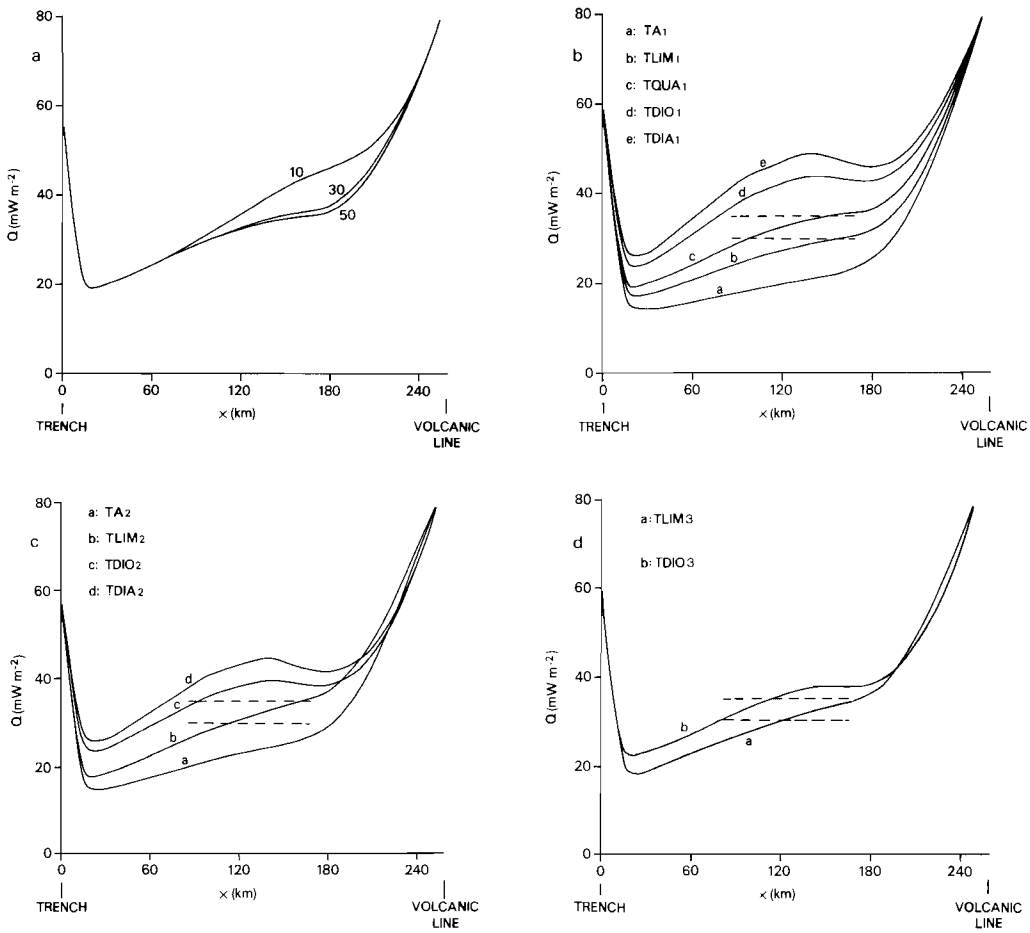

Figure 2.4. (a) Heat flow, 10, 30 and 50 Myr after the initiation of subduction for model TQUA1. (b) Heat flow, 50 Myr after the initiation of subduction. Dashed lines give the interval for the average heat flow, inferred from heat flow data, in the central part of the arc-trench region for subduction zones, where subduction started more than 50 Myr ago. (c) Heat flow, 50 Myr after the initiation of subduction, for models TA2, TLIM2, TDIO2 and TDIA2. (d) Heat flow, 50 Myr after the initiation of subduction, for models TLIM3 and TDIO3.

an arc-trench region that falls within the interval of 30 - 35 mW m^{-2} inferred from heat flow data.

Model calculations have also been made for models similar to the models TA1 - TDIA1, but with a different radiogenic heat production rate A_r in the crustal part of the upper plate. Variations in A_r have a much greater influence on temperatures near the surface than on temperatures at the plate contact. The heat flow for the models TA2,

TLIM2 (with a high estimate for A_r of 0.9 $\mu W\ m^{-3}$), TDIO2 and TDIA2 (with a low estimate of 0.4 $\mu W\ m^{-3}$) are given in Fig. 2.4c. Of these models, model TLIM2 meets both the constraint on heat flow and that on the depth of the brittle-ductile transition. Model TDIO2 exhibits a heat flow that is slightly too high. Models similar to model TDIO2, but with a lower value for γ (between 0.05 and 0.075) are acceptable, however.

A large number of model calculations have been made for different flow laws, and different values for A_r and γ. It was found that the constraints on heat flow and the depth of the brittle-ductile transition could not be satisfied for models with a flow law for a diabase. Models without heat production by friction could not meet the heat flow constraint. Acceptable models, with a limestone, quartzite or diorite rheology to model plastic deformation, exhibit a brittle-ductile transition between 30 and 50 km and shear stresses for brittle deformation between 2.5 and 7.5 % of the lithostatic pressure (γ between 0.025 and 0.075). For a given flow law, a lower value for γ leads to a brittle-ductile transition at greater depth. Temperature distributions for the models TLIM3, TQUA1 and TDIO3 are given in Fig. 2.5. Of all acceptable models, the models TLIM3 and TDIO3 exhibit the lowest and highest temperatures respectively. These two models also give a lower and upper bound for the magnitude of shear stresses at the plate contact. Temperatures and shear stresses at the plate contact, as a function of depth, are given in Fig. 2.6.

Calculations have been made for models with a quartzite flow law and convergence velocities of 4 and 12 cm/yr. Most of the subduction zones have convergence velocities between these two values. The influence of velocities on the thermal structure turns out to be very small (see Fig. 2.7a). The effect of an increased cooling, due to the faster subduction, approximately cancels the effect of an increased heat production by friction. Fig. 2.7b shows temperatures at the plate contact for two models similar to model TQUA1, but with a young (30 Myr) and a very old (150 Myr) subducting oceanic lithosphere. The influence of the age of the oceanic lithosphere on the thermal structure is greater than that of the convergence velocity. Differences between models for which the age of the subducting plate varies are small, however, compared to the differences between the models TLIM3, TQUA1 and TDIO3. Acceptable models with an age of the subducting plate of 30 or 150 Myr show a very similar range in temperatures and shear stresses as the models TLIM3 and TDIO3.

From our thermo-mechanical modelling it can be concluded that temperatures at and above the plate contact in an arc-trench region are mainly determined by the way the upper part of the slab heats up, during its descent, as a consequence of frictional heating. About 85 to 90 % of the frictional heat generated at the plate contact is used to heat up downgoing material in the upper part of the slab and only a small fraction contributes to the surface heat flow. Unless subduction takes place of very young oceanic lithosphere or with a very low convergence velocity, the age of the subducting lithosphere and the convergence velocity will not have a large influence on the temperatures at and above the plate contact. During brittle deformation, friction causes heating up to temperatures which enable plastic

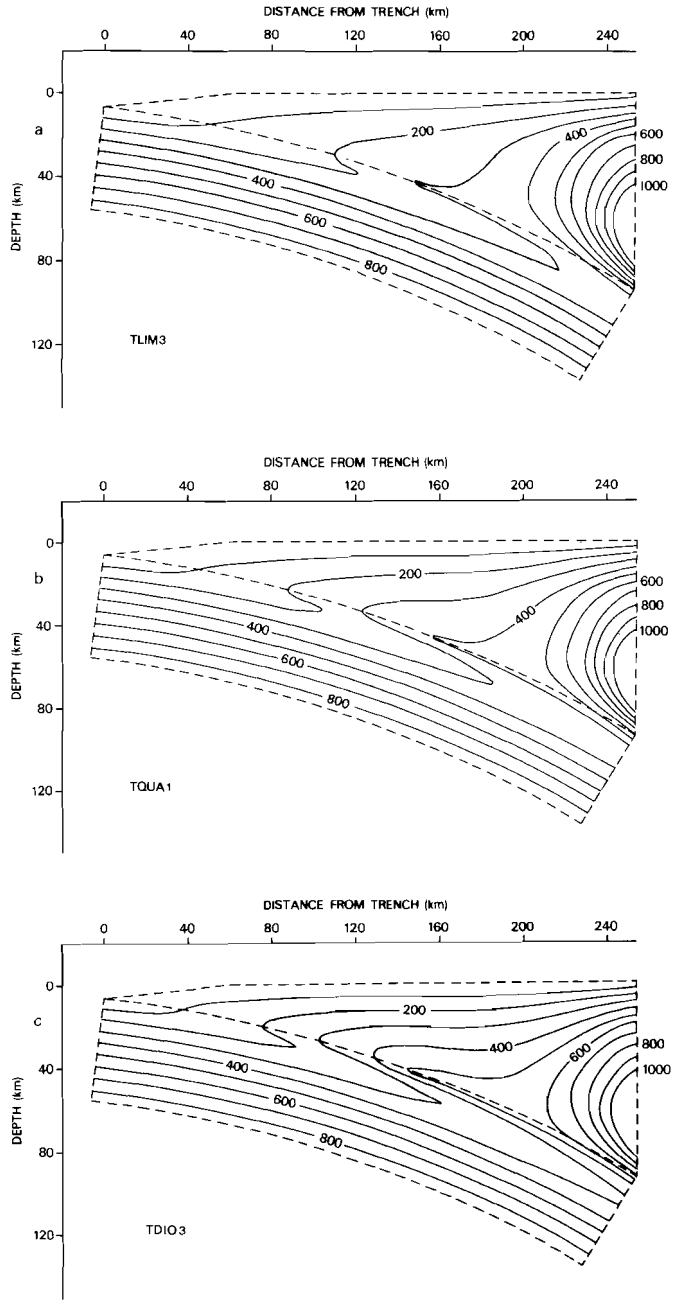

Figure 2.5. Temperature distributions for models TLIM3 (Fig. 2.5a), TQUA1 (Fig. 2.5b) and TDIO3 (Fig. 2.5c), 50 Myr after the initiation of subduction.

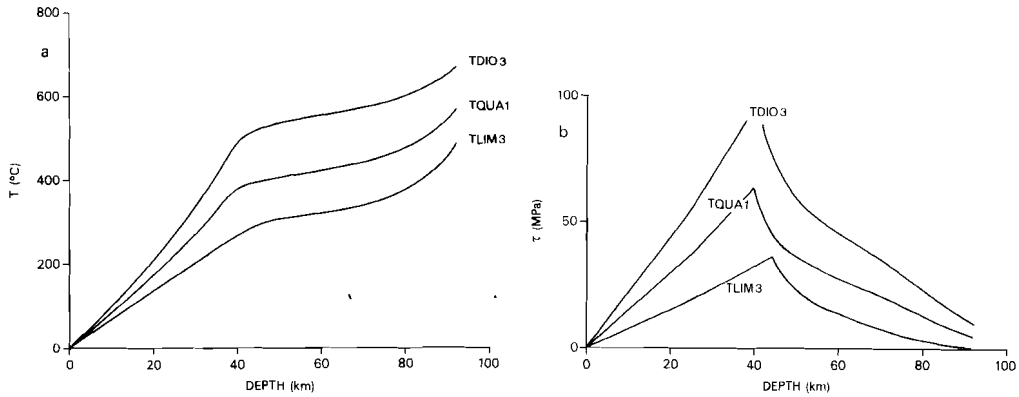

Figure 2.6. (a) Temperatures at the upper surface of the slab (line AB in Fig. 2.2), 50 Myr after the initiation of subduction, for models TLIM3, TQUA1 and TDIO3. (b) Shear stresses at the upper surface of the slab, 50 Myr after the initiation of subduction, for models TLIM3, TQUA1 and TDIO3.

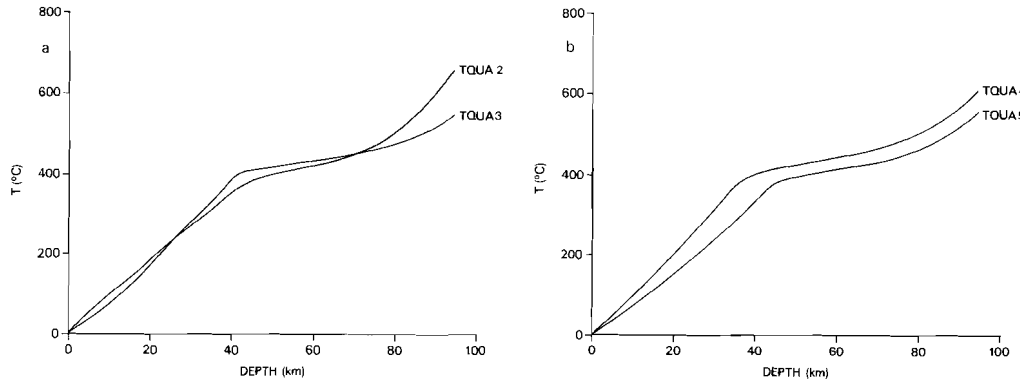

Figure 2.7. (a) Temperatures at the upper surface of the slab, 50 Myr after the initiation of subduction, for models TQUA2 and TQUA3. (b) Temperatures at the upper surface of the slab, 50 Myr after the initiation of subduction, for models TQUA4 and TQUA5.

flow to take place. At depths greater than that of the brittle-ductile transition friction only leads to a small increase of temperature with depth at the plate contact. A low level of interplate seismicity may exist at depths of about 40 to 80 km, since shear stresses for plastic deformation do not fall off rapidly to values near zero. Average shear stresses at the plate contact (between points A and B in Fig. 2.2) are 12 MPa (model TLIM3), 24 MPa (model TQUA1) and 38 MPa (model TDIO3). These values are primarily determined by the flow law that is used to model plastic deformation and are, for a wide range of convergence velocities (4 - 12 cm/yr) and ages of the subducting oceanic plate (30 - 150

Myr), essentially independent of these parameters. Average shear stresses for the models TQUA2 - TQUA5 range from 21 to 26 MPa.

2.5 High-pressure metamorphism

Subduction of oceanic lithosphere can lead to the formation of an accretionary wedge, which consists of sedimentary material. In a high-pressure metamorphic belt, such as the Franciscan Complex of California, material that was once part of an accretionary wedge and situated at substantial depths (up to about 40 km) is now exposed at the surface. High-pressure metamorphic belts are characterized by mineral assemblages that form at relatively low temperatures, which are generally thought to be related to the low temperatures that exist in the upper part of a subduction zone (e.g. Oxburgh and Turcotte, 1971). An increase in both metamorphic grade and radiometric ages exists in the direction from the former trench to the former volcanic arc (e.g. Ernst, 1977).

From observed mineral assemblages and experimentally determined or calculated phase equilibria estimates can be made of the pressure-temperature conditions to which the material in a high-pressure metamorphic belt has been subjected. Since sedimentary material in downward movement is expected to be close to the upper surface of the descending slab, P-T conditions during prograde metamorphism will give an estimate of the conditions at the upper surface of the slab during metamorphism. It must be kept in mind, however, that the P-T conditions inferred from mineral assemblages need not always represent a steady state thermal structure (as our model temperatures do) but may also represent relatively high temperatures shortly after the initiation of subduction.

Fig. 2.8 gives P-T conditions for material from the Franciscan Complex. For zones A to D the grade of metamorphism increases, whereas the volume of material, now exposed, decreases (Coleman and Lee, 1963). Zone D represents high-grade blueschist blocks (some meters in extent), which have been emplaced tectonically into lower grade metamorphic material of regional extent (zone A to C). Zone E represents material that has been metamorphosed at relatively high temperatures in contact with peridotite (Brown et al., 1982).

Radiometric ages for zones D and E span a relatively small time range of about 140 to 160 Myr (Brown et al., 1982; Cloos, 1985). These ages are close to the age of 155 to 165 Myr for the Coast Range Ophiolite (Hopson et al., 1981) and indicate that metamorphism took place during, or shortly after, the initiation of the subduction episode that lead to the formation of the Franciscan. Radiometric ages for zones B and C range from about 70 to 150 Myr, a time range similar to that for Franciscan fossils (Suppe and Armstrong, 1972; Cloos,1985). This greater time range and the regional extent of the metamorphic rocks from zones A to C indicate that the P-T conditions for zones A to C represent a steady state thermal situation. Note that, although it takes about 30 Myr for an arc-trench region as a whole to reach a steady state thermal structure, temperatures at the plate contact do so

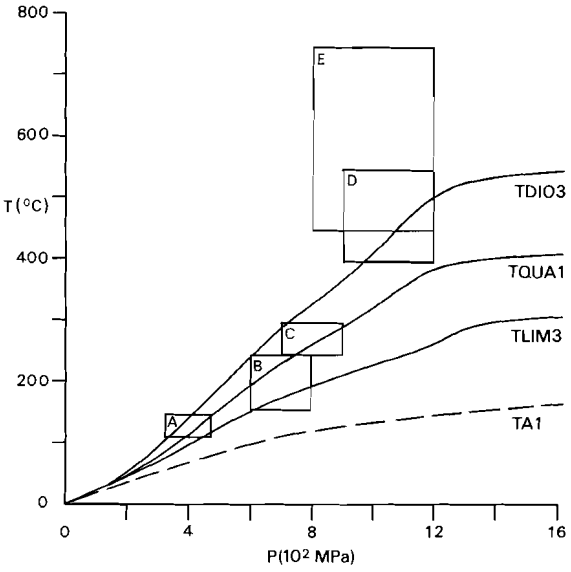

Figure 2.8. Temperatures at the upper surface of the descending slab, as a function of pressure, for models TA1, TLIM3, TQUA1 and TDIO3. Temperatures 5 km above the upper surface of the slab differ less than 25°C. Zones A to E represent P-T conditions during metamorphism for material in the Franciscan Complex, California. Zone A: Franciscan material at Diablo Range (Bostick, 1974). Zone B: Franciscan blueschist facies metasedimentary material from Diablo Range (Moore and Liou, 1979). Zone C: Franciscan blueschist facies material from northern California Coast Ranges (Black Butte and Ball Rock areas) and Panoche Pass region (Brown and Ghent, 1983). Zone D: High-grade blueschist blocks, generally metabasalts, emplaced tectonically into a melange of lower-grade Franciscan material (Taylor and Coleman, 1968; Brown and Bradshaw, 1979; Moore, 1984). Zone E: Amphibolite and barroisite schists, metamorphosed in contact with peridotite, from Shuksan Metamorphic Suite (Brown et al., 1982). All estimates for temperatures are based on mineral parageneses, except for zone A where temperatures are inferred from the maturation of organic material.

within a few Myr and temperatures within the upper plate, where its thickness is less than 30 km, do so within about 10 Myr (see Fig. 2.4b).

Fig. 2.8 also gives temperatures at the upper surface of the descending slab for the models TA1, TLIM3 and TDIO3. Models TLIM3 and TDIO3 provide a lower and an upper limit for temperatures in an arc-trench region. Thermal models in which heat production by friction is not included or very low (model TA1 in Fig. 2.8; see also Wang and Shi, 1984) give temperatures that are considerably lower than the temperatures for zones A to C. Such models can only give temperatures in agreement with P-T conditions for zones A to C if subduction takes place with a very low velocity of about 1 cm/yr or less (Wang and Shi, 1984). No present-day subduction zone has a subduction rate near 1 cm/yr and it seems unlikely that subduction of oceanic lithosphere with such low velocities has

been widespread in the past. On the other hand, the range of P-T conditions for the preferred thermal models (TLIM3, TQUA1 and TDIO3) turns out to be in very good agreement with P-T conditions for metamorphic rocks from zone A to C. The good agreement between P-T conditions for these rocks, likely to be the result of a steady state thermal situation, and our preferred models is an additional support for our modelling. As is the case for temperatures in an arc-trench region as a whole, temperatures in the accretionary wedge and P-T conditions for high-pressure metamorphism are heavily influenced by frictional heating near the upper surface of the slab and thus by pore fluid pressures and the rheological properties of material near the shear zone.

Temperatures for material from zone E are considerably higher than model temperatures. Metamorphism took place in contact with peridotite and Brown et al. (1982) have proposed that these higher temperatures are caused by hot ultramafic material within the hanging wall during the initiation of subduction. Similar high-temperature metamorphic rocks have been found directly below well-preserved ophiolites (e.g. Ghent and Stout, 1981). The radiometric ages and the basaltic composition of the high-grade tectonic blocks (zone D) suggest that they have been sheared-off from the subducting oceanic plate shortly after the initiation of subduction. Possibly their P-T conditions represent an early phase of subduction when temperatures at the plate contact were already determined by the rheological properties of material at the plate contact, but may have been somewhat higher than the temperatures during later phases, due to a lesser amount of weakening (see also Pavlis, 1986).

Within an accretionary wedge uplift may take place as a consequence of underplating and deep-seated movements of low-strength sediments (Cloos, 1982; Moore et al., 1982; Silver et al., 1985). We expect that upward velocities of sediments will be very small compared to the convergence velocity between the two plates. Firstly, it takes at least 20 - 30 Myr for blueschists to reach the surface (Ernst, 1972). Secondly, observed uplift rates of accretionary complexes are only a few tenths of a mm/yr (Pavlis and Bruhn, 1983). Calculations have been made for models similar to model TQUA1 but with an upward velocity (in the direction perpendicular to the upper surface of the slab) within the upper plate. Although movements within an accretionary wedge will certainly exhibit a much more complex pattern, such models can give an estimate of the influence of possible large scale movements of sediments. Differences in temperature between a model with an upward velocity of 0.3 mm/yr within the upper plate and model TQUA1 are less than 5 °C at the upper surface of the slab and less than 20 °C within the part of the upper plate where the slab is at depths less than 30 km. Even for a model with a velocity within the upper plate that is as high as 3 mm/yr, temperatures at the upper surface of the slab differ less than 20 °C everywhere. Thus even if significant movements of sediments in an accretionary wedge occur, conditions for high-pressure metamorphism will still be primarily determined by the way the upper part of the slab heats up as a result of frictional heating.

2.6 Discussion

The first step of the process that leads to subduction related volcanism is melting of material in the crust of the slab or in the asthenospheric wedge (e.g. Wyllie, 1979; Gill, 1981). In both cases high temperatures in the asthenospheric wedge above the slab are required for melting. From heat flow data we have inferred that the asthenospheric wedge does not extend significantly into the arc-trench region. The asthenospheric wedge does exist, however, below the back-arc region (as follows from the high heat flow data in this region) and below the volcanic zone (as follows from the composition of arc-basalt magmas; Tatsumi et al., 1983). Thus the volcanic line and the boundary of the asthenospheric wedge approximately coincide. We think it likely that the location of the volcanic line is determined by the extent of the asthenospheric wedge and that the part of the arc-trench region near the volcanic line is a transition zone, where equilibrium exists between cooling (caused by the nearby cold slab) and heating (caused by the nearby asthenospheric wedge). The absence of earthquakes in this region (the aseismic zone from Yoshii (1979)) can be attributed to higher temperatures in material that is still part of the lithosphere. During subduction, the volcanic line may slowly migrate, with a velocity less than 1 km/Myr (Dickinson, 1973). Because the thermal relaxation time of the upper plate in an arc-trench region is relatively short (see Fig. 2.4b), this will not have a large influence on the overall thermal structure of an arc-trench region.

Endothermic dehydration reactions for water-containing minerals in the crust of the descending slab start at a depth of about 75 km (Delany and Helgeson, 1978). The influence of these reactions on the thermal structure of an arc-trench region will be limited to temperatures in the upper part of the slab below this depth. The heat needed for the reactions will be readily supplied by the nearby asthenospheric wedge.

Frictional heating during brittle deformation depends on the pore fluid pressure and the coefficient of friction of material near the shear zone. For accretionary wedges, observed pore fluid pressures range from about 67.5 % to nearly 100 % of the lithostatic pressure (Davis et al., 1983). Chu et al. (1981) and Bird (1984) give values of 0.2 - 0.3 for the coefficient of friction for clays or clayey fault gouges. Shear stresses within clay-rich material at the base of an accretionary wedge, subjected to the observed range of pore fluid pressures, will range from 0 % to about 10 % of the lithostatic pressure (eqn. (3); see also Davis et al., 1983), corresponding to values for γ between 0 and 0.1. This agrees well with the interval for γ of 0.025 (model TLIM3) to 0.075 (model TDIO3) for the preferred thermal models. During thermal modelling γ is assumed to be independent of depth, whereas in reality γ may vary (Zhao et al., 1986). Values for γ in our thermal models should be seen as average values over the brittle part of the shear zone. In addition, it should be noted that the sharp peak of the shear stress near the brittle-ductile transition (see Fig. 2.6b) is a simplification. In reality this transition will be more gradual (e.g. Kirby, 1983).

From theoretical considerations on mantle convection McKenzie and Jarvis (1980)

infer that the average shear stress at the plate contact in an arc-trench region is unlikely to exceed 50 MPa. On the base of a force balance Bird (1978) has made estimates of the average shear stress at the plate contact at depths less than 100 km for two subduction zones where back-arc spreading occurs. The estimates are 16.5 ± 7.5 MPa for the Mariana and 22 ± 10 MPa for the Tonga subduction zone. These values are in good agreement with the average shear stress between the trench and the volcanic line for the models TLIM3 (12 MPa) and TQUA1 (24 MPa). The average shear stress for model TDIO3 is higher (38 MPa).

In spite of the relatively low strength of material at the plate contact (compared to the strength of material within a plate), frictional heating does have a large influence on the thermal structure of an arc-trench region. For shear stresses during brittle deformation that are about 5 % of the lithostatic pressure, frictional heating at strike-slip faults, such as the San Andreas fault, would lead to a very small heat flow anomaly, that would probably go undetected (Lachenbruch and Sass, 1980). The greater influence of frictional heating on the thermal structure of an arc-trench region is caused by the continuous advection of cold material, which leads to relatively low temperatures in an arc-trench region and thus, for a given pressure and temperature dependent rheology for material at the plate contact, to relatively high shear stresses. For an arc-trench region the depth to which frictional heating occurs is much greater than for a strike-slip fault and, for a given rheology for material at the plate contact, the average shear stress will be higher.

The total resistive force (per unit-length of trench), caused by friction in the upper part of a subduction zone, can be obtained by integrating shear stresses over the total down-dip length of the plate contact. This resistive force ranges from about 3 x 10^{12} N/m (model TLIM3) to 10 x 10^{12} N/m (model TDIO3). Estimates of the gravitational forces that drive the plates (ridge push and slab pull forces), as given by Wortel and Cloetingh (1983), are of the same order of magnitude. This indicates that this resistive force can be of major importance for intraplate stress fields and plate kinematics.

2.7 Conclusions

(1) From published heat flow data it can be inferred that, for older subduction zones (subduction started more than 50 Myr ago), the average heat flow in the central part of the arc-trench region is 30 - 35 mW m^{-2}.

(2) From our thermo-mechanical modelling it follows that shear stresses at the upper surface of the descending slab are relatively low. The average shear stress between the trench and the volcanic line lies between 10 and 40 MPa. During brittle deformation, shear stresses are about 2.5 - 7.5 % of the lithostatic pressure. Despite these low shear stresses, frictional heating has a large influence on temperatures near the plate contact and within the upper plate in an arc-trench region. For a wide range of convergence velocities (4 - 12 cm/yr) and ages of the subducting oceanic lithosphere (30 - 150 Myr), temperatures and

shear stresses are essentially independent of these parameters.

(3) Temperatures at the upper surface of the slab, for models that are in agreement with heat flow data and for which a steady state thermal structure has been reached, are in good agreement with P-T conditions for high-pressure metamorphism inferred from mineral assemblages in the Franciscan Complex of California. Conditions for high-pressure metamorphism are heavily influenced by frictional heating, and thus by pore fluid pressures and the rheological properties of material near the shear zone.

Acknowledgements. We thank dr. Sierd Cloetingh and prof. N.J. Vlaar for many helpful discussions.

References

Anderson, R.N., 1980. 1980 Update of heat flow in the East and Southeast Asian seas. In: D.E. Hayes (Editor), The tectonic and geologic evolution of Southeast Asian seas and islands. Geophys. Monogr. 23, Am. Geophys. Union, Washington D.C., pp. 319-326.

Anderson, R.N., DeLong, S.E. and Schwarz, W.M., 1978. Thermal model for subduction with dehydration in the downgoing slab. J. Geol., 86: 731-739.

Anderson, R.N., DeLong, S.E. and Schwarz, W.M., 1980. Dehydration, asthenospheric convection and seismicity in subduction zones. J. Geol., 88: 445-451.

Andrews, D.J. and Sleep, N.H., 1974. Numerical modelling of tectonic flow behind island arcs. Geophys. J. R. Astr. Soc., 38: 237-251.

Bird, P., 1978. Stress and temperature in subduction shear zones. Geophys. J. R. Astr. Soc., 55: 411-434.

Bird, P., 1984. Hydration-phase diagrams and friction of montmorillonite under laboratory and geologic conditions, with implications for shale compaction, slope stability and strength of fault gouge. Tectonophysics, 107: 235-260.

Blackwell, D.D., Ziagos, J. and Mooser, F., 1977. Heat flow and the thermal effects of subduction in southern Mexico. EOS, Trans. Am. Geophys. Union, 58: 1233.

Blackwell, D.D., Bowen, R.G., Hull, D.A., Riccio, J. and Steele, J.L., 1982. Heat flow, arc volcanism, and subduction in northern Oregon. J. Geophys. Res., 87: 8735-8754.

Bostick, N.H., 1974. Phytoclasts as indicators of thermal metamorphism, Franciscan assemblage and Great Valley sequence (upper Mesozoic), California. Geol. Soc. Am., Spec. Paper, 153: 1-17.

Brown, E.H. and Bradshaw, J.Y., 1979. Phase relations of pyroxene and amphibole in greenstone, blueschist and eclogite of the Franciscan complex, California. Contrib. Mineral. Petrol., 71: 67-83.

Brown, E.H. and Ghent, E.D., 1983. Mineralogy and phase relations in the blueschist facies of the Black Butte and Ball Rock areas, northern California Coast Ranges. Am. Mineral., 68: 365-372.

Brown, E.H., Wilson, D.L., Armstrong, R.L. and Harakal, J.E., 1982. Petrologic, structural, and age relations of serpentinite, amphibolite, and blueschist in the Shuksan Suite of the Iron Mountain-Gee Point area, North Cascades, Washington. Geol. Soc. Am., Bull., 93: 1087-1098.

Byerlee, J.D., 1978. Friction of rocks. Pure Appl. Geophys., 116: 615-626.

Caristan, Y., 1982. The transition from high-temperature creep to fracture in Maryland diabase. J. Geophys. Res., 87: 6781-6798.

Chu, C.L., Wang, C.Y. and Lin, W., 1981. Permeability and frictional properties of San Andreas fault gouge. Geophys. Res. Lett., 8: 565-568.

Cloetingh, S.A.P.L., Wortel, M.J.R. and Vlaar, N.J., 1982. Evolution of passive continental margins and initiation of subduction zones. Nature, 297: 139-142.

Cloos, M., 1982. Flow melanges: Numerical modeling and geologic constraints on their origin in the Franciscan subduction complex, California. Geol. Soc. Am. Bull., 93: 330-345.

Cloos, M., 1985. Thermal evolution of convergent plate margins: thermal modeling and reevaluation of isotopic Ar-ages for blueschists in the Franciscan complex of California. Tectonics, 4: 421-434.

Coleman, R.G. and Lee, D.E., 1963. Glaucophane-bearing metamorphic rock types of the Cazadero area, California. J. Petrol., 4: 260-301.

Coney, P.J. and Reynolds, S.J., 1978. Overview of Mesozoic-Cenozoic Cordilleran plate tectonics. In: R.B. Smith and G.P. Eaton (Editors), Cenozoic tectonics and regional geophysics of the western Cordillera. Geol. Soc. Am., Memoir, 152: 51-92.

Crough, S.T., 1975. Thermal model of oceanic lithosphere. Nature, 256: 388-390.

Davies, J. and House, L., 1979. Aleutian subduction zone seismicity, volcano-trench separation and their relation to great thrust-type earthquakes. J. Geophys. Res., 84: 4583-4591.

Davis, D., Suppe, J. and Dahlen, F.A., 1983. Mechanics of fold-and-thrust belts and accretionary wedges. J. Geophys. Res., 88: 1153-1172.

Delany, J.M. and Helgeson, H.C., 1978. Calculation of the thermodynamic consequences of dehydration in subducting oceanic crust to 100 kbar and 800 °C. Am. J. Sci., 278: 638-686.

Dickinson, W.R., 1973. Widths of modern arc-trench gaps proportional to past duration of igneous activity in associated magmatic arcs. J. Geophys. Res., 78: 3376-3389.

Dickinson, W.R., 1974. Sedimentation within and beside ancient and modern magmatic arcs. In: Modern and ancient geosynclinal sedimentation. Soc. Econ. Paleontol. Mineral., Spec. Pub., 19: 230-239.

Dickinson, W.R and Seely, D.R., 1979. Structure and stratigraphy of forearc regions. Am. Assoc. Petrol. Geol. Bull., 63: 2-31.

Ernst, W.G., 1972. occurrence and mineralogic evolution of blueschist belts with time. Am. J. Sci., 272: 657-668.

Ernst, W.G., 1977. Mineral parageneses and plate tectonic settings of relatively high-pressure blueschist belts. Fortschr. Mineral., 54: 192-222.

Furlong, K.P., Chapman, D.S. and Alfeld, P.W., 1982. Thermal modeling of the geometry of subduction with implications for the tectonics of the overriding plate. J. Geophys. Res., 87: 1786-1802.

Ghent, E.D. and Stout, M.Z., 1981. Metamorphism at the base of the Semail ophiolite. J. Geophys. Res., 86: 2557-2571.

Gill, J., 1981. Orogenic andesites and plate tectonics. Springer, Berlin, 390 pp.

Hansen, F.D. and Carter, N.L., 1982. Creep of selected crustal rocks at 1000 MPa. EOS, Trans. Am. Geophys. Union, 63: 437.

Henry, S.G., 1981. Terrestrial heat flow overlying the Andean subduction zone. Ph. D. Thesis, Univ. of Michigan, Ann Arbor, 194 pp.

Hilde, T.W.C., Uyeda, S. and Kroenke, L., 1977. Evolution of the western Pacific and its margin. Tectonophysics, 38: 145-165.

Honda, S., 1985. Thermal structure beneath Tohoku, Northeast Japan. A case study for understanding the detailed thermal structure of the subduction zone. Tectonophysics, 112: 69-102.

Honda, S. and Uyeda, S., 1983. Thermal process in subduction zones, a review and preliminary approach on the origin of arc volcanism. In: D. Shimozura and I. Yokoyama (Editors), Arc volcanism: physics and tectonics. Terra Scientific Publishing, Tokyo, pp. 117-140.

Hopson, C.A., Mattinson, J.M. and Pessango, E.A., 1981. Coast Range ophiolite, western California. In: W.G. Ernst (Editor), The geotectonic development of California. Prentice Hall, New-York, pp. 418-510.

Hsui, A.T. and Toksöz, M.N., 1979. The evolution of thermal structures beneath a subduction zone. Tectonophysics, 60: 43-60.

Hyndman, R.D., 1976. Heat flow measurements in the inlets of southwestern British Columbia. J. Geophys. Res., 81: 337-349.

Isacks, B.L. and Barazangi, M., 1977. Geometry of Benioff zones: lateral segmentation and downwards bending of subducted lithosphere. In: M. Talwani and W.C. Pitman, III (Editors), Island arcs, deep sea trenches and back-arc basins. Am. Geophys. Union, Washington D.C., pp. 99-114.

Isacks, B.L. and Molnar, P., 1971. Distribution of stresses in the descending lithosphere from a global survey of focal mechanism solutions of mantle earthquakes - Rev. Geophys. Space Phys., 9: 103-174.

Isacks, B.L., Cardwell, R.K, Chatelain, J.L., Barazangi, M., Marthelot, J.M., Chinn, D. and Louat, R., 1981. Seismicity and tectonics of the central New Hebrides island arc. In: D.W. Simpson and P.G. Richards (Editors), Earthquake prediction, an international review. Am. Geophys. Union, Washington, D.C., pp. 93-116.

Karig, D.E., Caldwell, R.K., Moore, G.F. and Moore, D.G., 1978. Late Cenozoic subduction and continental-margin truncation along the northern Middle America trench. Geol. Soc. Am. Bull., 89: 265-276.

Kirby, S.H., 1983. Rheology of the lithosphere. Rev. Geophys. Space Phys., 21: 1458-1487.

Kobayashi, K., 1983. Fore-arc volcanism and cycles of subduction. In: D. Shimozura, D. and I. Yokoyama (Editors), Arc volcanism: physics and tectonics. Terra Scientific Publishing, Tokyo, pp. 153-163.

Koch, P.S., Christie, J.M. and George, R.P., 1980. Flow law of "wet" quartzite in the α-quartz field. EOS, Trans. Am. Geophys. Union, 61: 376.

Lachenbruch, A.H. and Sass, J.H., 1980. Heat flow and energetics of the San Andreas fault system. J. Geophys. Res. 85: 6185-6222.

LeFevre, L.V. and McNally, K.C., 1985. Stress distribution and subduction of aseismic ridges in the Middle America subduction zone. J. Geophys. Res., 90: 4495-4510.

McCann, W.R., Nishenko, S.P., Sykes, L.R. and Krause, J., 1979. Seismic gaps and plate tectonics: seismic potential for major boundaries. Pure Appl. Geophys., 117: 1082-1147.

McKenzie, D. and Jarvis, G., 1980. The conversion of heat into mechanical work by mantle convection. J. Geophys. Res., 85: 6093-6096.

Meissner, R. and Strehlau, J., 1982. Limits of stresses in continental crust and their relation to the depth-frequency distribution of shallow earthquakes. Tectonics, 1: 73-89.

Minear, J.W. and Toksöz, M.N., 1970. Thermal regime of a downgoing slab and new global tectonics. J. Geophys. Res., 75: 1397-1419.

Moore, D.E., 1984. Metamorphic history of a high-grade blueschist exotic block from the Franciscan complex, California. J. Petrol., 25: 126-150.

Moore, D.E. and Liou, J.G., 1979. Mineral chemistry of some Franciscan blueschist facies metasedimentary rocks from the Diablo Range, California. Geol Soc. Am., Bull., 90: 1089-1091.

Moore, J.C., Watkins, J.S. and Shipley, T.H., 1982. Summary of accretionary processes, deep sea drilling project leg 66: offscraping, underplating, and deformation of the slope apron. Init. Repts. DSDP, 66: 825-836.

Nakamura, Y. and Wakita, H., 1982. Terrestrial heat flow around the aseismic front of the Japanese island arc. Tectonophysics, 81: T25-T36.

Oxburgh, E.R. and Turcotte, D.L., 1971. Origin of paired metamorphic belts and crustal dilation in island arc regions. J. Geophys. Res., 76: 1315-1327.

Palacios, C.M., 1984. Considerations about the plate tectonic model, volcanism and continental crust in the southern part of the central Andes. Tectonophysics, 106: 205-214.

Pavlis, T.L., 1986. The role of strain heating in the evolution of megathrusts. J. Geophys. Res., 91:

12407-12422.
Pavlis, T.L. and Bruhn, R.L., 1983. Deep-seated flow as a mechanism for the uplift of broad forearc ridges and its role in the exposure of high P/T metamorphic terranes. Tectonics, 2: 473-497.
Pollack, H.N. and Chapman, D.S., 1977. On the regional variation of heat flow, geotherms, and lithospheric thickness. Tectonophysics, 38: 279-296.
Ruff, L. and Kanamori, H., 1983. Seismic coupling and uncoupling at subduction zones. Tectonophysics, 99: 99-117.
Schatz, J.F. and Simmons, G., 1972. Thermal conductivity of earth materials at high temperatures. J. Geophys. Res., 77: 6966-6983.
Schmid, S.M., 1976. Rheological evidence for changes in the deformation mechanism of Solenhofen limestone towards low stresses. Tectonophysics, 31: T21-T28.
Silver, E.A., Ellis, M.J., Breen, N.A. and Shipley, T.H., 1985. Comments on the growth of accretionary wedges. Geology, 13: 6-9.
Smirnov, Y. and Sugrobov, V.M., 1982. Terrestrial heat flow in the northwestern Pacific. Tectonophysics, 83: 109-122.
Suppe, J. and Armstrong, R.L., 1972. Potassium-argon dating of Franciscan metamorphic rocks. Am. J. Sci., 272: 217-233.
Sykes, L.R. and Quittmeyer, R.C., 1981. Repeat times of great earthquakes along simple plate boundaries. In: In: D.W. Simpson and P.G. Richards (Editors), Earthquake prediction, an international review. Am. Geophys. Union, Washington, D.C., pp. 217-247.
Tatsumi, Y., Sakuyama, M., Fukuyama, H. and Kushiro, I., 1983. Generation of arc basalt magmas and thermal structure of the mantle wedge in subduction zones. J. Geophys. Res., 88: 5815-5825.
Taylor, H.P. and Coleman, R.G., 1968. $^{18}O/^{16}O$ ratios of coexisting minerals in glaucophane-bearing metamorphic rocks. Geol. Soc. Am. Bull, 79: 1727-1755.
Tsenn, M.C. and Carter, N.L., 1987. Upper limits of power law creep of rocks. Tectonophysics, 136: 1-26.
Uyeda, S. and Watanabe, T., 1982. Terrestrial heat flow in western South America. Tectonophysics, 83: 63-70.
van der Houwen, P.J., 1977. Construction of integration formulas for initial value problems. North-Holland, Amsterdam, 269 pp.
Verwer, J.G., 1977. A class of stabilized three-step Runge Kutta methods for the numerical integration of parabolic equations. J. Comp. Appl. Math., 3: 155-166.
von Huene, R., 1984. Tectonic processes along the front of modern convergent margins. Ann. Rev. Earth Planet. Sci., 12: 359-381.
Wang, C.Y. and Shi, Y.L., 1984. On the thermal structure of subduction complexes; a preliminary study. J. Geophys. Res., 89: 7709-7718.
Watanabe, T., Langseth, M.G. and Anderson, R.N., 1977. Heat flow in back-arc basins of the western Pacific. In: M. Talwani and W.C. Pitman, III (Editors), Island arcs, deep sea trenches and back-arc basins. Am. Geophys. Union, Washington D.C., pp. 137-160.
Weaver, B.L. and Tarney, J., 1984. Empirical approach to estimating the composition of the continental crust. Nature, 310: 575-577.
Wiens, D.A. and Stein, S., 1983. Age dependence of oceanic intraplate seismicity and implications for lithospheric evolution. J. Geophys. Res., 88: 6455-6468.
Wortel, R., 1982. Seismicity and rheology of subducted slabs. Nature, 296: 553-556.
Wortel, R. and Cloetingh, S., 1983. A mechanism for fragmentation of oceanic plates. In: J.S. Watkins and C.L. Drake (Editors), Studies in continental margin geology. Am. Assoc. Petr. Geol., Memoir, 34: 793-801.
Wyllie, P.J., 1979. Magmas and volatile components - Am. Mineral., 64: 469-500.
Yoshii, T., 1979. A detailed cross section of the deep seismic zone beneath Northeast Honshu, Japan. Tectonophysics, 55: 349-360.

Yoshii, T., 1983. Cross sections of some geophysical data around the Japanese islands. In: T.W.C. Hilde and S. Uyeda (Editors), Geodynamics of the western Pacific-Indonesian region. Am. Geophys. Union, Washington D.C., pp. 343-354.

Yuen, D.A., Fleitout, L., Schubert, G. and Froidevaux, C., 1978. Shear deformation zones along major transform faults and subducting slabs. Geophys. J. R. Astr. Soc., 54: 93-119.

Zhao, W.L., Davis, D.M., Dahlen, F.A. and Suppe, J., 1986. Origin of convex accretionary wedges: Evidence from Barbados. J. Geophys. Res., 91: 10246-10258.

Chapter 3

Thermal modelling of the Cascadia subduction zone: a case study for the subduction of young oceanic lithosphere

Abstract. A two-dimensional thermal model is presented of the Cascadia subduction zone of southwestern Canada. It is found that in spite of the prolonged subduction of very young oceanic lithosphere (with an age less than 10 Myr) the subduction process still leads to relatively low temperatures at the plate contact and within the upper plate. This is primarily due to the downward movement of slab material. Endothermic dehydration reactions within the crustal part of the downgoing plate are of much smaller influence. Our modelling results indicate that the small age of the subducting plate does not preclude the existence of significant shear stresses at the plate contact.

3.1 Introduction

Thermal models of subduction zones (see van den Beukel and Wortel, 1988, and references therein) have generally focused on the subduction of medium-age or older oceanic lithosphere (about 30 to 150 Myr old). For such an age-range, van den Beukel and Wortel (1988) found that the age of the subducting plate has only minor influence on the thermal structure of the upper part of a subduction zone, the region between the trench and the volcanic arc. In all cases, the subduction process was found to lead to relatively low

temperatures within this region. The subduction of a spreading centre, on the other hand, will result in relatively high temperatures and a phase of high-T, low-P metamorphism within the upper plate near the trench (James et al., 1989). If the age of the subducting plate becomes very small, this is expected to lead to higher temperatures at the plate contact and to increasing aseismic slip, as a result of ductile deformation (Kanamori and Astiz, 1985; Heaton and Hartzell, 1987). It is not clear, at what age of the subducting plate the thermal structure in the upper part of a subduction zone starts to deviate significantly from that for the subduction of medium-age or older oceanic lithosphere and starts to resemble the thermal structure during a ridge-trench interaction.

Examples of the subduction of young oceanic lithosphere include the subduction zones of S. Chile, the Cascades, and S.W. Japan. The Cascadia subduction zone provides a good opportunity to model the thermal consequences of the subduction of young oceanic lithosphere. Data acquired by the Canadian Lithoprobe program across the Cascadia subduction zone include seismic reflection profiles, which constrain the geometry of the subducting plate (e.g., Clowes et al., 1987a), as well as an extensive heat flow data set (Lewis et al, 1988). Further, plate reconstruction studies (e.g., Engebretson et al., 1985) provide information on the age of the subducting plate and the convergence velocity between the upper and the subducting plate, as a function of time. In this paper, we present a 2-D finite difference thermal model of the Cascadia subduction zone near Vancouver Island, S.W. Canada. It is the aim of our modelling to investigate the thermal consequences of the subduction of the relatively young Juan de Fuca plate (with an age less than 10 Myr); e.g., to assess whether it can still act as a significant heat sink during the early phase of its subduction, leading to relatively low temperatures within the upper plate.

3.2 Model description

The geometry of the subducting plate in our model is chosen to be in agreement with pertinent data on the geometry of the subducting plate. Clusters of Benioff seismicity (labeled 1 and 2) within the subducting slab are shown in Figure 3.1a. We have required that these clusters should fall within the subducting plate, although not necessarily in its mantle part. Seismicity within the crustal part of the downgoing plate may be caused by the basalt to eclogite phase transition (Pennington, 1984). In addition, we have required that a band of dipping reflectors (labeled E in Figure 3.1a), situated above the top of the subducting plate (Clowes et al., 1987a, 1987b), should fall within the upper plate. This band is thought to be related to a dipping zone of trapped pore water (Hyndman, 1988). The adopted geometry of the model, as given in Figure 3.1a, satisfies these constraints. The dip of the subducting plate in the model decreases gradually from 7° beneath the trench to about 27° at a distance of 220 km from the trench. The thickness of the crustal part of the

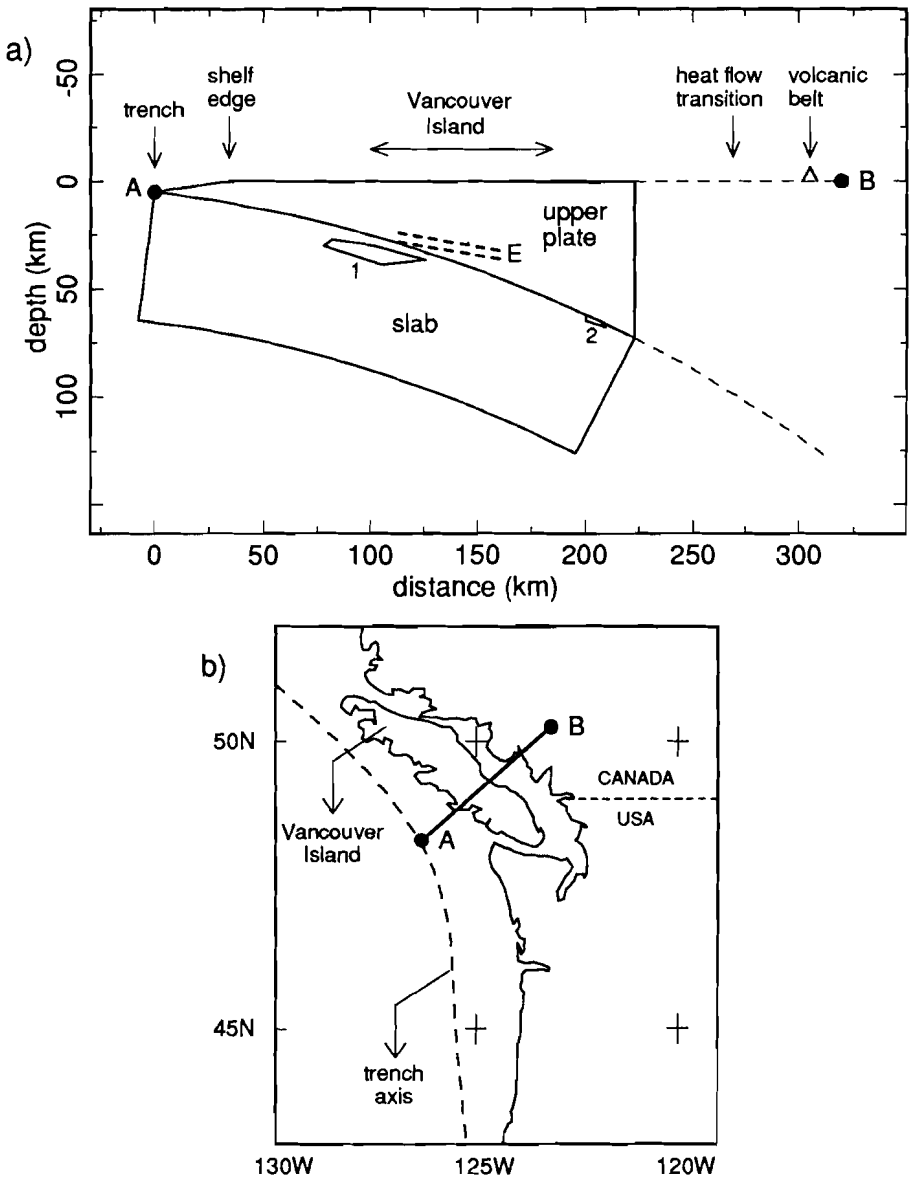

Figure 3.1. a) Geometry of the model. Dashed lines (labeled E) denote a dipping band of reflectors below Vancouver Island (Clowes, 1987a; 1987b). Clusters of Benioff seismicity within the subducting plate (from Rogers; as given in Lewis et al., 1988) are labeled 1 and 2. b) Position of the profile, shown in Fig. 3.1a.

upper and lower plate is taken to be 40 and 6 km, respectively.

Temperatures are determined by conduction, the downward movement of material

within the subducting plate and various sources of heat production (friction at the plate contact, radiogenic heating, dehydration reactions in the crustal part of the subducting plate). A more detailed description of the model can be found in van den Beukel and Wortel (1988). Unless otherwise stated, the values of various parameters for crustal and mantle material are the same as those given in van den Beukel and Wortel (1987; 1988).

Temperatures at the surface are kept at 0 °C. Temperatures at the left side of the model depend upon the age of the subducting oceanic lithosphere and are calculated using a boundary layer model for the cooling of oceanic lithosphere (Crough, 1975). We have adopted an age of the oceanic lithosphere of 8 Myr and a convergence velocity between the two plates of 5 cm/yr. These values are close to the present age of the Juan de Fuca plate, subducting below the southern part of Vancouver Island (e.g., Heaton and Hartzell, 1987), and the average convergence velocity between the two plates here during the last 6 Myr (Riddihough, 1984). Plate motion studies indicate that similar values for these parameters have prevailed for a period of time of at least 30 Myr (Engebretson et al., 1985).

It is noted that Crough's model is a relatively simple model for the thermal structure of very young oceanic lithosphere. Hydrothermal convection within the oceanic crust may lower temperatures. On the other hand, sediment deposition may lead to higher temperatures within an oceanic plate. Sedimentary sequences within the trench may be about 1 - 2 km thick. Most of these sediments represent a recent trench-fill deposit (Scholl, 1974), however, which is unlikely to have influenced the thermal structure of the underlying oceanic plate significantly.

Following Lewis at al. (1988), we have adopted a radiogenic heat production rate for the crustal part of the upper plate of 0.2 $\mu W\ m^{-3}$ (for material at depths greater than 10 km). At depths smaller than 10 km, this radiogenic heat production rate is taken to be 0.5 $\mu W\ m^{-3}$.

Anderson et al. (1976) have estimated that, depending upon its composition, the dehydration of 1 kg of oceanic crustal material requires about 0.4 to 1.7 x 10^5 J. Stability limits for various hydrous minerals, as a function of pressure and temperature, are given by Tatsumi (1989). We have here assumed that the gradual dehydration of the oceanic crust, between 50 and 80 km depth, requires 1 x 10^5 J per kg of material.

The amount of frictional heating at the plate contact depends linearly on the magnitude of shear stresses and the convergence velocity between the two plates. Shear stresses at the plate contact for brittle deformation (τ_{br}) are taken to depend linearly on the lithostatic pressure P (=ρgz):

$$\tau_{br} = \gamma P \quad . \tag{1}$$

For ductile deformation, shear stresses (τ_{du}) were inferred from a steady state flow law for a wet quartzite (Koch et al., 1980), adopting a strain rate of 1 x 10^{-12} s^{-1}. For a given place at the plate contact, the lowest of the two values for τ_{br} and τ_{du} has been used to infer the

amount of frictional heating.

The model does not include the effects of fluid flow or of underplating of sedimentary material beneath the upper plate. For the Cascadia subduction zone, a major episode of underplating may have taken place during Eocene times (Clowes et al., 1987a). In view of the limited time, needed for the upper plate to reach thermal equilibrium (less than 10 Myr where its thickness is less than about 30 km; see also van den Beukel and Wortel (1988)), we have not considered the effects of underplating in the present model. Modelling of the thermal consequences of fluid flow (Reck, 1987) indicates that the amount of fluids is insufficient to influence the overall thermal structure of the accretionary wedge. Restriction of fluid flow into narrow zones may influence temperatures and surface heat flow locally, however. Exothermic hydration reactions may retard the cooling of the upper plate shortly after the initiation of subduction (Peacock, 1987), but are unlikely to have a significant influence for a case in which there has been long-term subduction of oceanic lithosphere.

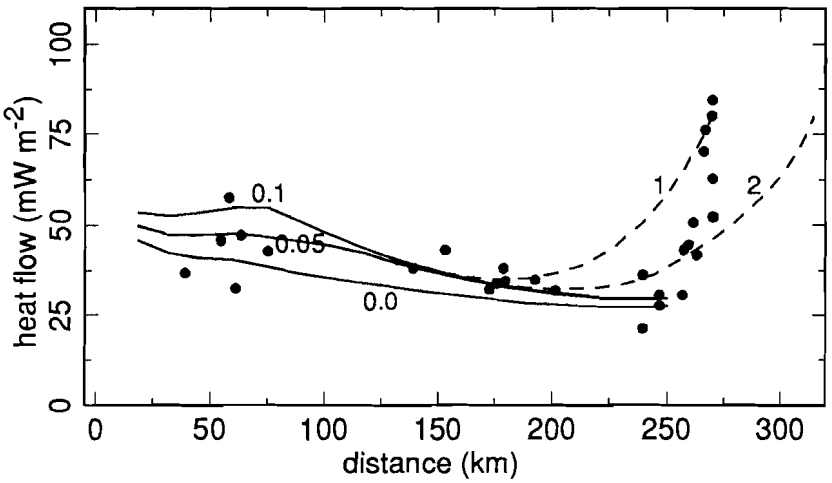

Figure 3.2. Heat flow data (from Lewis et al., 1988) at the Cascadia subduction zone, along the profile shown in Fig. 3.1b. Solid lines denote surface heat flow for models for which γ (which determines shear stresses during brittle deformation) is 0.0 (lower curve), 0.05 or 0.1 (upper curve). Dashed lines denote models with γ equal to 0.05, for which temperatures within the upper plate beneath the heat flow transition zone (curve 1) or beneath the volcanic belt (curve 2) are kept at constant values, corresponding to a continental geotherm with a surface heat flow of 80 mW m^{-2}.

Heat flow data (from Lewis et al., 1988) for a profile across the southern part of Vancouver Island are given in Figure 3.2. Going landward, heat flow decreases gradually from about 50 mW m^{-2}, near the shelf edge, to a level of about 30 mW m^{-2}. For the comparison with modelling results, we have primarily used the data at a distance of 140 - 200 km from the trench, for which the spread in the data is relatively small. A sharp

increase in heat flow occurs at a distance of about 260 - 270 km, about 30 km seaward from the volcanic belt. The sharpness of the heat flow transition indicates that the relatively high heat flow, just landward of the heat flow transition zone, is primarily related to relatively high temperatures at shallow depths only, or alternatively that relatively high temperatures at greater depths have only recently been established. Otherwise, a more gradual heat flow transition would be expected (see also below). It seems likely that the emplacement of magmas at relatively shallow depths, beneath and landward of the heat flow transition zone, has determined the shape of the heat flow transition (Lewis et al., 1988).

Thermal modelling results will only be given for the region shown in Figure 3.1a, which extends over a distance of about 220 km. The actual right boundary of the model is situated at a distance of more than 100 km landward from the heat flow transition zone. This setup has the advantage that the boundary condition at the right side of the model (where temperatures are kept constant) does not influence temperatures within the region shown in Figure 3.1a.

3.3 Results

Modelling results are shown in Figure 3.3. Shown are thermal structures for three models, with γ (which determines the amount of frictional heating during brittle deformation; see above) equal to 0.0, 0.05 and 0.1. These models will be referred to as the standard models. A value for γ of 0.0 implies that shear stresses at the plate contact are zero everywhere. Thermal structures are shown at a time 100 Myr after the onset of subduction, which ensures that the initial thermal structure is of no influence. Surface heat flow for these models is shown in Figure 3.2. Models with γ equal to 0.05 or 0.1 are in good agreement with the heat flow data. Larger values for γ would give relatively high heat flow for the region near the trench. For the model with γ equal to zero, model heat flow falls below the heat flow data at distances of 140 - 200 km from the trench.

Models without any frictional heating are only found to be in agreement with the data if the radiogenic heat production rate in the crustal part of the upper plate is increased (e.g., from 0.2 to 0.5 $\mu W\ m^{-3}$ for material at depths greater than 10 km). Such a model would exhibit a similar thermal structure as that given in Figure 3.3a, as an increase in radiogenic heat production rates primarily influences surface heat flow and has only minor influence on temperatures at depth.

Dashed lines in Figure 3.2 denote models for which temperatures within the upper plate beneath the heat flow transition zone or beneath the volcanic belt are kept at constant values, corresponding to a continental geotherm with a surface heat flow of 80 $mW\ m^{-2}$. Based on these modelling results, it can be excluded that temperatures beneath the heat flow transition zone, at greater depths, have been kept at a relatively high level for a prolonged period of time. It can not be ruled out that temperatures beneath the volcanic belt, at greater depths, have been kept at a relatively high level, e.g., as a consequence of

induced mantle flow in the asthenospheric wedge. For the region shown in Figure 3.3, the differences in temperature and surface heat flow between such a model and the standard model are very small, however.

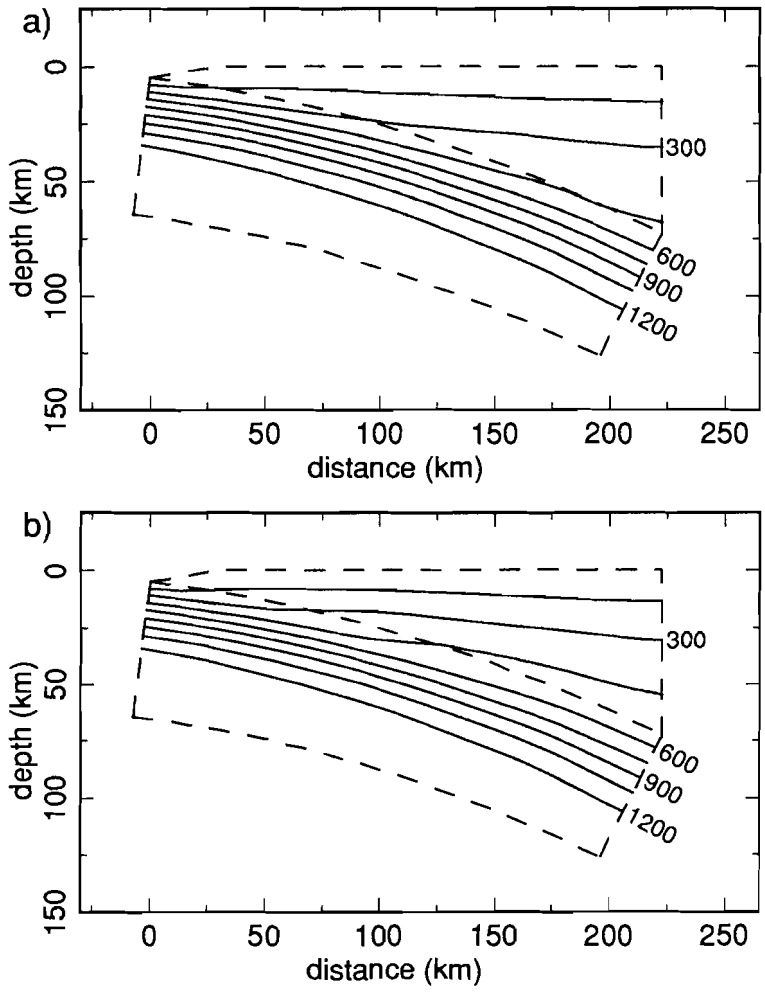

Figure 3.3. Thermal modelling results for the Cascadia subduction zone near the southern part of Vancouver Island. Age of the subducting plate is 8 Myr; convergence velocity between the two plates is 5 cm/yr. Temperature difference between adjacent isotherms is 150 °C. a) For a model with γ equal to 0.0. b) For a model with γ equal to 0.05. c) For a model with γ equal to 0.1.

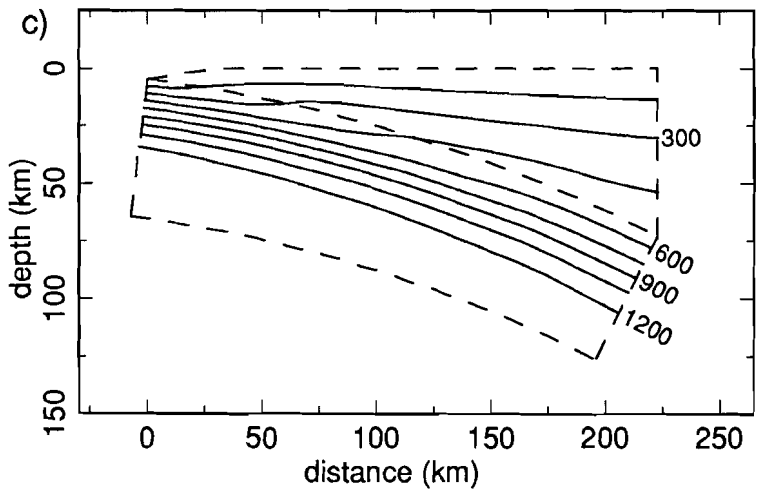

Figure 3.3 (continued).

Shear stresses at the plate contact for models with γ equal to 0.05 or 0.1 are shown in Figure 3.4a. For older oceanic lithosphere (> 30 Myr old), γ was inferred to fall within a range of 0.025 to 0.075 (van den Beukel and Wortel, 1988). If for the subduction of relatively young oceanic lithosphere, γ has similar values, significant shear stresses may exist at the plate contact, in spite of the relatively high temperatures within the subducting plate. The average shear stress at the plate contact (within the region shown in Figure 3.1a) for the model with γ equal to 0.05 is about 14 MPa, about half of the average shear stress for a similar model for which the age of the subducting plate is greater than 30 Myr.

Figures 3.4b and 3.4c show temperatures at the top of the subducting crust and surface heat flow for models with γ equal to 0.05. In addition to the standard model, results are shown for a model in which the effect of endothermic dehydration reactions is not included. For such a model, temperatures at the plate contact are less than 50 °C higher than those for the standard model. It is concluded that the low temperatures within the modelled region are primarily due to the downward movement of slab material and that the influence of dehydration reactions is much smaller. At least for the subduction of young oceanic lithosphere, the influence of dehydration reactions on subduction zone temperatures seems to be more limited than suggested by Anderson et al. (1976).

Prior to about 30 Myr ago, the convergence velocity and possibly the age of the subducting plate may have been significantly greater than the present-day values of these parameters (Engebretson et al., 1985). The lower curve in Figure 3.4c denotes the surface heat flow for a model in which, at times between 100 and 30 Myr ago, the convergence velocity has been 10 cm/yr and the age of the subducting plate has decreased gradually from 70 to 8 Myr. The maximum difference in surface heat flow between this model and the corresponding standard model is about 1.5 mW m^{-2} only.

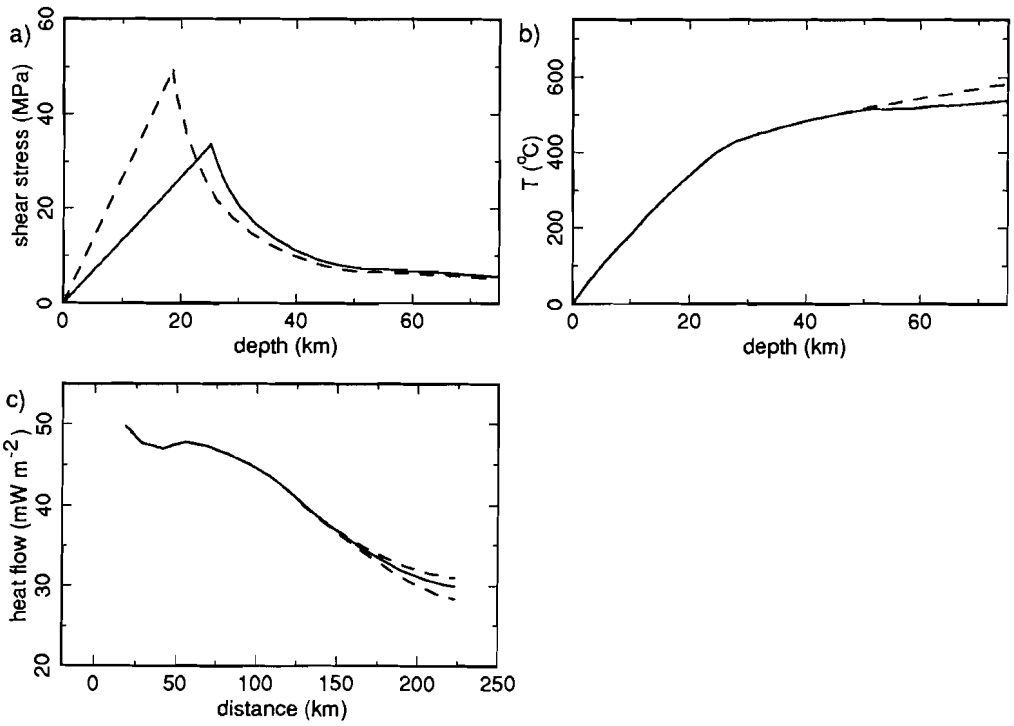

Figure 3.4. a) Shear stresses at the plate contact, as a function of depth beneath the top of the upper plate, for standard models with γ equal to 0.05 (solid line) or 0.1 (dashed line). A distance of 100 or 200 km corresponds to a depth of the plate contact of about 25 km or 62 km respectively. b) Temperatures at the plate contact, as a function of depth beneath the top of the upper plate, for the standard model (solid line; with γ equal to 0.05) and for a similar model, for which the effect of endothermic dehydration reactions within the crustal part of the downgoing plate is not included (dashed line). c) Surface heat flow for the standard model, with γ equal to 0.05 (solid line). Upper dashed line denotes a similar model, for which the effect of endothermic dehydration reactions is not included. Lower dashed line denotes surface heat flow for a model for which, between 100 and 30 Myr ago, the convergence velocity has been 10 cm/yr and the age of the subducting plate has decreased gradually from 70 to 8 Myr.

The relatively low magnitude of heat flow data (see Figure 3.2) points to relatively low temperatures within the upper plate for the Cascadia subduction zone at the southern part of Vancouver Island. Thermal modelling results were found to be in good agreement with the heat flow data. Based on our modelling results, we conclude that the low temperatures within the upper plate are primarily caused by the downward movement of the subducting plate, in spite of the prolonged subduction of very young oceanic lithosphere at the Cascadia subduction zone. Endothermic dehydration reactions within the subducting crust were found to be of lesser influence.

3.4 Discussion

We have here focused on the thermal consequences of the subduction of young oceanic lithosphere. The subduction of young oceanic lithosphere will also lead to a much reduced strength of the subducting plate. The results of mechanical modelling, which indicate that the interaction between a relatively fast spreading ridge and a subduction zone can lead to the break-up of very young oceanic lithosphere during the early phase of subduction, will be presented elsewhere (van den Beukel, 1989).

Shear stresses at the plate contact for the Cascadia subduction zone (see Figure 3.4a) are considerably lower than those inferred for the Taiwan fold-and-thrust belt (Barr and Dahlen, 1989). This is likely to be due to higher pore fluid pressures at the plate contact, leading to lower shear stresses during brittle deformation. For the subaerial Taiwan fold-and-thrust belt, pore fluid pressures are lower than those commonly observed for submarine accretionary wedges (Davis et al., 1983).

Hyndman (1988) has proposed that the top of the band of reflectors (labeled E in Figure 3.1a) coincides with a transition from high to low permeability, near the boundary between greenschist and blueschist facies metamorphic conditions at a temperature of about 400 °C. This is good agreement with the thermal models for which frictional heating is included. For these models, the top of the band of reflectors is nearly isothermal, at temperatures of about 380 °C (γ = 0.05) or 390 °C (γ = 0.1). Temperatures for the model without frictional heating are considerably lower (about 290 - 320 °C).

A study of the observed stress field near the Cascadia subduction zone, augmented by finite element modelling of stresses within the Juan de Fuca plate and the adjoining part of the North American plate indicates relatively strong coupling between the two plates, with an average shear stress at the plate contact that may range between about 5 and 25 MPa (Spence, 1989). The best agreement between model results and the observed stress field was found to occur for models in which the coupling between the two plates was not concentrated at the trench itself, but rather at a distance of about 100 km from the trench. Thermal models for which friction at the plate contact is included (given in Figure 3.3b and 3.3c) exhibit an average shear stress at the plate contact of about 14 to 18 MPa. Highest shear stresses are reached at a distance of 80 to 100 km from the trench.

Several independent lines of evidence thus indicate that these thermal models give a better approximation of the actual thermal structure of the Cascadia subduction zone, than a thermal model without any frictional heating (as given in Figure 3.3a). In any case, it is clear that, if shear stresses during brittle deformation are similar to those inferred for older oceanic lithosphere (γ between 0.025 and 0.075), subduction of very young oceanic lithosphere can still lead to significant coupling between the subducting and the overriding plate. Thus, one of the conditions for the generation of interplate thrust earthquakes, the existence of significant shear stresses at the plate contact, is likely to be fulfilled for the Cascadia subduction zone.

References

Anderson, R.N., S. Uyeda, and A. Miyashiro, Geophysical and geochemical constraints at convergent plate boundaries, Part I: Dehydration in the downgoing slab, *Geophys. J. R. Astr. Soc., 44,* 333-357, 1976.

Barr, T.D., and F.A. Dahlen, Brittle frictional mountain building 2. Thermal structure and heat budget, *J. Geophys. Res., 94,* 3923-3947, 1989.

Clowes, R.M., M.T. Brandon, A.G. Green, C.J. Yorath, A. Sutherland Brown, E.R. Kanasewich, and C. Spencer, LITHOPROBE-southern Vancouver Island: Cenozoic subduction complex imaged by deep seismic reflections, *Can. J. Earth Sci., 24,* 31-51, 1987a.

Clowes, R.M., C.J. Yorath, and R.D. Hyndman, Reflection mapping across the convergent margin of western Canada, *Geophys. J. R. Astr. Soc., 89,* 79-84, 1987b.

Crough, S.T., Thermal model of oceanic lithosphere, *Nature, 256,* 388-390, 1975.

Davis, D., J. Suppe, and F.A. Dahlen, Mechanics of fold-and-thrust belts and accretionary wedges, *J. Geophys. Res., 88,* 1153-1172, 1983.

Engebretson, D. C., A. Cox, and R. G. Gordon, Relative motions between oceanic plates of the Pacific Basin, *Geol. Soc. Am. Spec. Paper, 206,* 59 pp., 1985.

Heaton, T.H., and S.H. Hartzell, Earthquake hazards on the Cascadia subduction zone, *Science, 236,* 162-168, 1987.

Hyndman, R.D., Dipping seismic reflectors, electrically conductive zones, and trapped water in the crust over a subducting plate, *J. Geophys. Res., 93,* 13391-13405, 1988.

James, T.S., L.S. Hollister, and W.J. Morgan, Thermal modeling of the Chugach metamorphic complex, *J. Geophys. Res., 94,* 4411-4423, 1989.

Kanamori, H., and L. Astiz, The 1983 Akita-Oki earthquake (M_W = 7.8) and its implications for systematics of subduction earthquakes, *Earthq. Predict. Res., 3,* 305-317, 1985.

Koch, P.S., J.M. Christie, and R.P. George, Flow law of "wet" quartzite in the α-quartz field (abstract), *Eos Trans. AGU, 61,* 376, 1980.

Lewis, T.J., W.H. Bentkowski, E.E. Davis, R.D. Hyndman, J.G. Souther, and J.A. Wright, Subduction of the Juan de Fuca plate: Thermal consequences, *J. Geophys. Res., 93,* 15207-15225, 1988.

Peacock, S.M., Thermal effects of metamorphic fluids in subduction zones, *Geology, 15,* 1057-1060, 1987.

Pennington, W.D., The effect of oceanic crustal structure on phase changes and subduction, *Tectonophysics, 102,* 377-398, 1984.

Reck, B.H., Implications of measured thermal gradients for water movement through the northeast Japan accretionary prism, *J. Geophys. Res., 92,* 3683-3690, 1987.

Riddihough, R., Recent movements of the Juan de Fuca plate system, *J. Geophys. Res., 89,* 6980-6994, 1984.

Scholl, D.W., Sedimentary sequences in the North Pacific trenches, in *The geology of continental margins,* edited by C. A. Burk and C. L. Drake, pp. 261-283, Springer, Berlin, 1974.

Spence, W, Stress origins and earthquake potentials in Cascadia, *J. Geophys. Res., 94,* 3076-3088, 1989.

Tatsumi, Y., Migration of fluid phases and genesis of basalt magmas in subduction zones, *J. Geophys. Res., 94,* 4697-4707, 1989.

van den Beukel, J. and R. Wortel, Temperatures and shear stresses in the upper part of a subduction zone, *Geophys. Res. Lett., 14,* 1057-1060, 1987.

van den Beukel, J. and R. Wortel, Thermo-mechanical modelling of arc-trench regions, *Tectonophysics, 154,* 177-193, 1988 (Chapter 2 of this thesis).

van den Beukel, J., Break-up of young oceanic lithosphere in the upper part of a subduction zone: Implications for the emplacement of ophiolites, *Tectonics, in press,* 1989 (Chapter 4 of this thesis).

Chapter 4

Break-up of young oceanic lithosphere in the upper part of a subduction zone: implications for the emplacement of ophiolites

Abstract. It is investigated, by means of numerical modelling, whether the interaction between young oceanic lithosphere and a subduction zone can lead to the break-up of a young and thin oceanic plate. First, a thermal model of the upper part of a subduction zone (the region between the trench and the volcanic arc) is presented. Temperatures are modelled for situations in which the age of the subducting oceanic lithosphere gradually decreases, culminating in the arrival of a spreading ridge at the trench. Temperatures are used to infer the strength of material within the subducting plate from a pressure and temperature dependent rheology. Next, it is investigated by means of finite element modelling whether the forces acting upon young subducting oceanic lithosphere, recently created at a spreading centre in the vicinity of a subduction zone, can lead to its break-up. Our modelling results show that very young oceanic lithosphere may indeed break up during the early phase of its subduction. Whether break-up occurs depends upon the spreading velocity and the length of the ridge segment that interacts with the trench. If break-up occurs, some young oceanic lithosphere situated in the upper part of the subduction zone and in the region between the ridge and the trench will be detached from the other parts of the subducting plate. The detached sheet of thin oceanic lithosphere will

This chapter is to be published as:

van den Beukel, J., Break-up of young oceanic lithosphere in the upper part of a subduction zone: implications for the emplacement of ophiolites, *Tectonics, in press*, 1989.

not be subducted to mantle depths. Instead, subduction of the trailing plate, at the opposite side of the ridge, can lead to the incorporation of this sheet into the forearc region. Our modelling provides a mechanism to incorporate thin oceanic lithosphere into an arc-trench region and eventually, upon closure of the ocean basin, into an orogenic belt. It is shown that a large subset of ophiolites (those with a harzburgite-dominated mantle section) has properties in good agreement with an emplacement history in which the break-up of young oceanic lithosphere in the upper part of a subduction zone is the first phase.

4.1 Introduction

Using numerical modelling techniques we investigate whether oceanic lithosphere involved in the subduction process may break up, leading to a situation where some oceanic lithosphere remains at the surface or at relatively shallow depths. Our modelling results have implications for the emplacement of ophiolites; oceanic crust and upper mantle that has apparently escaped the usual fate of oceanic lithosphere (i.e. subduction into the mantle).

It is generally accepted that ophiolites are fragments of oceanic crust and upper mantle. Dike complexes which, in most cases, form part of the crustal section point to a spreading centre origin. Ophiolites are mostly exposed within orogenic belts (e.g., the well exposed Semail ophiolite of Oman and the Troodos ophiolite of Cyprus), in which case exposure is thought to be due to underthrusting by continental lithosphere [e.g., Moores, 1982]. In some cases, in which exposure is not related to underthrusting by continental lithosphere, ophiolites are found in (former) forearc regions, such as the Zambales ophiolite in the northern Philippines [Karig, 1982] and the Coast Range ophiolite in California [Ingersoll, 1982]. The initial tectonic setting at which ophiolites have been created is not clear. Models for the origin and emplacement of ophiolites invoke both the creation at a mid-ocean ridge [e.g., Nicolas and Le Pichon, 1980; Boudier and Coleman, 1981; Boudier et al., 1988] and creation at a spreading centre above a subducting plate, in the arc or back-arc region [e.g., Pearce et al., 1981; Harper and Wright, 1984; Thy and Moores, 1988].

In many cases it has been found that there is only a small difference in age (less than about 10 Myr) of an ophiolite itself and of the metamorphic rocks directly below an ophiolite [e.g., Lanphere, 1981; Spray, 1984]. Apparently, many ophiolites were still very young during the early phase of deformation at their base. Shearing at the base of these ophiolites thus started when they were still at a relatively small distance from the spreading centre at which they were created, and it seems likely that the relatively low strength of young oceanic lithosphere has played an important role [Vlaar and Cloetingh, 1984; Meissner and Wever, 1988]. It is not clear what mechanism and what plate tectonic setting can account for compression and shearing at the base of an ophiolite, shortly after that it has been created at an extensional spreading centre. One of the possibilities that has been considered is that the arrival of very young oceanic lithosphere (possibly a ridge crest) at a

subduction zone can lead to the break-up of a young and thin oceanic plate, followed by shearing within the plate or at its base [Christensen and Salisbury, 1975; Nicolas and Le Pichon, 1980]. It is the aim of our numerical modelling to investigate theoretically whether young oceanic lithosphere can break up just prior to or during the early phase of its subduction.

We have recently [van den Beukel and Wortel, 1987, 1988] studied the thermal structure of the upper part of a subduction zone. Heat flow data, in combination with rheological arguments and the distribution of interplate seismicity, have been used to constrain the thermal structure of this region and the magnitude of shear stresses at the plate contact between the downgoing and the upper plate. These shear stresses result in a resistive force, opposing subduction, that has the same order of magnitude as the plate driving ridge push and slab pull forces. For the subduction of oceanic lithosphere with an age greater than 30 Myr, temperatures at and above the plate contact as well as shear stresses at the plate contact were found to be essentially independent of the age of the subducting plate and the convergence velocity between the two plates. In the thermal models presented here, we focus on temperatures and shear stresses during the subduction of relatively young oceanic lithosphere. During the thermal modelling, the age of the subducting oceanic lithosphere will be decreased gradually until a spreading ridge has reached the trench. It is investigated whether, for the subduction of such young oceanic lithosphere, friction at the plate contact in the upper part of a subduction zone still leads to a substantial resistive force. At various stages during the evolution of the convergent plate margin it will then be investigated, by means of finite element modelling, whether the forces acting upon a young subducting plate can lead to the break-up of young oceanic lithosphere just prior to or during the early phase of its subduction. A pressure and temperature dependent rheology will be used to infer the strength of material within the subducting slab from the thermal models.

4.2 Thermal modelling

The geometry of the thermal model is given in Figure 4.1. The model encompasses the upper part of a subduction zone, the region between the trench and the volcanic line (arc-trench region). The volcanic line is the boundary, in the direction of the trench, of the volcanic arc. The top of the subducting plate is part of a circle, which gives a reasonable approximation of the actual geometry of a slab during the early phase of its subduction [e.g., Furlong et al., 1982]. At the right side of the model, the upper surface of the slab has reached a depth that is slightly less than 100 km. The thickness of the subducting oceanic crust is 6 km; the thickness of the crustal and sedimentary part of the upper plate is 25 km. Conduction of heat, the movement of the slab (which causes temperatures in an arc-trench region to be relatively low) and frictional heating at the plate contact (line A-B in Figure 4.1) primarily determine the thermal structure of an arc-trench region. The differential equation to be solved, the employed finite difference techniques, and values of different

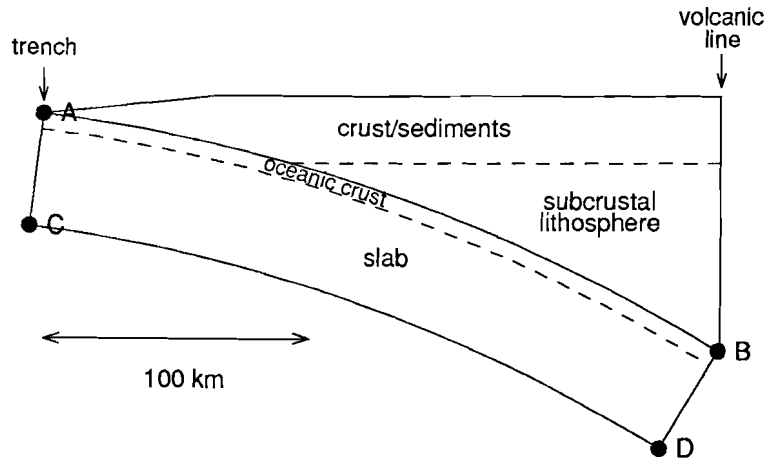

Figure 4.1. Geometry of the thermal model.

parameters (e.g., densities, thermal conductivities) are given in van den Beukel and Wortel [1987, 1988]. During thermal modelling it is assumed that the subducting plate does not break up. Velocities within the slab are taken to be constant, except for a small effect due to bending of the plate.

Temperatures at the surface are assumed to be 0 °C. Temperatures at the right side of the model (below the volcanic line), at depths less than about 85 km, are those for a geotherm with a relatively high surface heat flow of 80 mW m^{-2}, in keeping with observations that temperatures here remain relatively high as a consequence of processes below the volcanic arc and the back-arc region [see van den Beukel and Wortel, 1988]. Temperatures below the trench, at the left side of the model, are calculated using a boundary layer model for the cooling of oceanic lithosphere from Crough [1975]. Temperatures here depend upon the age of the oceanic lithosphere that arrives at the trench, which is varied during model calculations. During the subduction of gradually younger oceanic lithosphere, the age A(t) of the subducting oceanic plate as a function of time is given by:

$$A(t) = A_0 - \frac{v_c - v_{sp}}{v_{sp}} t \qquad (1)$$

where v_c is the convergence velocity between the two plates and v_{sp} the half-spreading rate for the ridge at which the subducting plate was created (both taken to be constant). A_0 is the age of the subducting plate at a moment that the reference time t is equal to zero. It has been assumed that the subduction of gradually younger oceanic lithosphere has been preceded by the subduction of oceanic lithosphere with a constant age of 70 Myr for a period of time of 30 Myr. The start of the subduction of oceanic lithosphere with a decreasing age took place at t = 0. For A_0 we have obviously adopted a value of 70 Myr.

The age of the subducting lithosphere (as a function of time), for v_{sp} equal to 5 cm/yr and v_c equal to 12 cm/yr, is given in Figure 4.2.

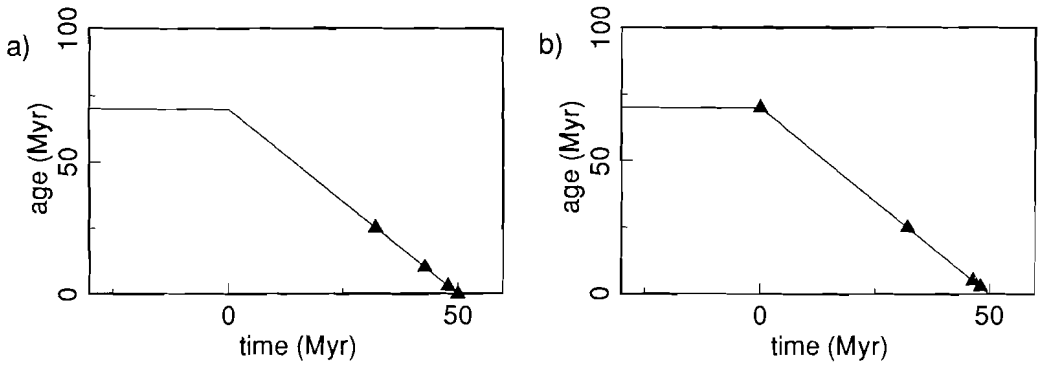

Figure 4.2. Age of the subducting oceanic lithosphere below the trench, as a function of time, for v_c equal to 12 cm/yr and v_{sp} equal to 5 cm/yr. *(a)* Symbols denote times at which thermal modelling results are given in Figure 4.3. *(b)* Symbols denote times at which mechanical modelling results are given in Figure 4.5.

Shear stresses at the plate contact determine both frictional heating and the resistive force, caused by coupling between the two plates, that must be overcome in order to continue subduction. Van den Beukel and Wortel [1987, 1988] have modelled these shear stresses with a pressure and temperature dependent rheology, using heat flow data from arc-trench regions and the distribution of thrust earthquakes at the plate contact as constraints for the magnitude of these shear stresses. In agreement with the results obtained by van den Beukel and Wortel [1987], we here adopt the following shear stresses at the plate contact:

$$\text{Brittle deformation: } \tau_{br} = 0.05\ P \tag{2}$$

$$\text{Ductile deformation: } \tau_{du} = 0.5\ (\dot{\varepsilon}/A)^{1/n} \exp(E/nRT) \tag{3}$$

For brittle deformation, at relatively small depths and low temperatures, shear stresses depend linearly on the lithostatic pressure P. The lithostatic pressure P has been calculated assuming a density of 2700 kg m^{-3} for crustal and sedimentary material and a density of 3300 kg m^{-3} for mantle material. The relatively low shear stresses during brittle deformation are likely to be caused by high pore fluid pressures and a low coefficient of friction, related to the subduction of sediments and fluids [Davis et al., 1983; Shi and Wang, 1988]. For ductile deformation, values for the material constants A and n, and the activation energy E are those for a steady state flow law for a quartzite under wet conditions [from Koch et al., 1980]. R is the universal gas constant and T the temperature (in K). Models for ductile deformation at subduction shear zones exhibit a typical strain

rate of about 10^{-12} s^{-1} [Yuen et al., 1978]. Here, the strain rate $\dot{\varepsilon}$ depends linearly on v_c, and is taken to be (v_c/8) x 10^{-12} s^{-1} (v_c in cm/yr). For the subduction of oceanic lithosphere older than 30 Myr, the adopted rheology gives an average shear stress at the plate contact, within the modelled region, of 20 - 25 MPa [van den Beukel and Wortel, 1988]. This is in good agreement with values of approximately 20 MPa, inferred by Bird [1978] by means of a force balance, for the average shear stress at the plate contact in the upper part of the Tonga and Mariana subduction zones. A similar value of about 20 - 30 MPa has been obtained by Sleep [1979] for the Aleutian subduction zone. The adopted shear stresses result in a limited amount of frictional heating, which causes pressure-temperature conditions at the plate contact in thermal models to be in good agreement with pressure-temperature conditions inferred for material in high-pressure metamorphic belts [van den Beukel and Wortel, 1988].

The strength of material within the subducting plate has been modelled with pressure and temperature dependent rheologies which incorporate both pressure-dependent brittle deformation and temperature-dependent ductile deformation. Differential stresses that cause normal faulting have been inferred from (see Sibson [1974]):

$$(\sigma_1 - \sigma_3) = \frac{R' - 1}{R'} (1-\lambda) P \tag{4}$$

with

$$R' = ((1 + \mu^2)^{1/2} - \mu)^{-2} \tag{5}$$

σ_1 and σ_3 are maximum and minimum principal stresses and λ is the pore fluid factor. A value of 0.75 has been adopted for the coefficient of friction μ [Byerlee, 1978]. For ductile deformation, the strength of material is inferred from steady state power-law creep flow laws, which have the form:

$$(\sigma_1 - \sigma_3) = (\dot{\varepsilon}/A)^{1/n} \exp(E/nRT) \tag{6}$$

We have used both a relatively weak and a relatively strong rheology for the strength of material within the subducting plate. A low estimate for the strength of material has been obtained using a value of 1/3 for the pore fluid factor λ, which implies near-hydrostatic pore fluid pressures, and by inferring the strength for ductile deformation of mantle material from a flow law for olivine under wet conditions (Aheim dunite; from Chopra and Paterson [1981]), and the strength for ductile deformation of material within the oceanic crust from a flow law for a diorite under wet conditions [from Hansen and Carter, 1982]. A high estimate for the strength of material has been obtained using a value of zero for λ and by inferring the strength for ductile deformation of mantle material from a power-law creep flow law for olivine under dry conditions (for differential stresses less than 200 MPa) or from a Dorn-creep flow law (for differential stresses greater than 200 MPa). Parameters of these two flow laws, as well as the constitutive equation for Dorn-creep, are given by Goetze and Evans [1979]. The strength for ductile deformation of crustal material is inferred from a flow law for diabase under dry conditions [from Caristan, 1982]. The strain

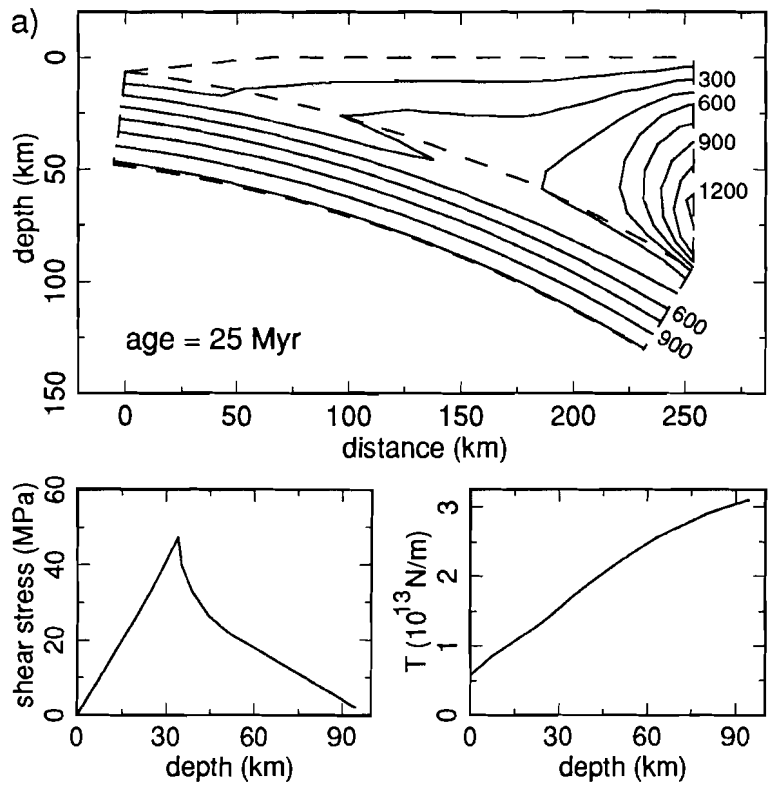

Figure 4.3. Temperatures (in °C) within the upper part of a subduction zone during the subduction of gradually younger oceanic lithosphere: *(a)* at a moment when the age of the subducting plate below the trench is 25 Myr; *(b)* when the age of the subducting plate is 10 Myr; *(c)* when the age of the subducting plate is 3 Myr; *(d)* when the ridge has reached the trench. Insets in the lower left show shear stresses at the plate contact (line AB in Figure 4.1) as a function of depth below the surface. Insets in the lower right show the strength T of the subducting slab for extensional deformation, per unit length of trench, as a function of the depth to which the upper surface of the slab has been subducted.

rate for material within the subducting plate is taken to be 10 % of the strain rate for material at the plate contact.

Results of our modelling of the thermal evolution of an arc-trench region during the subduction of gradually younger oceanic lithosphere are given in Figure 4.3. Results are shown for a model with a convergence velocity between the two plates of 12 cm/yr and a half-spreading rate for the approaching ridge of 5 cm/yr. For these velocities it takes 50 Myr for the age of the subducting plate to decrease from its initial value of 70 Myr to 0 Myr (see also Figure 4.2). Thermal structures are shown at times when the age of the subducting oceanic lithosphere at the trench is 25, 10, 3 and 0 Myr. Shortly before the arrival of the ridge at the subduction zone, temperatures within the upper plate increase

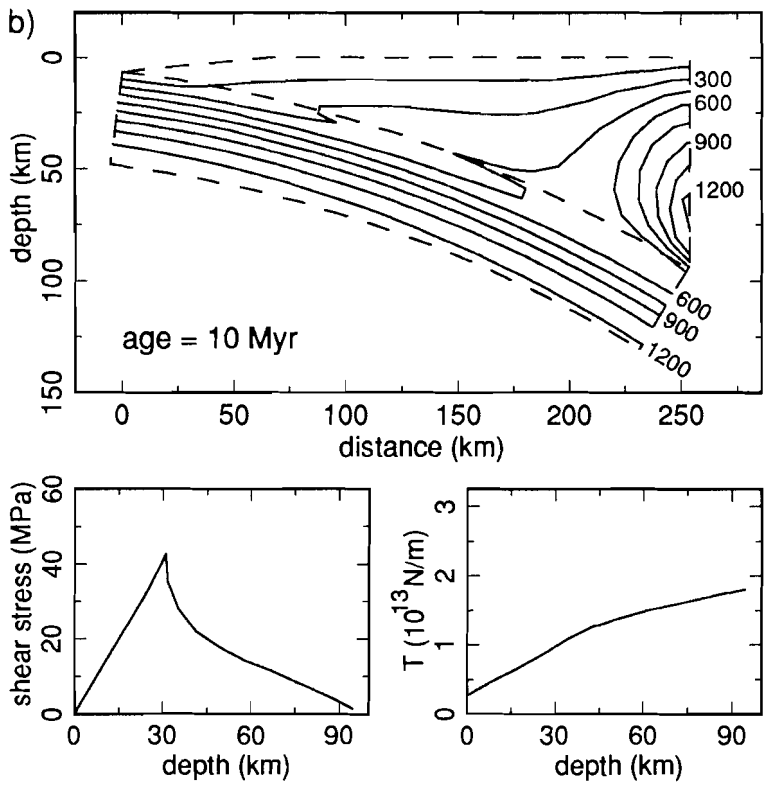

Figure 4.3 (continued).

significantly, especially in the region near the trench.

Insets in the lower left of Figures 4.3a - 4.3d give shear stresses at the plate contact, as a function of depth below the surface. Going along the plate contact from point A to B (see Figure 4.1), shear stresses at the plate contact first increase with depth. For this part of the plate contact, temperatures are less than about 400 °C and deformation is brittle (shear stresses given by equation (2)). At the deeper part of the plate contact, shear stresses decrease with depth, as increasing temperatures lead to decreasing strengths for ductile deformation. At this part of the plate contact, temperatures are greater than about 400 °C and deformation is ductile (shear stresses determined by equation (3)). During the subduction of gradually younger oceanic lithosphere, the increasing temperatures at the plate contact lead to decreasing shear stresses; especially at the deeper parts of the plate contact where ductile deformation prevails.

Insets in the lower right of Figures 4.3a - 4.3d give the strength of the subducting plate for extensional deformation, as a function of the depth below the surface to which the top of the plate has been subducted. The strength of the plate has been obtained by integrating

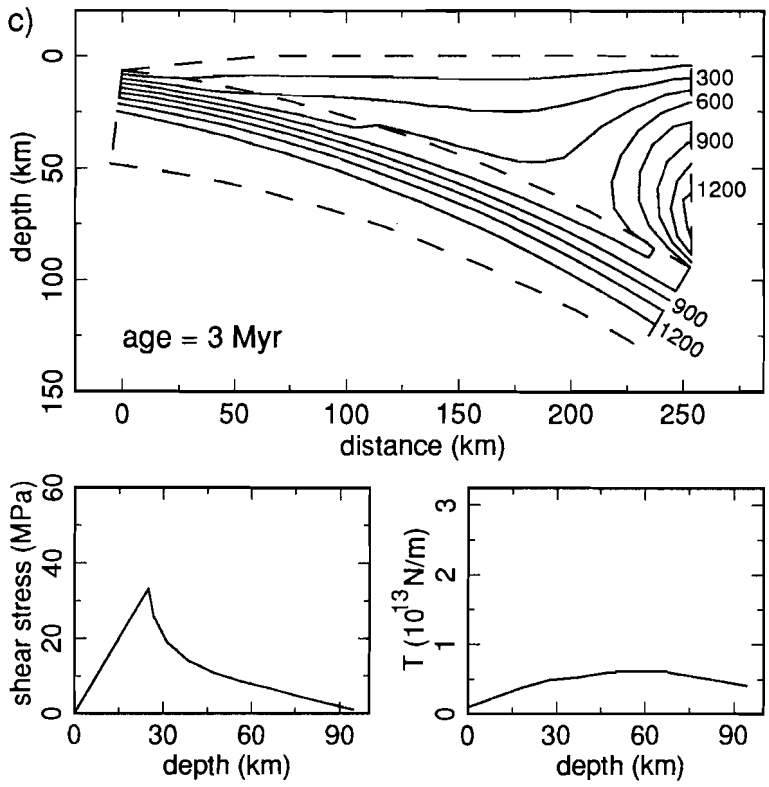

Figure 4.3 (continued).

yield strengths, inferred from equations (4) and (6), over a profile through the slab (e.g., lines A - C and B - D in Figure 4.1). The strength of the slab generally increases with the depth to which its upper surface has been subducted (e.g., from about 0.6 x 10^{13} N/m below the trench to about 3 x 10^{13} N/m at the right side of the model in Figure 4.3a). This is caused by the increasing pressure, leading to greater strengths for brittle deformation, and the relatively small rise of temperatures within the slab during subduction to depths less than about 100 km.

At this stage of our modelling, an important observation can already be made. As can be seen in the insets in Figure 4.3, shear stresses at the plate contact (and thus the resistive force caused by friction at the plate contact) decrease much more slowly during the subduction of gradually younger oceanic lithosphere than the strength of the subducting plate. At the moment that the ridge arrives at the trench, the average shear stress at the plate contact is still about 35 % of the average shear stress in Figure 4.3a, where the subducting plate is still 25 Myr old. The average strength of the subducting plate in the modelled region is, at the time that the ridge reaches the trench, only about 3 % of the average

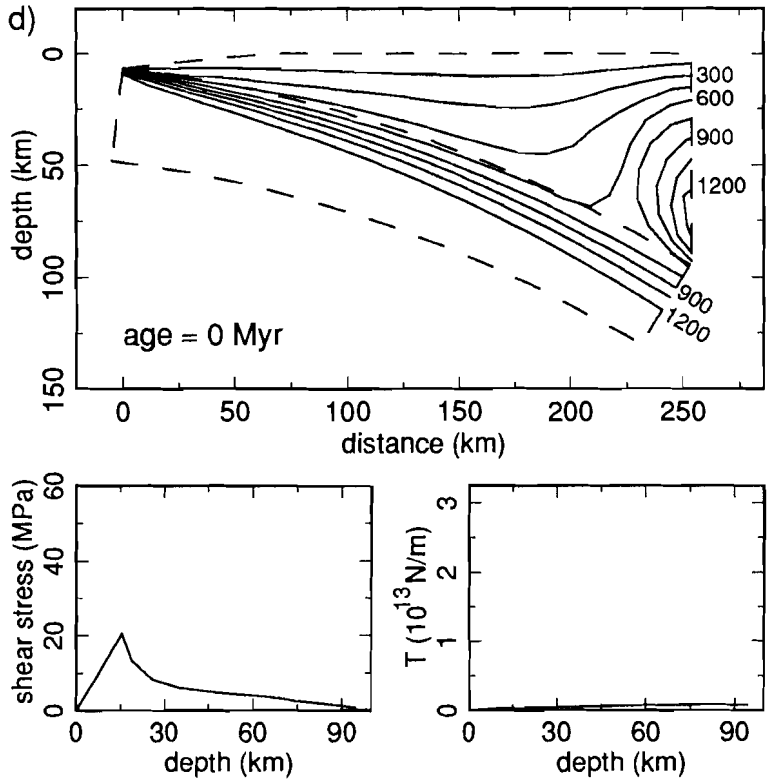

Figure 4.3 (continued).

strength in Figure 4.3a. The relatively slow decrease of resistive forces caused by friction in the upper part of the subduction zone and the relatively fast decrease of the strength of the subducting plate, during the subduction of gradually younger oceanic lithosphere, suggests that break-up of oceanic lithosphere in the upper part of a subduction zone will become more likely if the age of the subducting plate becomes smaller.

4.3 Finite element modelling

4.3.1 Model description

During the thermal modelling it has been assumed that a subducting young oceanic plate does not break up during the early phase of its subduction. We will now investigate, by means of finite element modelling, whether this is indeed the case. We model deformation and stresses for the subducting slab within the arc-trench region (the region

encompassed by the thermal model) as well as for the oceanic plate between the ridge and the trench. If the ridge is at a distance greater than 400 km from the trench, only that part of the oceanic plate at a distance less than 400 km from the trench has been included in the finite element models.

The geometry of a finite element model is shown in Figure 4.4. Point E represents the position of the trench in the thermal models. Calculations have been made at different stages of the evolution of the convergent plate margin. The different finite element models consist of about 200 - 300 elements. Element strengths are inferred from pressure and temperature dependent rheologies. Calculations have been made both for a relatively weak and a relatively strong rheology (see above). The brittle strength for material in compression is probably greater than the brittle strength for material in extension. Because plate bending generally does not imply compression in the upper part of the plate (that part where temperatures are relatively low and where failure will mostly be related to brittle deformation), the differential brittle strength for material in compression could be taken to be equal to that in tension (given by equation (4)), without significantly affecting the results. Temperatures are inferred from our thermal models or, for the part of the plate that has not yet reached the trench, are calculated using the model for the thermal evolution of oceanic lithosphere from Crough [1975]. For those regions where the pressure and temperature dependent strength is not reached, material behaves elastically. We have adopted a Young's modulus of 7 x 10^{10} N m^{-2} and a Poisson's ratio of 0.25. Following Bodine et al. [1981], we define a strength level (in this case 30 MPa) which determines the location of the base of the mechanically strong part of the subducting oceanic lithosphere. Except for the area near the ridge, the base of the finite element models is situated at the depth where the strength falls below 30 MPa.

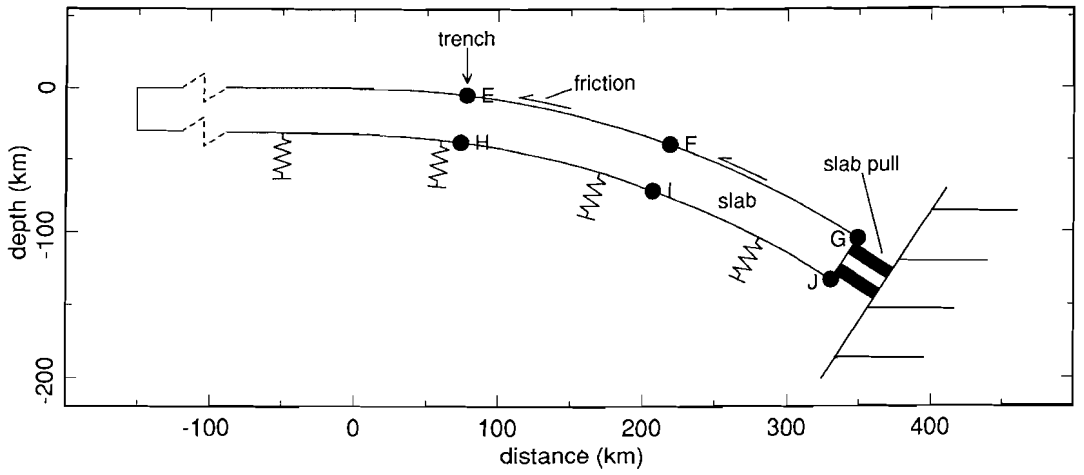

Figure 4.4. Geometry of a finite element model.

Finite element calculations have been carried out with a modified version of the NONSAP program for nonlinear finite element analysis [Bathe et al., 1974]. An extensive description of the finite element method can be found in Zienkiewicz [1977]. As constant strain elements are not well suited for an analysis of a bending plate, we have used linear strain (eight-node) elements (see also Cloetingh [1982]).

Isostasy has been incorporated by the implementation of springs at the base of the model, resulting in an elastic foundation with a stiffness equal to $(\rho_m - \rho_w)g$, where g is the acceleration due to gravity and $(\rho_m - \rho_w)$ is the density difference between the mantle and the medium overlying the subducting and upper plate (taken to be water with density ρ_w equal to 1000 kg/m^3). Initially, for a situation in which the oceanic plate is horizontal, with its upper surface at z = 0 km (for distance x less than 0 km; see Figure 4.4) or where it has a constant radius of curvature equal to that in the thermal model (for x > 0 km), the hydrostatic restoring forces exerted by the springs at the base of the model are taken to be zero. It is noted that this leads to a relatively simple geometry of the subducting plate, as the radius of curvature will approximately be constant throughout the upper part of the subduction zone. The actual geometry may be more complicated; in particular for the region near the trench.

Forces at the plate contact, opposing subduction, are due to friction and are determined by the magnitude of shear stresses at the plate contact in the thermal models. The total resistive force due to friction can be obtained by integrating shear stresses over the total length of the plate contact and ranges from about 2 x 10^{12} N (at the moment that the ridge arrives at the trench; see Figure 4.3d) to about 6 x 10^{12} N (for the subduction of oceanic lithosphere with an age of 70 Myr) per unit length of trench.

The relatively low density of the basaltic crust (prior to the basalt-eclogite phase change) and of the underlying depleted mantle material will also lead to a resistive force, opposing subduction. Upwards directed buoyancy forces acting upon subducting material within the downgoing slab have been taken to depend linearly upon $\Delta\rho$, the difference in density between material within the slab and material, situated at the same depth z, at x = 0:

$$\Delta\rho = \rho(0,z) - \rho(x,z) \qquad (7)$$

A value of 450 kg/m^3 has been adopted for the difference in density (due to the difference in composition) between undepleted mantle material and basaltic crust; a value of 60 kg/m^3 for the difference in density between undepleted and depleted mantle material, and a value of -200 kg/m^3 for the difference in density between undepleted mantle material and eclogite [Oxburgh and Parmentier, 1977]. The basalt-eclogite phase change probably takes place at a depth between about 40 and 80 km [Ahrens and Schubert, 1975]. We have assumed a gradual transition from basalt to eclogite between 40 and 60 km depth. The thickness of the crust is taken to be 6 km; the thickness of the layer of depleted mantle material immediately below it is taken to be 20 km. For mantle material, a thermal component of buoyancy forces has been included, which is determined by a density

difference;

$$\Delta\rho_{th} = \rho_m \alpha (T(x,z) - T(0,z)) \quad (8)$$

adopting a value for the thermal expansion coefficient α of 4×10^{-5} °C^{-1}.

As we focus here on the subduction of very young oceanic lithosphere, the neglect of ridge push forces does not significantly influence the modelling results. Slab pull forces have been incorporated in the model, however, and act upon the right boundary of the model (line G - J in Figure 4.4). Slab pull forces need not to be specified explicitly. We do not permit any deformations at the right side of the model. As a result a force will be exerted upon the subducting plate at the right boundary of the model. For the first set of finite element models (set A), the magnitude of this force will be approximately equal to the sum of the resistive forces caused by friction at the plate contact and the components in the direction parallel to the slab of the buoyancy forces within the modelled region. This implies that resistive forces in the models are overcome by slab pull forces (due to density differences between the slab and the surrounding mantle at depths greater than about 100 km) in the same section of the subduction zone. As slab pull forces are expected to be relatively small for the subduction of young oceanic lithosphere (England and Wortel, 1980; Wortel, 1984), we have also considered a second set of models (set B) for which resistive forces are only in part overcome by slab pull forces, and in part by a compressive force (applied upon the left boundary of the model), or by distributed body forces.

4.3.2 Modelling results: set A

Set A represents finite element models in which resistive forces are overcome by slab pull forces, exerted upon the right boundary of the model, only. Modelling results, at times when the age of the subducting plate at the trench in the thermal models (point E in Figure 4.4) is 70, 25, 5 and 2.8 Myr are given in Figure 4.5. These models correspond to the overall thermal evolution for which the results of thermal modelling are given in Figure 4.3; the convergence velocity between the two plates is thus 12 cm/yr and the half-spreading rate of the approaching ridge at which the subducting plate was created is 5 cm/yr. Strengths have been inferred from thermal models, using the relatively weak rheology. The lower halves of Figure 4.5a - 4.5d give the stresses within the subducting plate. Straight lines with arrows denote tension; straight lines without arrows denote compression. Stresses are only given for a subset of elements. Black areas in the upper halves of Figure 4.5a - 4.5d denote material for which the yield strength has been reached; white areas denote the part of the plate that behaves elastically.

For the model given in Figure 4.5a, for which the age of the oceanic plate below the trench is still 70 Myr, bending of the plate primarily determines the stress field. Extension prevails in the upper half of the slab; compression in the lower half. Brittle failure within the upper part of the plate will lead to the formation of horsts and grabens near its upper surface [Wortel and Cloetingh, 1985]. Apart from bending, the strength of material also

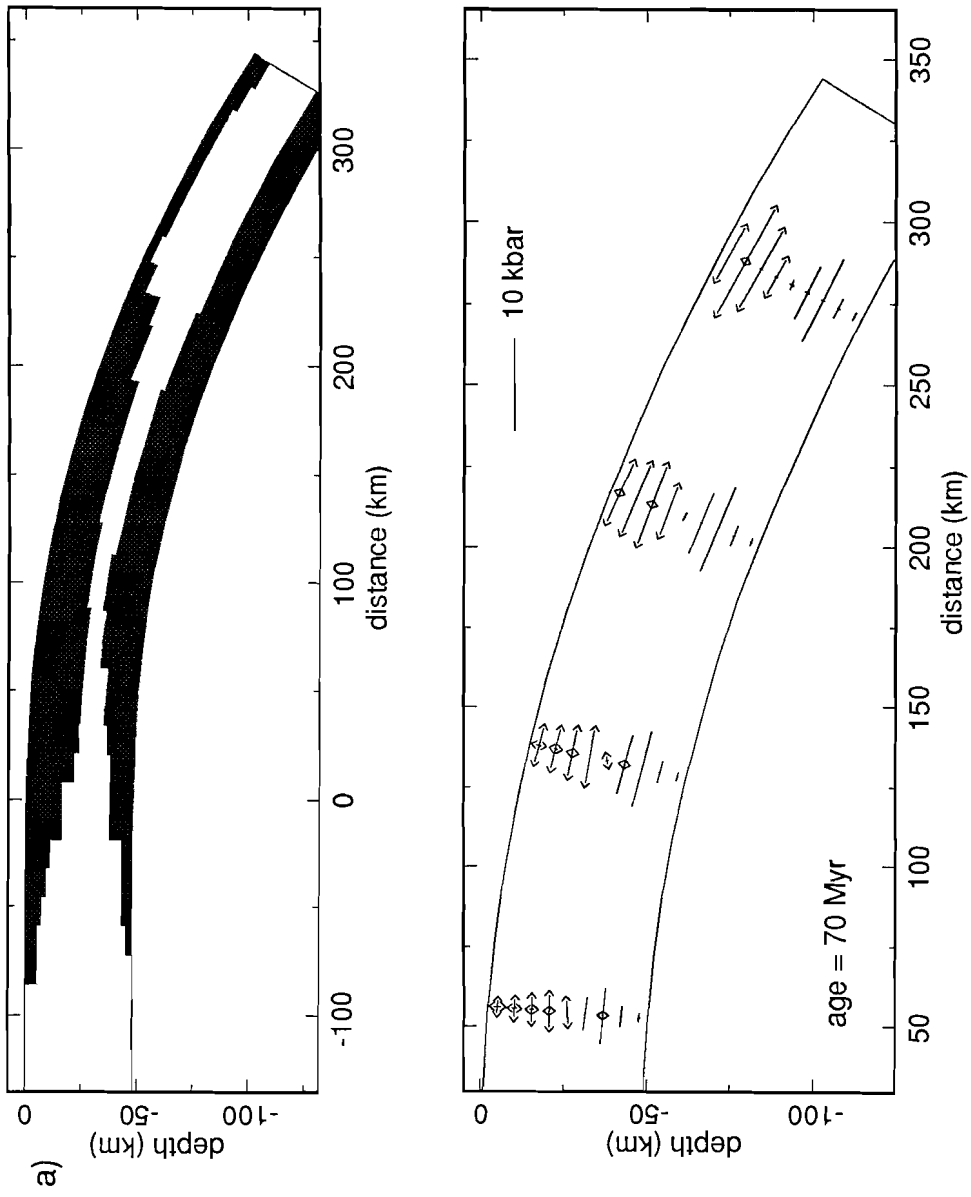

Figure 4.5. Results of finite element modelling for a model with a relatively low strength for material within the subducting plate and with a half-spreading rate v_{sp} equal to 5 cm/yr (v_c = 12 cm/yr). *(a)* At a moment when the age of the subducting plate below the trench is 70 Myr; *(b)* when the age of the subducting plate is 25 Myr; *(c)* when the age of the subducting plate is 5 Myr; *(d)* when the age of the subducting plate is 2.8 Myr (situation shortly after break-up of the slab near the right side of the model). Lower half of figures gives stresses within the subducting plate. Straight lines without arrows denote compression; straight lines with arrows denote tension. Upper half of figures gives areas in failure within the subducting plate. Black areas denote zones for which the strength of material has been reached and that are in failure. White areas within the subducting plate denote material that behaves elastically.

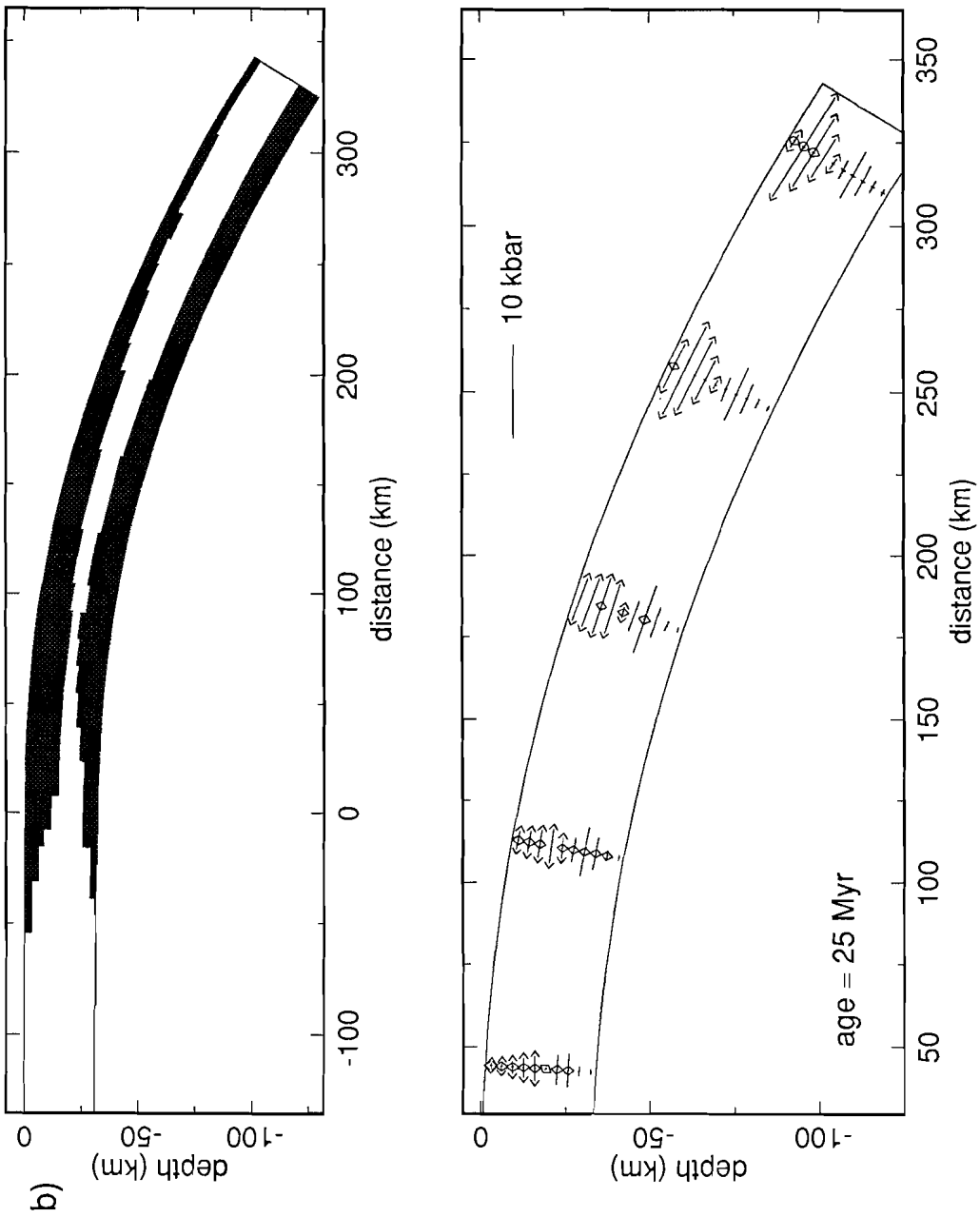

Figure 4.5 (continued).

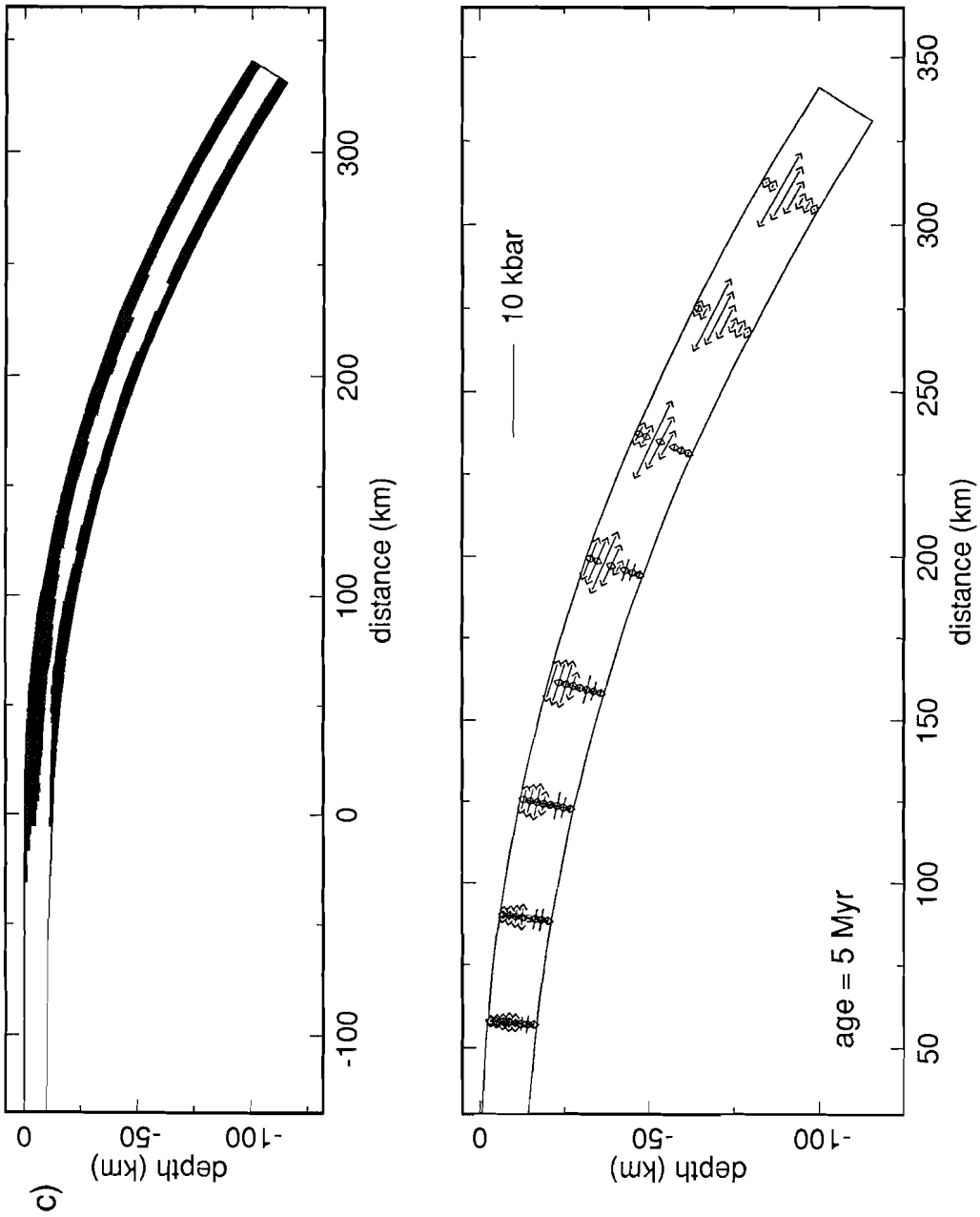

Figure 4.5 (continued).

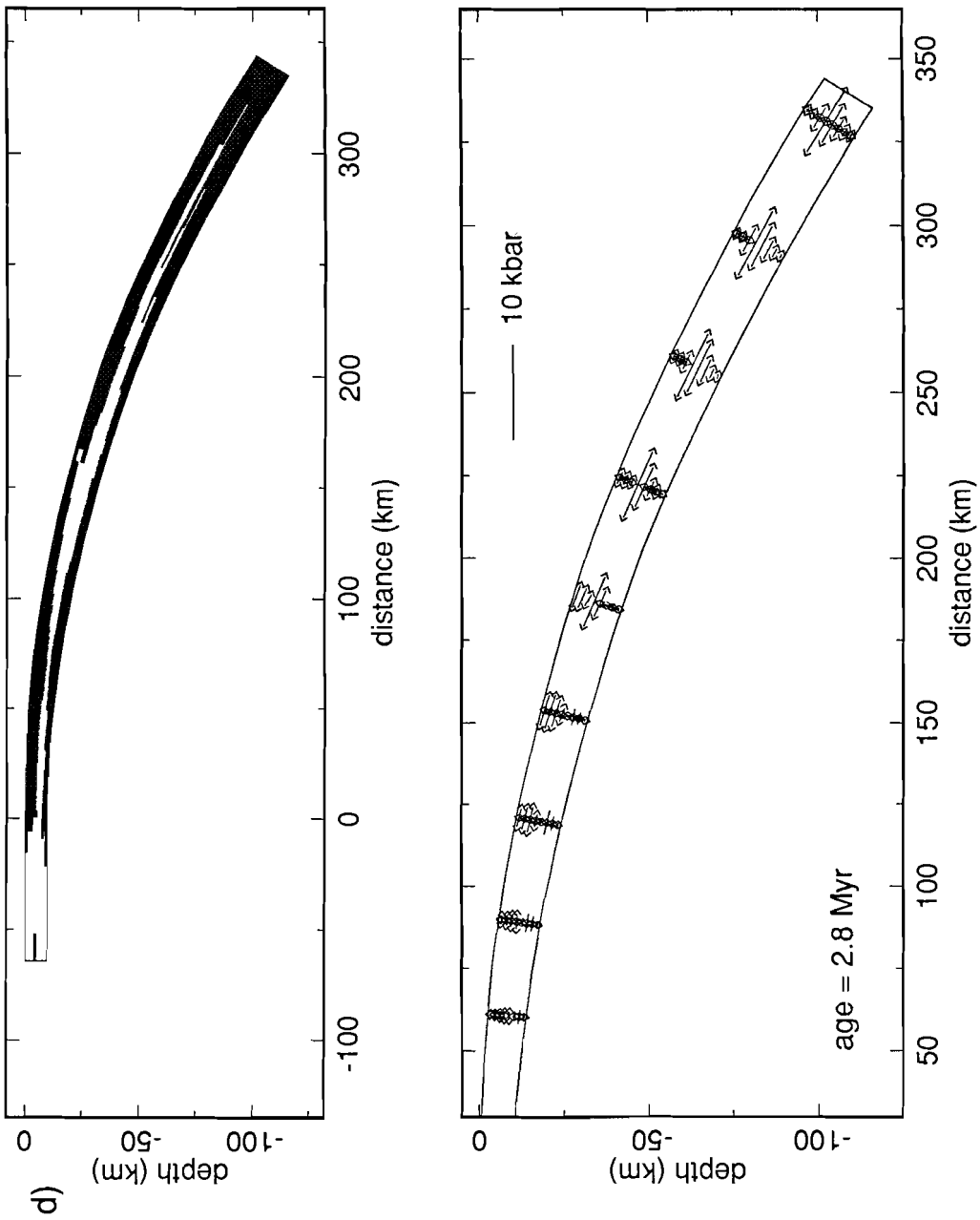

Figure 4.5 (continued).

influences the stress field given in Figures 4.5a. The low stresses near the base of the plate are due to the low strength of material here, caused by relatively high temperatures that lead to relatively low-strength ductile deformation. This also applies to the relatively low stresses within the crust of the slab, in the region where it has been subducted to depths greater than about 75 km. The largest stresses are reached for the mantle part of the slab that has been subducted to the greatest depths. This is caused by the increase of the strength for brittle deformation with pressure.

At a moment that the age of the subducting plate below the trench is 25 Myr (Figure 4.5b), the situation is still very similar to that given in Figure 4.5a. In both cases, it is expected that all of the lithospheric material that arrives at the trench will be subducted into the mantle.

During the gradual decrease of the age of the subducting plate, the magnitudes of the bending stresses tend to become smaller as the thickness of the subducting slab decreases. For models in which the age of the plate below the trench has become very small (Figures 4.5c and 4.5d), most material within the part of the plate for which the upper surface has been subducted to a depth greater than about 50 km is in extension. Extension in the deeper parts of the slab, during the subduction of very young oceanic lithosphere, is caused by the combination of resistive forces, which act primarily on slab material at depths less than about 50 km, and slab pull forces exerted upon the right boundary of the model. Extension in the deeper parts of the slab in the model is superimposed on the bending stresses. At a time that the subducting plate is 5 Myr old, about half of the material near the right side of the model is in extensional failure (see Figure 4.5c). Eventually, extensional failure throughout the subducting plate, near the right side of the model, occurs at a time when the oceanic plate at the trench is about 2.8 Myr old. At this time, a large slab of thin oceanic lithosphere, with a length of about 400 km, will be detached from the deeper parts of the subducting oceanic plate. Whereas the deeper parts can continue to subduct, the detached thin sheet of oceanic lithosphere at the surface or in the upper part of the subduction zone will remain at its present position. If detachment is followed by subduction of the trailing plate (at the opposite side of the ridge) the new plate contact will initially be situated at the base of the detached sheet, probably near the lithosphere-asthenosphere boundary, and the detached slab will be transferred to the upper plate. The geometry of the thin oceanic lithosphere, detached from the deeper parts of the slab, is given in Figure 4.6a. The base of the detached sheet has been taken to coincide with the 1200 °C isotherm, near the lithosphere-asthenosphere boundary. The use of a somewhat higher or lower isotherm, also close to mantle temperatures, would give only slightly different geometries.

At the time of break-up, resistive forces are primarily due to friction at the plate contact. The sum of the components, in the direction parallel to the slab, of buoyancy forces (due to both the thermal and the compositional structure of the slab) is about 10 % of the total resistive force due to friction. This fraction can be somewhat greater if the basalt-eclogite phase change takes place at a greater depth. If the phase change occurs gradually between 60 and 80 km depth, break-up takes place at a moment that the age of the subducting plate at the trench is about 3.2 Myr; at a time that the sum of the components of

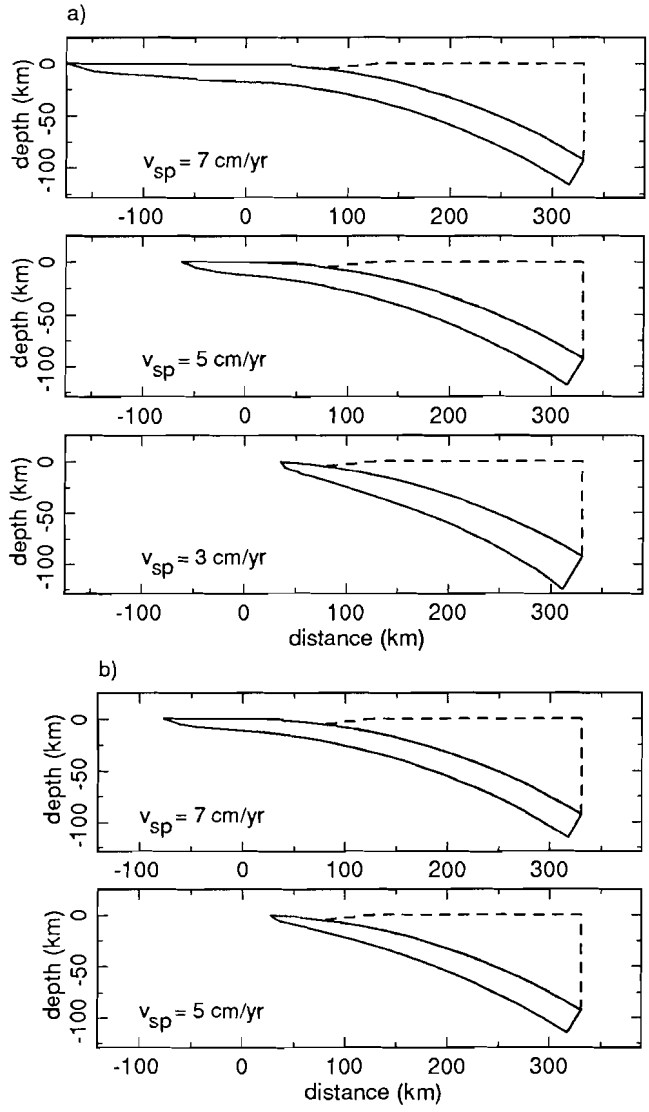

Figure 4.6. The geometry of the detached sheet. Dashed lines denote the geometry of the upper plate in the thermal model. The base of the detached sheet is taken to coincide with the 1200 °C isotherm in the thermal models. *(a)* for models with a relatively low strength for material within the subducting plate (defined in the section on thermal modelling), with a half-spreading rate v_{sp} equal to 3 cm/yr (v_c = 8 cm/yr), v_{sp} = 5 cm/yr (v_c = 12 cm/yr), and v_{sp} = 7 cm/yr (v_c = 14 cm/yr). The age of the subducting plate, at a time that break-up has just occurred, is 1.4 Myr (v_{sp} = 3 cm/yr), 2.8 Myr (v_{sp} = 5 cm/yr) or 3.6 Myr (v_{sp} = 7 cm/yr). For an alternative condition for detachment (see below), these ages are 1.4, 2.6 and 3.6 Myr respectively. *(b)* for models with a relatively high strength for material within the subducting plate (defined in the section on thermal modelling), with a half-spreading rate v_{sp} equal to 5 cm/yr (v_c = 12 cm/yr), and v_{sp} = 7 cm/yr (v_c = 14 cm/yr). The age of the subducting plate, at a time that break-up has just occurred, is 1.0 Myr (v_{sp} = 5 cm/yr) or 2.8 Myr (v_{sp} = 7 cm/yr). For the alternative condition for detachment (see below), break-up was found to have just occurred for the same ages of the subducting plate.

buoyancy forces parallel to the slab is about 30 % of the total resistive force due to friction.

Results of other thermal and mechanical calculations, for different half-spreading rates of the ridge that approaches the trench, are also shown in Figure 4.6a. No detachment was found to occur for models in which the ridge has a half-spreading rate of 1 cm/yr or 2 cm/yr. For the other models, the length of the detached sheet increases rapidly as the the half-spreading rate increases. For a model with a large half-spreading rate, the amount of low-strength very young oceanic lithosphere, that is situated in the upper part of a subduction zone and the region near the trench, can be much greater, and break-up takes place at an earlier time, when the ridge is still at a greater distance from the trench. This distance amounts to as much as about 250 km for a model with a half-spreading rate of 7 cm/yr. Other calculations (not shown) indicate that the geometry of the detached sheet and the time of break-up are primarily determined by the half-spreading rate of the ridge; the convergence rate between the two plates being of less importance.

It is clear, that in reality the convergence velocity and the half-spreading rate may vary as a function of time. The age of the subducting plate as a function of time is likely to exhibit a more complicated pattern than that shown in Figure 4.2. It is expected that the time of break-up will primarily be determined by the half-spreading rate during and just prior to the subduction of very young oceanic lithosphere. The half-spreading rate during earlier stages of the subduction process is likely to be of only minor influence.

Results of finite element models with a relatively strong rheology (as defined in the section on thermal modelling) for material within the subducting plate are shown in Figure 4.6b. For these models, detachment was found to occur at a later time (v_{sp} equal to 5 or 7 cm/yr), or no break-up was found to occur, prior to the arrival of the ridge at the trench (v_{sp} = 3 cm/yr). Subsequent finite element models use the relatively weak rheology for material within the subducting plate.

For all models, for which results are given in Figure 4.6, break-up takes place at the right boundary of the model. This is caused by the small decrease in the strength of the subducting plate near the right boundary, related to limited heating of the slab in this region (see Figure 4.3c). If no such heating of the slab would occur, break-up would take place shortly afterwards, at a place where the slab has been subducted to a somewhat smaller depth. The temperature gradient, just above the slab at the right boundary of the thermal model (below the volcanic line), is of similar magnitude, however, as temperature gradients here, in thermal models of subduction zones that include mantle flow in the region above the slab, below the volcanic zone and the back-arc region (e.g., Hsui et al., 1983).

4.3.3 Modelling results: set B

In the finite element models, of which the results are shown above (set A), it is assumed that resistive forces are overcome by slab pull forces exerted by earlier subducted oceanic lithosphere in the same section of the subduction zone. Although slab pull forces are indeed likely to be the main forces driving plate motion [e.g., Forsyth and Uyeda,

1975], this does not mean that for a given section of a subduction zone, resistive forces are overcome by slab pull forces, exerted by lithosphere subducted into the mantle in the same section of the subduction zone. Especially, subduction of young oceanic lithosphere (leading to relatively small slab pull forces) is likely to be due in part to slab pull forces exerted by oceanic lithosphere, that was of greater age when it reached the trench, in adjacent parts of the subduction zone [e.g., Wortel, 1984]. A rigorous analysis of the influence of forces, exerted by slab segments in adjacent parts of the subduction zone, requires three-dimensional finite element modelling. With the present two-dimensional finite element models, an estimate of the possible influence of these forces has been made by considering an additional set of finite element models (set B). For these models, resistive forces caused by friction at the plate contact and by buoyancy are only in part overcome by slab pull forces exerted upon the right boundary of the finite element models, and partly by distributed body forces or by a force exerted upon the left boundary of the model.

Figure 4.7a shows modelling results for a situation in which a compressive force is exerted upon the left boundary of the model. The magnitude of this force is equal to 33 % of the total resistive force (the sum of resistive forces due to friction and the components of buoyancy forces parallel to the slab) exerted upon the subducting plate. Other model parameters are equal to those of the model for which results are shown in Figure 4.5b. The force exerted upon the left boundary leads to compression within the oceanic plate and to a thin band of material in failure near the relatively weak upper boundary of the plate, prior to its subduction. It also leads to a small upwards shift of the part of the downbending plate that behaves elastically and to a decrease of the extensional stresses near the right boundary of the model, making break-up less likely.

No significant compressive forces can be exerted upon the left boundary of the model if the spreading ridge is situated at this boundary. Calculations have also been made for two additional sets of models, in which 33 or 67 % of the resistive forces are overcome by distributed body forces, exerted in the direction parallel to the slab. We have, somewhat arbitrary, assumed that these plate driving body forces have a magnitude that depends linearly on the strength of the element on which the force is exerted; the sum of the body forces being equal to 33 or 67 % of the sum of the resistive forces. Figures 4.7b and 4.7c show results of some of these calculations, for models for which 33 % of the total resistive force is overcome by distributed body forces, and for which other model parameters are the same as for the initial set of models (results shown in Figure 4.5). Break-up near the right boundary of the model here occurs when the age of the subducting slab, just prior to subduction, is about 1.8 Myr. Break-up for the initial set of models occurred for an age of about 2.8 Myr. The geometry of the detached sheet, at the time of break-up, is given in Figure 4.8b. Results of similar models, with a higher or lower half-spreading rate and convergence velocity, are also given in Figure 4.8. These results indicate that forces, exerted by slab segments in adjacent parts of the subduction zone, will cause break-up to occur at a later time and will lead to a significantly smaller length of the detached sheets. The geometry of the detached sheets, as given in Figure 4.6 (modelling results for set A), should be seen as giving an upper bound for their actual dimensions.

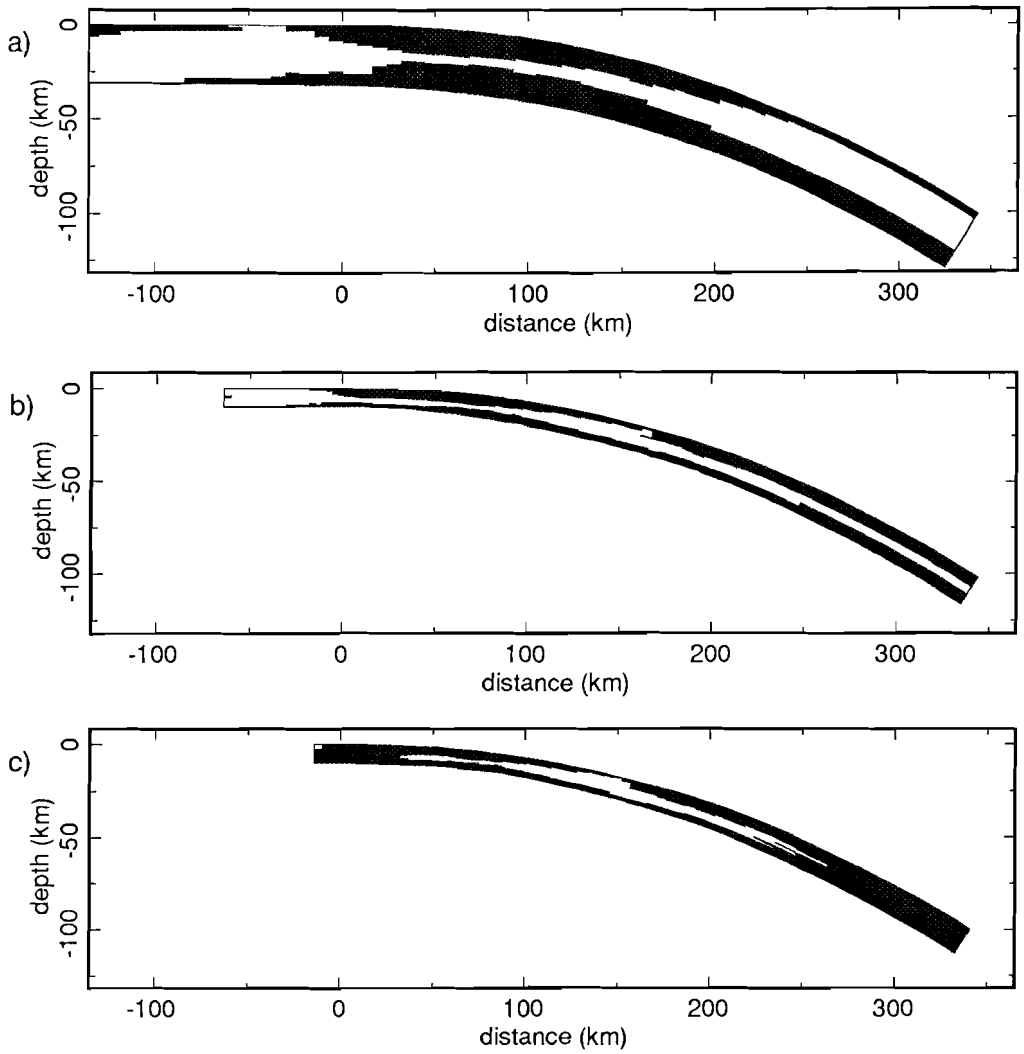

Figure 4.7. (a) Material that is in failure, for a model for which the age of the subducting plate at the trench is 25 Myr and for which a compressive force, equal to 33 % of the total resistive force (the sum of resistive forces due to friction and the components of buoyancy forces parallel to the slab), is exerted upon the left boundary of the model. Otherwise, model parameters are the same as for the model for which results are shown in Figure 4.5b. *(b)* Material that is in failure, for a model for which the age of the subducting plate at the trench is 2.8 Myr, and for which 33 % of the total resistive force (the sum of resistive forces due to friction and the components of buoyancy forces parallel to the slab) is overcome by distributed body forces. Otherwise, model parameters are the same as for the model for which results are shown in Figure 4.5d (v_{sp} equal to 5 cm/yr; v_c equal to 12 cm/yr). *(c)* Material that is in failure, for a model similar to that in Figure 4.7b, for which the age of the subducting plate at the trench is 1.8 Myr.

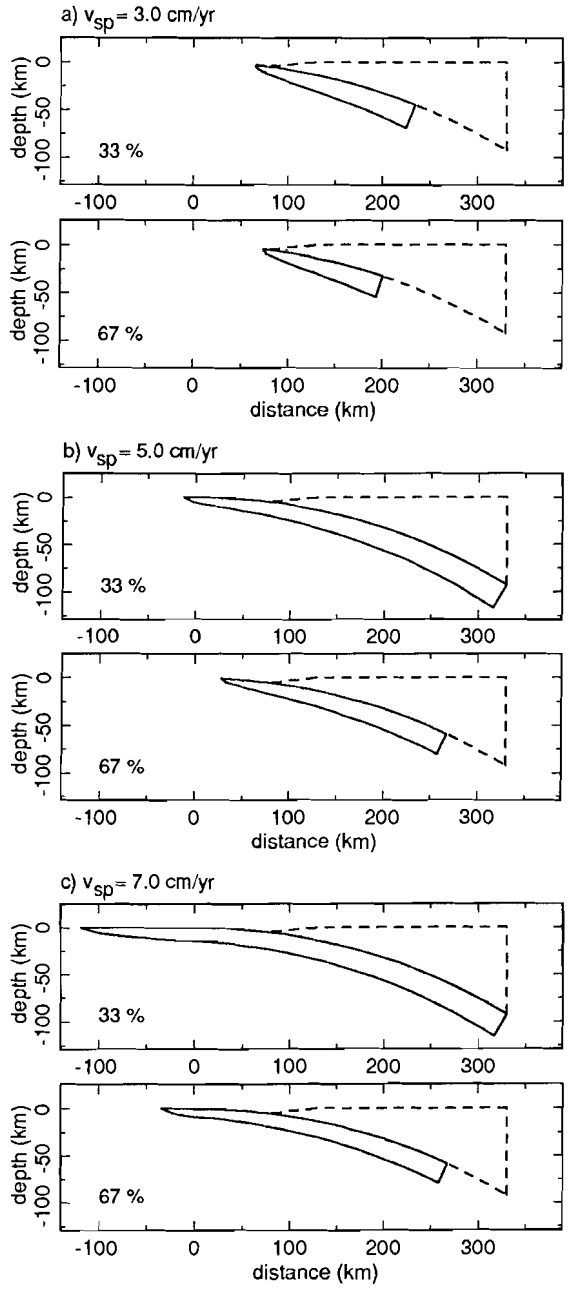

Figure 4.8. Geometry of the detached sheet, for models for which 33 % or 67 % of the total resistive force is overcome by distributed body forces. The position of the right boundary of the detached sheet is estimated from the finite element modelling results. *(a)* for v_{sp} = 3 cm/yr, v_c = 8 cm/yr, weak rheology; *(b)* for v_{sp} = 5 cm/yr, v_c = 12 cm/yr, weak rheology; *(c)* for v_{sp} = 7 cm/yr, v_c = 14 cm/yr, weak rheology.

Failure throughout the plate may also occur in the immediate vicinity of the ridge; at distances less than about 50 km (see Figure 4.7c). Here, however, failure is not related to extension (or compression) throughout the plate and is not expected to lead to detachment. Apparently, bending of the very thin and weak plate near the ridge leads to an elastic zone that is either very small (considerably less than the thickness of an element in the finite element models) or absent. Models, in which only the effects of bending are incorporated (and for which the resistive forces at the plate contact and buoyancy forces are taken to be zero) show a very similar stress field and regions were material is in failure, in the vicinity of the ridge. Note, that in the vicinity of the ridge the lower part of the crust may form a zone of relative weakness, compared to the crustal material above it and the mantle material below.

4.3.4 An alternative approach: a condition for detachment

An alternative assessment of the time of break-up has been obtained by taking into account that detachment of young oceanic lithosphere not only requires extensional failure of the slab itself, but also shearing at the transform faults and fracture zones that bound the young oceanic lithosphere recently created at the ridge segment (see Figure 4.9). An estimate of the time of break-up and the geometry of the detached sheet has been made by assuming that detachment of part of a young subducting plate will occur once that the following condition is reached:

$$F_{RES(F)}\, D_{trf} = F_{T(F,I)}\, D_{trf} + 2.0\, F_{S(trf)} \tag{9}$$

where $F_{RES(F)}$ is the sum (per unit length of trench) of the resistive force due to friction at the plate contact between points E and F (see Figure 4.4), which can be obtained by integrating shear stresses over the plate contact between points E and F, and the components in the direction parallel to the slab of buoyancy forces, exerted upon that part of the slab of which the upper surface has been subducted to a depth smaller than that of point F. $F_{T(F,I)}$ is the integrated strength (for tension) over a profile F - I (again per unit length of trench). D_{trf} is the length of the ridge segment that interacts with the subduction zone. $F_{S(trf)}$ is the total force that will be exerted upon the segment of young oceanic lithosphere during strike slip deformation at the transform faults or fracture zones that bound the part of the slab of which the upper surface has not yet reached the trench or has been subducted to a depth smaller than that of point F. It is obtained by integrating shear resistance over the transform faults or fracture zones. Shear resistance during frictional sliding at strike slip faults is taken from Sibson [1974]:

$$\tau = 0.5(\sigma_1 - \sigma_3) \sin 2\theta \tag{10}$$

where θ is the angle between the fault and σ_1, and where

$$\sin 2\theta = (1+\mu^2)^{-1/2} \tag{11}$$

$$(\sigma_1 - \sigma_3) = 2\, \frac{R' - 1}{R' + 1}\, (1 - \lambda)\, P \tag{12}$$

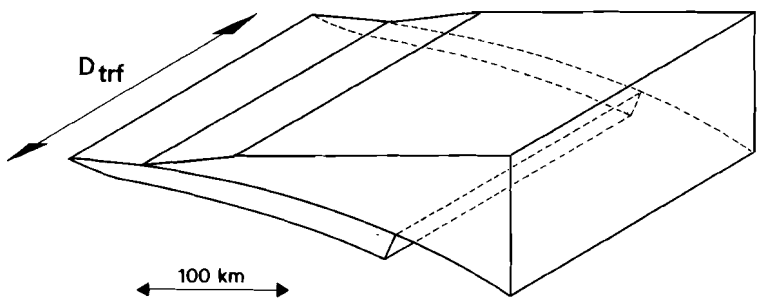

Figure 4.9. Schematic representation of the 3-D situation near the trench.

Equation (12) assumes that $\sigma_2 = (\sigma_1 + \sigma_3)/2$. Shear resistance for ductile deformation is obtained using the same flow laws that are used to determine in-plate strengths. We have also adopted the same values for μ and λ. We have thus assumed that material at a transform fault or fracture zone has similar strength as material within a plate, which may be an upper bound for the actual strength here [Engeln et al., 1986]. Temperatures at fracture zones are taken to be equal to those within the subducting young oceanic plate that is part of the thermal model, thus neglecting horizontal conduction across the fracture zones. For a two-dimensional situation (D_{trf} goes to ∞), the time of break-up, as predicted by equation (9), is in good agreement with the time of break-up that is predicted by finite element models that belong to set A (see also Figure 4.6).

The geometry of the thin oceanic lithosphere, detached from the deeper parts of the slab and the oceanic lithosphere adjacent to the ridge segment, is given in Figure 4.10. Results are shown for calculations with different half-spreading rates and with ridge segment lengths of 100 and 500 km, which seems a reasonable range for the distance between two major transform faults. Calculations have been made both for a high and a low estimate for the strength of material within the plate and at fracture zones or transform faults. In some cases, detachment occurs shortly after the arrival of the ridge at the trench. During thermal modelling of the situation after the arrival of the ridge at the trench, it has been assumed that the plate continues to subduct at the same velocity and that the gap with the trailing plate is filled with hot mantle material. It is clear that, apart from the half-spreading rate, the length of the ridge segment can also have a large influence on the geometry of the detached sheet. The length of the detached sheet increases as the length of the ridge segment and the half-spreading rate increase. Even for a ridge segment with a length as great as 500 km, the length of the detached sheet is significantly smaller, however, than that for the two-dimensional situation, as inferred for finite element models that belong to set A (compare Figures 4.6 and 4.10). At the time of break-up, resistive forces acting upon a detached sheet are primarily due to friction at the plate contact, although the influence of buoyancy forces may be somewhat greater than that for a two-dimensional model with a similar half-spreading rate. The sum of the components of buoyancy forces in the direction parallel to the slab may range up to about 40 % of the total resistive force due to friction.

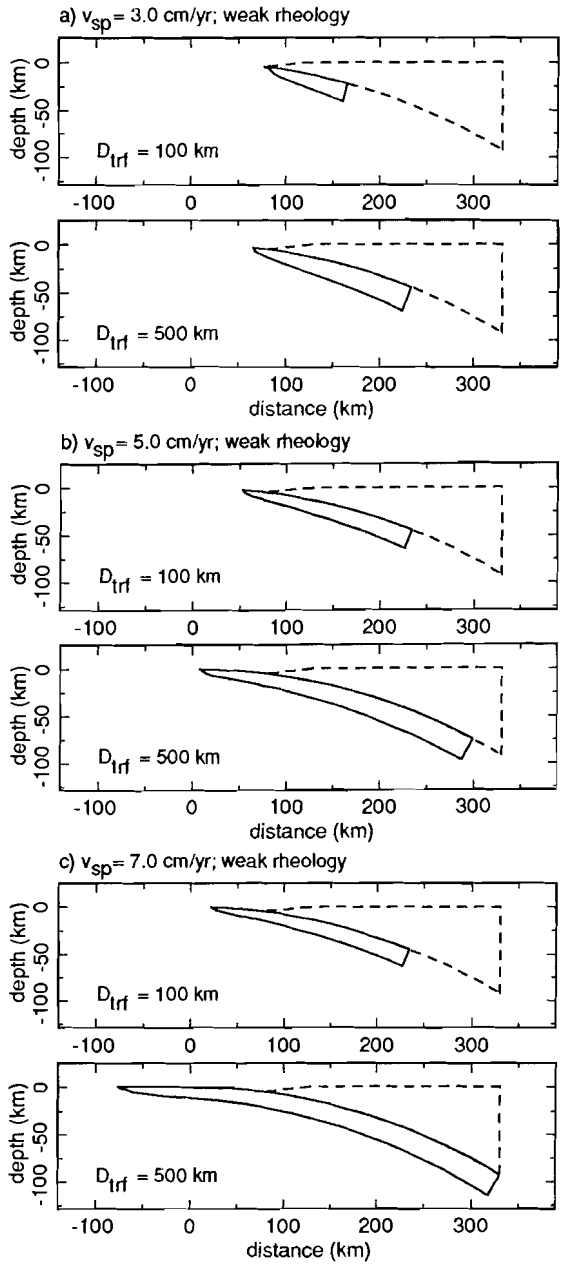

Figure 4.10. The geometry of the detached sheet as a function of the half-spreading rate and the length D_{trf} of the ridge segment that interacts with a subduction zone. Dashed lines denote the geometry of the upper plate in the thermal model. The base of the detached sheet is taken to coincide with the 1200 °C isotherm in the thermal models. *(a)* for v_{sp} = 3 cm/yr, v_c = 8 cm/yr, weak rheology; *(b)* for v_{sp} = 5 cm/yr, v_c = 12 cm/yr, weak rheology; *(c)* for v_{sp} = 7 cm/yr, v_c = 14 cm/yr, weak rheology; *(d)* for v_{sp} = 5 cm/yr, v_c = 12 cm/yr, strong rheology; *(e)* for v_{sp} = 7 cm/yr, v_c = 14 cm/yr, strong rheology.

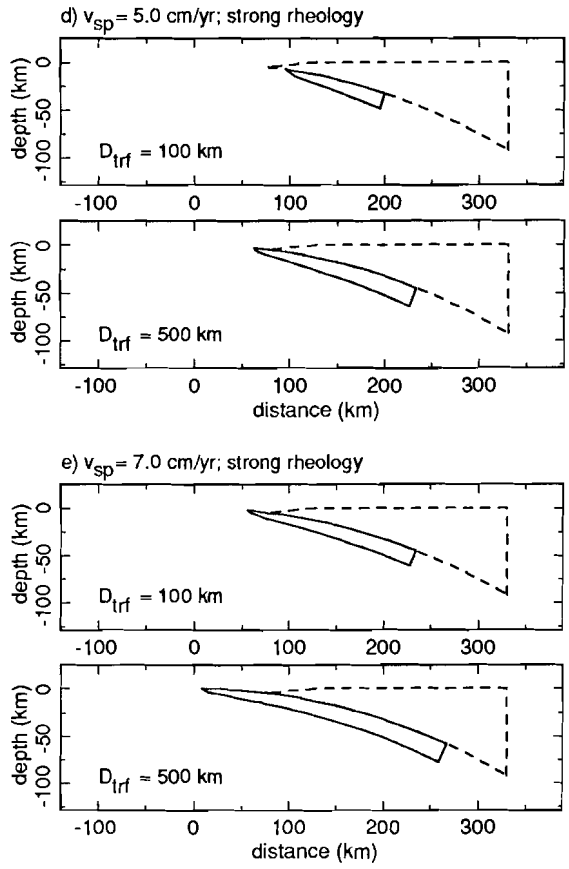

Figure 4.10 (continued).

Calculations have been made for a condition for detachment, similar to equation (9), which applies to the crustal part of the subducting plate only and which includes forces that can be exerted upon the base of the crust. These calculations indicate that in general the condition for detachment of both crust and subcrustal lithosphere is reached at an earlier time than the condition for detachment of the crust only. This is not always the case, however, for models with a length of the ridge segment of 100 km. It thus can not be excluded that in some cases only crustal material will be detached.

It is concluded that very young oceanic lithosphere, created at a moderately fast or fast spreading ridge (v_{sp} greater than about 3 to 4 cm/yr), may break up during the early phase of subduction. The geometry of the elongated sheet of detached oceanic lithosphere, which will remain at the surface or within the upper part of the subduction zone, is determined by the half-spreading rate and the length of the ridge segment at which it was created. Break-

up is caused by the relatively slow decrease of resistive forces in the upper part of a subduction zone (primarily due to friction at the plate contact and to a lesser extent to the compositional buoyancy of crustal and depleted mantle material) during the subduction of oceanic lithosphere with a gradually decreasing age.

4.4 Implications of modelling results for the emplacement of ophiolites

As follows from our modelling results, the interaction between a spreading ridge and a subduction zone can lead to the break-up of young oceanic lithosphere during the early phase of its subduction. In this chapter, we will first discuss the tectonic setting of the detached sheet of thin oceanic lithosphere, both during and after break-up. Next, we will try to asses whether recent, and thus relatively well-known, ridge-trench interactions have led to break-up of the subducting plate. Finally, we will discuss whether the properties of (some) ophiolites are in agreement with an emplacement history in which the break-up of young and thin oceanic lithosphere in the upper part of a subduction zone is the first phase.

4.4.1 Tectonic Setting of the Detached Sheet

Tectonic setting during detachment. The current record of plate motions indicates that the absolute velocity of a subducting oceanic plate increases as the average age of the subducting oceanic lithosphere, at the trenches that bound part of the plate, increases. For the Juan the Fuca plate, for which the average age of the subducting plate has a small value near 10 Myr, the absolute velocity is about 1 cm/yr only [Carlson et al., 1983]. This is probably related to the relatively low magnitude of slab pull forces for a relatively young subducting plate. Theoretical modelling of the slab pull force, which is thought to be the dominant force driving plate motion [Forsyth and Uyeda, 1975], predicts that it depends on the age of the subducting plate and that it will increase linearly with age$^{3/2}$ [e.g., England and Wortel, 1980]. It seems unlikely that, if the average age of a subducting plate is very small (and has been so during the last 5 - 10 Myr), a moderately fast or fast spreading ridge (v_{sp} greater than 3 - 4 cm/yr) can arrive at or near the trench.

Although the half-spreading rate of a ridge is thus expected to decrease as the ridge approaches the trench, there are at least two recent examples of the interaction between a relatively fast spreading ridge segment and a subduction zone. In both these cases, which are discussed below, subduction of very young oceanic lithosphere is contemporaneous with the subduction of much older oceanic lithosphere in other parts of the subduction zone. In general, we expect that an interaction between a relatively fast spreading ridge and a subduction zone will only occur if the subduction of very young oceanic lithosphere is contemporaneous with the subduction of significantly older oceanic lithosphere, belonging to the same plate, in other parts of the subduction zone, or (alternatively) if subduction of very young oceanic lithosphere has recently been preceded by the subduction of

considerably older oceanic lithosphere in the same section of the subduction zone.

Tectonic setting after detachment. In some cases, the interaction between a spreading ridge and a subduction zone will be followed by subduction of the trailing plate, that was initially situated at the opposite side of the ridge. In the southern part of the South American subduction zone, for instance, subduction of the Nazca plate has been followed, after the arrival of the Chile ridge at the subduction zone, by subduction of the Antarctic plate. For such a situation, our modelling results predict the following scenario (see also Figure 4.11). If ridge-trench interaction has led to break-up, a new plate contact will develop at the base of the detached sheet. Initially, friction at the new plate contact will be very low as a result of the high temperatures at the new plate contact, combined with the subduction of fluids, oceanic crust and sedimentary material below the detached sheet. Thus, the subducting trailing plate is unlikely to break up. If the detached sheet is very large, young and relatively buoyant oceanic lithosphere of the trailing plate will be moving sub-horizontally below the detached sheet for some time, in a situation that is essentially similar to the lithospheric doubling process, proposed by Vlaar [1983].

Subduction of oceanic crust, sediments and fluids below the detached sheet, which has mantle temperatures at its base, is likely to lead to a short phase of near-trench volcanism [e.g., Boudier et al., 1988]. Similar to the situation below a "normal" subduction-related volcanic arc [Gill, 1981], the first phase of the process that leads to volcanism may be either melting of the subducting crustal and sedimentary material itself, or melting of hot overlying mantle material, due to the migration of fluids. Due to the small thickness of the detached sheet, it will cool rapidly and the phase of near-trench volcanism will be very short. Generation of the sheet at a spreading centre, subsequent near-trench volcanism, and cooling of the detached sheet will take place within less than 10 to 15 Myr.

As a result of the subduction of the trailing plate, the detached slab will be transferred to the upper plate (see Figure 4.11). Continuation of subduction of the trailing plate may well lead to imbrication and dismemberment of the detached sheet. It will eventually result in the resumption of subduction-related arc volcanism in the region where the slab has reached a depth of about 100 - 200 km.

Underthrusting of the oceanic sheet by continental lithosphere, after the closure of the ocean basin and the arrival of continental lithosphere at the trench, will lead to the incorporation of the elongated sheet of thin oceanic lithosphere into an orogenic belt, as well as rapid uplift and sub-aerial exposure.

Our modelling provides us with a mechanism to incorporate thin oceanic lithosphere into a forearc region and, eventually, an orogenic belt. In the remaining part of this chapter we will try to assess whether recent ridge-trench interactions have led to the transfer of part of the subducting plate to the upper plate. In addition, we will compare the properties of ophiolites with our modelling results, in order to determine whether (some) ophiolites may have experienced an emplacement history as shown in Figure 4.11.

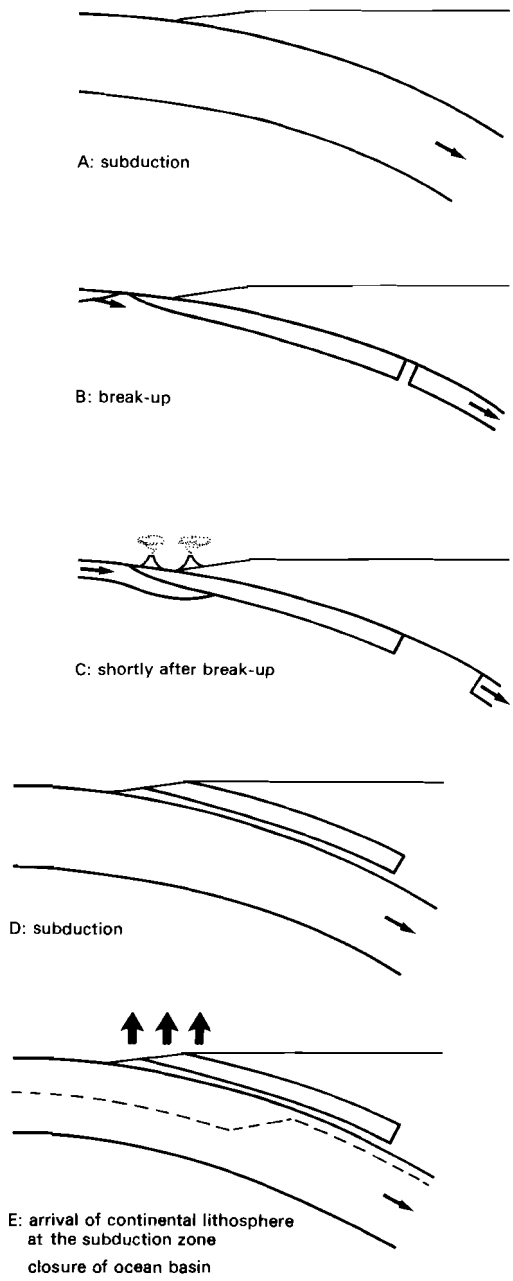

Figure 4.11. Schematic representation of the tectonic setting during and after break-up. Dashed lines denote the base of the crust in the subducting plate. The absolute velocity of the upper plate need not be zero; arrows denote relative rather than absolute velocities.

4.4.2 Recent Ridge-Trench Interactions

Some of the recent examples of the subduction of very young oceanic lithosphere have not led to the interaction between a relatively fast spreading ridge and a subduction zone. This is the case for the present-day subduction of the Juan de Fuca plate and the subduction of the (now largely subducted) Phoenix plate at the Pacific margin of the Antarctic Peninsula [Barker, 1982]. In these cases, the average age of the subducting oceanic lithosphere has been relatively small, which may preclude the arrival of fast spreading ridge segments at a trench (see above). In both cases, there is no evidence for a recent break-up of the subducting plate.

S. Chile. During the last 14 Myr, segments of the Chile Ridge have interacted with the southern part of the Peru-Chile subduction zone. For most of this time, the half-spreading rate at the Chile Ridge has been about 5 cm/yr. During the last 6 Myr, it has decreased to about 3 - 3.5 cm/yr [Cande et al., 1987]. North of the present-day triple junction, the Nazca plate is now subducting with a velocity of about 9 cm/yr below the South American plate. The average age of the subducting Nazca plate is about 40 Myr [Wortel, 1984]. South of the triple junction, the Antarctic plate is subducting with a velocity of about 2 cm/yr.

The last segment of the Chile Ridge that has reached the trench over its entire length did so about 2.5 to 4.0 Myr ago in the region between 46.5 and 47 °S. It had a length of about 50 km and was offset by relatively large transform faults [Cande et al., 1987]. For the region where this occurred, Forsythe et al. [1986] have reported the discovery of a small, fully-developed ophiolite complex at the Taitao Peninsula, directly bordering on the Pacific Ocean, and at a distance of only 10 - 15 km from the trench. A K-Ar age of 3.7 ± 0.6 Myr of the ophiolite indicates that its emplacement must indeed have been related to the interaction between the spreading ridge segment and the subduction zone [Forsythe et al., 1986]. Exposure of the ophiolite on Taitao Peninsula is probably caused by the short time span that has elapsed since the ridge-trench interaction. Prior to a ridge-trench interaction, the region near the trench will be uplifted significantly. Submergence of the ophiolite below sea-level is likely to occur within a few Myr, as the age of the subducting Antarctic plate will increase rapidly.

Solomon Island arc. Another example of a recent ridge-trench interaction occurs near the Solomon Island arc in the southwestern part of the Pacific Ocean. Since the initiation of seafloor spreading at the Woodlark spreading system, more than 3.5 Myr ago, a trench-ridge-trench triple junction exists South-West of the Solomon Island arc [Weissel et al., 1982]. The ridge is strongly oblique with respect to the trench, which may promote detachment as such a situation can lead to the prolonged arrival of very young low-strength oceanic lithosphere at the same section of the trench. Oceanic lithosphere of the Solomon Sea plate, part of which has been recently created at the Woodlark Rift (at a rate of ± 3.6

cm/yr), subducts at relatively high velocities (> 10 cm/yr) below the Solomon Island arc [Weissel et al., 1982]. South-East of the triple junction, subduction of the Solomon Sea plate has been followed by subduction of the Indo-Australian plate.

The tectonic development of this region has been discussed by Ridgway [1987]. Presently, subduction of very young oceanic lithosphere occurs at a trench South-West of the New Georgia Islands, causing anomalously near-trench volcanism at these islands, at a distance of only 25 - 50 km from the trench. A fossil trench can be recognized, however, to the North-East of these islands [Ridgway, 1987]. This fossil trench was still active during Late Miocene and Pliocene times, indicating that migration of the trench was contemporaneous with the interaction of the Woodlark spreading system and the subduction zone. Eruption of picritic and olivine basalts at the New Georgia Islands [Weissel et al., 1982] seems to be caused by the subduction of crust, sediments and fluids beneath a recently detached sheet of young and thin oceanic lithosphere.

Implications for forearc regions. Recent ridge-trench interactions indicate that during such an interaction some thin oceanic lithosphere can indeed be incorporated into an arc-trench region, in agreement with our modelling results. Forearc regions are thought to be frequently underlain by oceanic crust and upper mantle [e.g., Dickinson and Seely, 1979; Hamilton, 1988], which may thus in some cases be due to a ridge-trench interaction. Oceanic basement in forearc regions, however, is not well exposed. In general, it does not seem possible to determine the dimensions of oceanic crust and upper mantle in arc-trench regions and to compare them with the geometry of the detached sheets in our models.

An exception is the forearc region near Vancouver Island, western Canada, for which seismic reflection and refraction profiles delineate structures up to substantial depths. Based on these profiles, Green et al. [1986] have proposed that an elongated slab of oceanic lithosphere overlies the currently subducting Juan de Fuca plate in this arc-trench region. The upper surface of this slab is situated at depths of 10 - 20 km. The thickness of the slab is about 15 km, of similar magnitude as the thicknesses of the detached sheets in our models. Green et al. [1986] suggest that this slab has been transferred to the upper plate after a jump in the locus of subduction during the Eocene. Plate reconstructions from Engebretson et al. [1985] show that throughout the Tertiary the subducting plate in this region has been relatively young. In particular, our modelling predicts that the Late Eocene arrival of the still fast spreading (v_{sp} > 5 cm/yr) Farallon - Pacific ridge at the North American subduction zone, in the region near Vancouver Island, may well have led to break-up.

4.4.3 Observed Properties of Ophiolites; Comparison with Modelling Results

A review of the structure of ophiolite complexes is given in Moores [1982]. Here, we will focus on a number of properties of ophiolites that seem to be especially useful to

constrain the tectonic settings during the initial creation of the ophiolite and the subsequent emplacement history. A small subset of ophiolites, those with a lherzolite-dominated rather than harzburgite-dominated mantle section, is excluded from this discussion. Most ophiolites, including relatively well exposed and large ophiolites such as the Semail ophiolite (Oman) and the Troodos ophiolite (Cyprus), exhibit a harzburgite-dominated mantle section [Boudier and Nicolas, 1985].

Dimensions. Ophiolites generally form linear belts that extend along plate sutures over significant lengths. The length of a single ophiolite may range up to about 450 km and the exposed width may range up to about 90 km (for the Semail ophiolite, [Lippard et al., 1986]). Our modelling results indicate that break-up can occur when the ridge is still at a significant distance from the trench (up to about 100 to 200 km; see Figures 4.8 and 4.10). The thickness of ophiolites generally ranges between about 10 and 15 km [Christensen and Salisbury, 1975]. Estimates range up to about 14 - 20 km for the thickness of the northeastern part of the southern section of the Semail ophiolite [Hopson et al., 1981]. The narrow range of observed thicknesses of ophiolites is consistent with an emplacement history as envisaged in Figure 4.11. Near the ridge, cooling oceanic lithosphere rapidly reaches a thickness of about 5 to 10 km. At the time of break-up the detached sheets in our models, where situated at the surface, have a maximum thickness of about 10 to 15 km (for a relatively strong and a relatively weak rheology respectively, for ridge segment lengths up to 500 km).

Tectonic units below the ophiolite. The base of ophiolites, if exposed, is generally associated with a thin sheet of metamorphic material, the basal metamorphic sole, situated immediately below the ophiolite [Jamieson, 1986]. The basal metamorphic sole consists of metamorphosed basalts and sediments of oceanic origin [Searle and Malpas, 1982], that were emplaced during an early phase of underthrusting of material below the ophiolite. Going downward, the metamorphic grade decreases from granulite facies immediately below the ophiolite through amphibolite facies to greenschist facies. For the highest sub-ophiolite metamorphic rocks, temperatures during metamorphism have reached about 700 - 950 °C [Jamieson, 1986]. Partial melting may have occurred during the early phase of deformation below an ophiolite [Searle and Malpas, 1980; Boudier et al., 1988]. Temperatures of 700 - 950 °C are far in excess of temperatures that can be reached as a result of frictional heating during ductile deformation of crustal or sedimentary material. Thus, residual heat from the overlying ophiolite must have been the cause for the high initial temperatures at the shear zone below the ophiolite, in agreement with the emplacement history as envisaged above.

The ophiolite and the basal metamorphic sole are generally underlain by a series of thrust sheets of abyssal plain sediments, in some cases again underlain by passive margin sediments and continental lithosphere, indicating that large amounts of convergence have taken place below the ophiolite [e.g., Glennie et al., 1974; Moores, 1982]. Based on these structural relationships and on regional geologic considerations, Gealey [1977, 1980] has

proposed that many relatively well-exposed and large ophiolites (including Semail and Troodos) have, prior to underthrusting by continental lithosphere, been part of a forearc region.

Volcanic stratigraphy and trace element composition of the ophiolite crust. Geochemical studies have shown that at least parts of the crustal section of ophiolites have a trace element composition more similar to arc rocks than to mid-ocean ridge basalts [e.g., Pearce et al., 1981]. For the Troodos ophiolite, for instance, the extrusive sequence can be divided into a lower and an upper group. Lower pillow lavas can be correlated compositionally with the sheeted dike complex and the older (and upper) part of the gabbroic cumulates [Thy, 1987]. The basaltic and picritic upper pillow lavas, with relatively high MgO and low TiO_2 contents, have a composition that points to an origin in a subduction-related setting (e.g. melting of a depleted mantle source, induced by fluids derived from a subducting slab) and that is incompatible with a mid-ocean ridge origin [Pearce, 1980; Rautenschlein et al., 1985]. The upper pillow lavas contain boninites which, apart from their exposure in ophiolites, have only been found in forearc regions [Cameron et al., 1979; Bloomer and Hawkins, 1987]. The younger part of the cumulates can be correlated compositionally with the upper pillow lavas. Taken together, the geochemical evidence indicates that the crustal part of the Troodos ophiolite was formed by two distinct, chemically unrelated, systems. Lower pillow lavas, sheeted dikes, and the upper part of the cumulates where formed during an earlier event at a spreading centre; upper pillow lavas and the lower part of the cumulates were formed during a later event, after the termination of spreading, in a subduction-related setting. This later event seems to represent a short-lived phase of incipient island-arc volcanism [Rautenschlein et al., 1985; Thy, 1987; Thy and Moores, 1988].

The subduction of a trailing plate below a thin sheet of detached oceanic lithosphere, with mantle temperatures at its base, may well account for the arc nature of the upper part of the extrusive section of an ophiolite. A similar opinion is given by Boudier et al. [1988] and Ernewein et al. [1988], who relate the later stages of arc-like volcanism and crust formation of the Semail ophiolite to subduction of a ridge crest below another ridge crest. As the detached sheet of oceanic lithosphere will rapidly cool during the subduction of the trailing plate, the emplacement history as envisaged above (see Figure 4.11) can explain why the phase of arc-like volcanism has been so short-lived.

Age relations. A compilation of ages of ophiolites and their basal metamorphic soles, given in Spray [1984], gives differences in the age of the ophiolite itself and that of the basal metamorphic sole that range from 0 to about 20 Myr. In several well-documented cases, the age difference is less than 10 Myr.

For the Semail Ophiolite, a particularly accurate timing exists of events that took place during and shortly after the creation of the ophiolite. The lower volcanic Geotimes Unit, created at the spreading centre, contains intercalated sediments with an early Cenomanian

(± 95 Myr on the Cretaceous time scale of Kennedy and Odin [1982]) radiolarian assemblage [Tippit et al., 1981]. Sediments within, and directly overlying the upper volcanic sequences (Lasail and Alley Units) contain Cenomanian and early Turonian (± 95 - 89 Myr) radiolarian assemblages, indicating that all volcanic units were emplaced within a time span of about 6 Myr only [Tippit et al., 1981]. Amphibolites within the upper part of the basal metamorphic sole have a mean $^{40}Ar/^{39}Ar$ isotopic age of 90 ± 3 Myr [Lanphere; 1981]. This is a minimum age of formation of these rocks, as some diffusive loss of ^{40}Ar is expected to occur at the high temperatures that these rocks have initially been subjected to. It thus seems likely that the early phase of shearing at the base of the Semail ophiolite has been contemporaneous with the eruption of part of the volcanic sequences.

The relatively small time span between the initial creation at a spreading centre, arc-like volcanism, and the initiation of shearing at the base of an ophiolite is in keeping with the emplacement history as envisaged above.

Synthesis. Our modelling results indicate that a tectonic setting which is known to have occurred fairly frequently in the geological past (i.e. the interaction between a spreading centre and a subduction zone) will in some cases have led to the incorporation of a thin sheet of oceanic lithosphere into an arc-trench region and eventually into an orogenic belt. The properties of a large subset of ophiolites, those with a harzburgite-dominated mantle section, are in good agreement with our modelling results. We thus propose that these ophiolites are the result of the interaction between a mid-ocean spreading centre and a subduction zone.

A number of studies have proposed that the initiation of shearing at the base of an ophiolite, shortly after its creation at a spreading centre, was caused by the break-up of young oceanic lithosphere at a subduction zone as a result of bending [Nicolas and Le Pichon, 1980], or by the subduction of a ridge crest below another ridge crest [Boudier et al., 1982, 1988; Spray, 1983]. The situation during the initiation of shearing at the base of the detached oceanic lithosphere, as envisaged in Figure 4.11, contains elements of both these types of models, as it incorporates both break-up of oceanic lithosphere in the upper part of a subduction zone, and subduction of a ridge crest below another ridge crest.

The proposed model for the emplacement of ophiolites with a harzburgite-dominated mantle section, if correct, has significant implications. Initial generation of the ophiolite will have taken place at a spreading centre with an intermediate or high spreading rate (v_{sp} > 3 - 4 cm/yr). The largest ophiolites will have been generated at fast spreading ridge segments. During the creation of the ophiolite, spreading took place in the vicinity of a subduction zone, which may already have affected the composition of the crust [Abbott and Fisk, 1986]. Within a few Myr after its initial generation, the ophiolite will have experienced a second stage of volcanism, caused by subduction of fluids, sediments and oceanic crust beneath a thin sheet of oceanic lithosphere with mantle temperatures at its base.

4.5 Summary

Thermo-mechanical modelling indicates that very young oceanic lithosphere, recently created at a spreading ridge in the vicinity of a subduction zone, can break-up during the early phase of its subduction. Break-up is due to the relatively slow decrease of resistive forces, primarily caused by friction at the top of the subducting plate, and the relatively fast decrease of the strength of the subducting plate during the subduction of gradually younger oceanic lithosphere. Whether break-up occurs depends upon the spreading velocity and the length of the ridge segment that interacts with the trench. If break-up takes place, a thin sheet of oceanic lithosphere will be detached from the other parts of the slab. It will remain at the surface or, at relatively small depths, in the upper part of a subduction zone. The geometry of the detached slab of oceanic lithosphere will depend on the spreading velocity and the length of the ridge segment at which it was created in the vicinity of a subduction zone.

Break-up of young oceanic lithosphere during the early phase of subduction, followed by subduction of the trailing plate (at the opposite side of the ridge at which the young oceanic lithosphere was created), can lead to the incorporation of a thin sheet of oceanic lithosphere, less than about 15 to 20 km thick, into a forearc region. Finally, upon closure of the ocean basin, this sheet can be incorporated into an orogenic belt. It is proposed that ophiolites with a harzburgite-dominated mantle section have experienced such an emplacement history. If this is the case, these ophiolites represent oceanic lithosphere that was created at a ridge with an intermediate or high half-spreading rate (greater than 3 - 4 cm/yr), in the vicinity of a subduction zone, and that experienced a second stage of volcanism and crust formation within a few Myr after the initial generation at the spreading centre.

Acknowledgements. I thank N. J. Vlaar and Rinus Wortel for many useful discussions and for their insistence to continue my work with finite element models. I am indebted to Sierd Cloetingh for his help and advice on finite element modelling. Kevin Furlong and R. Meissner contributed helpful reviews. This work has been supported by a research grant from Royal Dutch/Shell.

References

Abbott, D., and M. Fisk, Tectonically controlled origin of three unusual rock suites in the Woodlark Basin, *Tectonics, 5,* 1145-1160, 1986.

Ahrens, T. J., and G. Schubert, Gabbro-eclogite reaction rate and its geophysical significance, *Rev. Geophys. Space Phys., 13,* 383-400, 1975.

Barker, P. F., The Cenozoic subduction history of the Pacific margin of the Antarctic Peninsula: Ridge crest-trench interactions, *J. Geol. Soc. London, 139,* 787-801, 1982.

Bathe, K. J., E. L. Wilson, and R. H. Iding, NONSAP a structural analysis program for static and

dynamic response of nonlinear systems, 73 pp., Univ. of California Structural Engineering Lab., Berkeley, 1974.

Bird, P., Stress and temperature in subduction shear zones, *Geophys. J. R. Astron. Soc., 55,* 411-434, 1978.

Bloomer, S. H., and J. W. Hawkins, Petrology and geochemistry of boninite series volcanic rocks from the Mariana trench, *Contrib. Mineral. Petrol., 97,* 361-377, 1987.

Bodine, J. H., M. S. Steckler, and A. B. Watts, Observations of flexure and the rheology of the oceanic lithosphere, *J. Geophys. Res., 86,* 3695-3707, 1981.

Boudier, F., and R. G. Coleman, Cross section through the peridotite in the Samail ophiolite, southeastern Oman Mountains, *J. Geophys. Res., 86,* 2573-2592, 1981.

Boudier, F., and A. Nicolas, Harzburgite and lherzolite subtypes in ophiolitic and oceanic environments, *Earth Planet. Sci. Lett., 76,* 84-92, 1985.

Boudier, F., A. Nicolas, and J. L. Bouchez, Kinematics of oceanic thrusting and subduction from basal sections of ophiolites, *Nature, 296,* 825-828, 1982.

Boudier, F., G. Ceuleneer, and A. Nicolas, Shear zones, thrusts and related magmatism in the Oman ophiolite: Initiation of thrusting on an oceanic ridge, *Tectonophysics, 151,* 275-296, 1988.

Byerlee, J. D., Friction of rocks, *Pure Appl. Geophys., 116,* 615-626, 1978.

Cameron, W. E., E. G. Nisbet, and V. J. Dietrich, Boninites, komatiites and ophiolitic basalts, *Nature, 280,* 550-553, 1979.

Cande, S. C., R. B. Leslie, J. C. Parra, and M. Hobart, Interaction between the Chile Ridge and Chile Trench: Geophysical and geothermal evidence, *J. Geophys. Res., 92,* 495-520, 1987.

Caristan, Y., The transition from high-temperature creep to fracture in Maryland diabase, *J. Geophys. Res., 87,* 6781-6798, 1982.

Carlson, R. L., T. W. C. Hilde, and S. Uyeda, The driving mechanism of plate tectonics: Relation to the age of the lithosphere at trenches, *Geophys. Res. Lett., 10,* 297-300, 1983.

Chopra, P. N., and M. S. Paterson, The experimental deformation of dunites, *Tectonophysics, 78,* 453-473, 1981.

Christensen, N. I., and M. H. Salisbury, Structure and constitution of the lower oceanic crust, *Rev. Geophys. Space Phys., 13,* 57-86, 1975.

Cloetingh, S. A. P. L., Evolution of passive continental margins and initiation of subduction zones, Ph. D. thesis, 111 pp., Univ. of Utrecht, Utrecht, 1982.

Crough, S. T., Thermal model of oceanic lithosphere, *Nature, 256,* 388-390, 1975.

Davis, D., J. Suppe, and F. A. Dahlen, Mechanics of fold-and-thrust belts and accretionary wedges, *J. Geophys. Res., 88,* 1153-1172, 1983.

Dickinson, W. R., and D. R. Seely, Structure and stratigraphy of forearc regions, *Am. Assoc. of Pet. Geol. Bull., 63,* 2-31, 1979.

Engebretson, D. C., A. Cox, and R. G. Gordon, Relative motions between oceanic plates of the Pacific Basin, *Geol. Soc. Am. Spec. Paper, 206,* 59 pp., 1985.

Engeln, J. F., D. A. Wiens, and S. Stein, Mechanisms and depths of Atlantic transform earthquakes, *J. Geophys. Res., 91,* 548-578, 1986.

England, P., and R. Wortel, Some consequences of the subduction of young slabs, *Earth Planet. Sci. Lett., 47,* 403-415, 1980.

Ernewein, M., C. Pflumio, and H. Whitechurch, The death of an accretion zone as evidenced by the magmatic history of the Sumail ophiolite (Oman), *Tectonophysics, 151,* 247-274, 1988.

Forsyth, D., and S. Uyeda, On the relative importance of the driving forces of plate motion, *Geophys. J. R. Astron. Soc., 43,* 163-200, 1975.

Forsythe, R. D., E. P. Nelson, M. J. Carr, M. E. Kaeding, M. Herve, C. Mpodozis, J. M. Soffia, and S. Harambour, Pliocene near-trench magmatism in southern Chile: A possible manifestation of ridge collision, *Geology, 14,* 23-27, 1986.

Furlong, K. P., D. S. Chapman, and P. W. Alfeld, Thermal modeling of the geometry of subduction

with implications for the tectonics of the overriding plate, *J. Geophys. Res., 87,* 1786-1802, 1982.

Gealey, W. K., Ophiolite obduction and the geologic evolution of the Oman Mountains and adjacent areas, *Geol. Soc. Am. Bull., 88,* 1183-1191, 1977.

Gealey, W. K., Ophiolite obduction mechanism, in *Ophiolites, Proc. Int. Ophiolite Symp. Cyprus,* edited by A. Panayiotou, pp. 228-243, 1980.

Gill, J., *Orogenic andesites and plate tectonics,* 390 pp., Springer, Berlin, 1981.

Glennie, K. W., M. G. A. Boeuf, M. W. Hughes Clarke, M. Moody-Stuart, W. F. H. Pilaar, and B. M. Reinhardt, Geology of the Oman Mountains, *Kon. Ned. Geol. Mijnbouwkundig Genootschap, Verhandelingen, 31,* 423 pp., 1974.

Goetze, C., and B. Evans, Stress and temperature in the bending lithosphere as constrained by experimental rock mechanics, *Geophys. J. R. Astron. Soc., 59,* 463-478, 1979.

Green, A. G., R. M. Clowes, C. J. Yorath, C. Spencer, E. R. Kanasewich, M. T. Brandon, and A. Sutherland Brown, Seismic reflection imaging of the subducting Juan de Fuca plate, *Nature,* 319, 210-213, 1986.

Hamilton, W. B., Plate tectonics and island arcs, *Geol. Soc. Am. Bull., 100,* 1503-1527, 1988.

Hansen, F. D., and N. L. Carter, Creep of selected crustal rocks at 1000 MPa (abstract), *Eos Trans. AGU, 63,* 437, 1982.

Harper, G. D., and J. E. Wright, Middle to Late Jurassic tectonic evolution of the Klamath Mountains, California-Oregon, *Tectonics, 3,* 759-772, 1984.

Hopson, C. A., R. G. Coleman, R. T. Gregory, J. S. Pallister, and E. H. Bailey, Geologic section through the Samail ophiolite and associated rocks along a Muscat-Ibra transect, southeastern Oman Mountains, *J. Geophys. Res., 86,* 2527-2544, 1981.

Hsui, A. T., B. D. Marsh, and M. N. Toksöz, On melting of the subducted oceanic crust: Effects of subduction induced mantle flow, *Tectonophysics, 99,* 207-220, 1983.

Ingersoll, R. V., Initiation and evolution of the Great Valley forearc basin of northern and central California, U.S.A. , in *Trench-forearc geology: Sedimentation and tectonics on modern and ancient active plate margins, Geol. Soc. London Spec. Publ., 10,* edited by J. K. Leggett, pp. 459-467, Oxford, 1982.

Jamieson, R. A., P-T paths from high temperature shear zones beneath ophiolites, *J. Metamorphic Geol., 4,* 3-22, 1986.

Karig, D. E., Initiation of subduction zones: Implications for arc evolution and ophiolite development, in *Trench-forearc geology: Sedimentation and tectonics on modern and ancient active plate margins, Geol. Soc. London Spec. Publ., 10,* edited by J. K. Leggett, pp. 563-576, Oxford, 1982.

Kennedy, W. J., and G. S. Odin, The Jurassic and Cretaceous time scale in 1981, in *Numerical dating in stratigraphy,* edited by G. S. Odin, pp. 557-592, Wiley, Chichester, 1982.

Koch, P. S., J. M. Christie, and R. P. George, Flow law of "wet" quartzite in the α-quartz field (abstract), *Eos Trans. AGU, 61,* 376, 1980.

Lanphere, M.A., K-Ar ages of metamorphic rocks at the base of the Samail ophiolite, Oman, *J. Geophys. Res., 86,* 2777-2782, 1981.

Lippard, S. J., Shelton, A. W., and I. G. Gass, *The ophiolite of northern Oman, Geol. Soc. London, Memoir, 11,* 178 pp., 1986.

Meissner, R., and T. Wever, Lithospheric rheology: Continental versus oceanic unit, *J. Petrol., Special Lithosphere Issue,* 53-61, 1988.

Moores, E. M., Origin and emplacement of ophiolites, *Rev. Geophys. Space Phys., 20,* 735-760, 1982.

Nicolas, A., and X. Le Pichon, Thrusting of young lithosphere in subduction zones with special reference to structures in ophiolitic peridotites, *Earth Planet. Sci. Lett., 46,* 397-406, 1980.

Oxburgh, E. R., and E. M. Parmentier, Compositional and density stratification in oceanic lithosphere - causes and consequences, *J. Geol. Soc. London, 133,* 343-355, 1977.

Pearce, J. A., Geochemical evidence for the genesis and eruptive setting of lavas from Tethyan

ophiolites, in *Ophiolites, Proc. Int. Ophiolite Symp. Cyprus*, edited by A. Panayiotou, pp. 261-272, 1980.

Pearce, J. A., T. Alabaster, A. W. Shelton, and M. P. Searle, The Oman ophiolite as a Cretaceous arc-basin complex: Evidence and implications, *Phil. Trans. R. Soc. London, A 300*, 299-317, 1981.

Rautenschlein, M., G. A. Jenner, J. Hertogen, A. W. Hofmann, R. Kerrich, H.-U. Schmincke, and W. M. White, Isotopic and trace element composition of volcanic glasses from the Akaki canyon, Cyprus: Implications for the origin of the Troodos ophiolite, *Earth Planet. Sci. Lett., 75*, 369-383, 1985.

Ridgway, J., Neogene displacements in the Solomon Islands arc, *Tectonophysics, 133*, 81-93, 1987.

Searle, M. P., and J. Malpas, Structure and metamorphism of rocks beneath the Semail ophiolite of Oman and their significance in ophiolite obduction, *Trans. Roy. Soc. Edinburgh, Earth Sci., 71*, 247-262, 1980.

Searle, M. P., and J. Malpas, Petrochemistry and origin of sub-ophiolite metamorphic and related rocks in the Oman Mountains, *J. Geol. Soc. London, 139*, 235-248, 1982.

Shi, Y., and C.Y. Wang, Generation of high pore pressures in accretionary prisms: inferences from the Barbados subduction complex, *J. Geophys. Res., 93*, 8893-8910, 1988.

Sibson, R. H., Frictional constraints on thrust, wrench and normal faults, *Nature, 249*, 542-544, 1974.

Sleep, N. H., The double seismic zone in downgoing slabs and the viscosity of the mesosphere, *J. Geophys. Res., 84*, 4565-4571, 1979.

Spray, J. G., Lithosphere-asthenosphere decoupling at spreading centres and initiation of obduction, *Nature, 304*, 253-255, 1983.

Spray, J. G., Possible causes and consequences of upper mantle decoupling and ophiolite displacement, in *Ophiolites and oceanic lithosphere, Geol. Soc. London, Spec. Publ., 14*, edited by I. G. Gass, S. J. Lippard, and A. W. Shelton, pp. 255-268, Oxford, 1984.

Thy, P., Magmas and magma chamber evolution, Troodos ophiolite, Cyprus, *Geology, 15*, 316-319, 1987.

Thy, P., and E. M. Moores, Crustal accretion and tectonic setting of the Troodos ophiolite, Cyprus, *Tectonophysics, 147*, 221-245, 1988.

Tippit, P. R., E. A. Pessagno, and J. D. Smewing, The biostratigraphy of sediments in the volcanic unit of the Samail ophiolite, *J. Geophys. Res., 86*, 2756-2762, 1981.

van den Beukel, J., and R. Wortel, Temperatures and shear stresses in the upper part of a subduction zone, *Geophys. Res. Lett., 14*, 1057-1060, 1987.

van den Beukel, J., and R. Wortel, Thermo-mechanical modelling of arc-trench regions, *Tectonophysics, 154*, 177-193, 1988 (Chapter 2 of this thesis).

Vlaar, N. J., Thermal anomalies and magmatism due to lithospheric doubling and shifting, *Earth Planet. Sci. Lett., 65*, 322-330, 1983.

Vlaar, N. J., and S. A. P. L. Cloetingh, Orogeny and ophiolites: Plate tectonics revisited with reference to the Alps, *Geol. Mijnbouw, 63*, 159-164, 1984.

Weissel, J. K., B. Taylor, and G. D. Karner, The opening of the Woodlark Basin, subduction of the Woodlark spreading system, and the evolution of northern Melanesia since mid-Pliocene time, *Tectonophysics, 87*, 253-277, 1982.

Wortel, R., Spatial and temporal variations in the Andean subduction zone, *J. Geol. Soc. London, 141*, 783-791, 1984.

Wortel, M. J. R., and S. A. P. L. Cloetingh, Accretion and lateral variations in tectonic structure along the Peru-Chile trench, *Tectonophysics, 112*, 443-462, 1985.

Yuen, D. A., L. Fleitout, G. Schubert, and C. Froidevaux, Shear deformation zones along major transform faults and subducting slabs, *Geophys. J. R. Astron. Soc., 54*, 93-119, 1978.

Zienkiewicz, O. C., *The finite element method*, 787 pp., McGraw-Hill, Maidenhead, 1977.

Chapter 5

Some thermo-mechanical aspects of the subduction of continental lithosphere

Abstract. Based on thermal and mechanical modelling, it is concluded that the subduction of continental lithosphere can lead to its break-up and the formation of a new plate contact within the middle or lower crust. As a result, (part of) the subducting continental crust is transferred to the upper plate. Break-up is caused by the resistive forces acting upon subducting continental crust, due to the buoyancy of crustal material and to friction at the plate contact, as well as the decrease in strength of the subducting crust once that it has been subducted to a depth of a few tens of km. The crustal thickness and the thermal and compositional structure of the continental crust just before the onset of subduction have a large influence on the depth to which continental crust can be subducted (prior to its break-up). The depth to which continental crust can be subducted coherently decreases as the surface heat flow or the crustal thickness of the subducting continental plate increases. In many cases, break-up is found to occur at a time when the upper surface of the continental plate has been subducted to a depth of 25 - 50 km. The subduction of a cold continental shield or of continental lithosphere with a relatively small crustal thickness, on the other hand, may lead to the subduction of both upper and lower crust to mantle depths.

This chapter has been submitted for publication as:

van den Beukel, J., Some thermo-mechanical aspects of the subduction of continental lithosphere, *submitted to Tectonics*, 1989.

5.1 Introduction

In this paper, the subduction[1] of continental lithosphere is studied by means of thermal and mechanical modelling. In particular, it is investigated whether (and if so, due to what processes) continental lithosphere may break up during the early phase of its subduction.

Orogenic belts such as the Alps and the Himalayas are associated with the collision of continents. Such a collision has generally been preceded by the subduction of oceanic lithosphere. Large amounts of convergence can take place between two continental plates during a continental collision. Balanced cross-sections of external fold and thrust belts generally show a minimum shortening of about 100 km (Boyer and Elliot, 1982; Williams, 1985). Much greater amounts of shortening are obtained if more internal parts of an orogenic belt, where thrusting has also occurred within the crystalline basement, are included in the balanced cross section (e.g., Butler, 1986). For the Himalayas, paleomagnetic data indicate an amount of convergence, related to deformation and subduction of the Indian continent as well as deformation of the Eurasian plate, of 2600 ± 900 km (Patriat and Achache, 1984).

Subduction of continental lithosphere (also termed A-subduction) can lead to the detachment of the upper part of the crust and the formation of a large thrust sheet with a thickness of about 10 - 20 km (e.g., Burchfiel (1980) and Gillet et al. (1986) for the European Alpine system; Allègre et al. (1984) and Mattauer (1986) for the Himalayas). We will refer to this process as break-up of a subducting continental plate, although it is noted that it does not necessarily involve the break-up of an entire section of continental lithosphere but rather the break-up and detachment of its upper part only. The relatively small amounts of lower crust and mantle material (originating from the subducting plate) observed in orogenic belts indicate that these parts of the continental lithosphere are subducted to greater depths, possibly into the mantle.

Emplacement of such relatively large crystalline thrust sheets requires decoupling, presumably in relatively weak zones within the middle or lower part of the crust (Bally, 1981; Meissner, 1986). The causes for thrust sheet emplacement are, however, not well known. Mostly, it is assumed that the buoyancy of crustal material plays a key role in inhibiting the subduction of continental crust, and continental lithosphere as a whole (e.g., McKenzie, 1969). Molnar and Gray (1979) have modelled the resistive forces, due to the buoyancy of continental crust, that act upon subducting continental lithosphere and have compared them with driving forces (exerted by earlier subducted oceanic lithosphere and subcrustal continental lithosphere, possibly augmented by forces exerted by adjacent slab

1. With subduction we mean the movement of material within a downgoing plate at convergent plate margins. It does not imply that the material reaches mantle depths.

segments). They concluded that the buoyancy of continental crust in itself can not prevent the subduction of significant amounts of continental crust to mantle depths, in particular if the subducting continental plate is still attached to earlier subducted oceanic lithosphere. In an analysis, such as that given in Molnar and Gray (1979), the subducting continental plate is treated like a coherent plate that does not deform or break up. Even if sufficient driving forces are available, however, the limited strength of continental crust may still lead to its break-up, and thus inhibit its subduction to greater depths. In the present analysis, the strength of subducting continental crust is compared with the forces acting upon it, in order to constrain the depth to which continental crust can be subducted.

We here present a thermo-mechanical model of a convergent plate margin, where subduction of oceanic lithosphere is followed by the subduction of a limited amount of continental lithosphere. It is the aim of our modelling to assess whether continental lithosphere may break up during the early phase of its subduction. We model the strength of material within subducting continental lithosphere (which is inferred from pressure and temperature), as well as the magnitude of the resistive forces opposing the subduction of a continental plate. Two aspects appear to control the break up of continental lithosphere in the upper part of a subduction zone. First, the relatively low strength of the crustal part of the continental plate. Second, the resistive forces opposing the subduction of continental lithosphere. These resistive forces are not only due to the relatively low density of the continental crust but also to friction at the upper surface of the subducting continental plate.

5.2 Thermal modelling

The geometry of the thermal model is given in Figure 5.1. The plate contact between the upper plate and the subducting lower plate is part of a circle. Temperatures are modelled for the upper part of a subduction zone only. At the right boundary of the model, the downgoing plate has been subducted to a depth that is slightly less than 100 km. For the subduction of oceanic lithosphere, which is assumed to have preceded the subduction of continental lithosphere for a period of time of 30 Myr, the region encompassed in the model coincides with the region between the trench and the volcanic arc. For a detailed investigation of the thermal structure of this model, it is not necessary to include the entire slab and back-arc region in the thermal model (see also van den Beukel and Wortel, 1988). For the situation shown in Figure 5.1, continental lithosphere has already been subducted to a depth of a few tens of km.

Temperatures are determined by conduction, the downward movement of material within the lower plate, and by heat production due to radiogenic heating and to friction at the plate contact. Temperatures are calculated by means of a finite difference method. The differential equation to be solved as well as values for different parameters (e.g., densities, thermal conductivities) for material within the upper plate and the subducting oceanic plate are given in van den Beukel and Wortel (1987; 1988). In the present study, the thickness of the subducting plate is 75 km and the distance between gridpoints (situated at lines

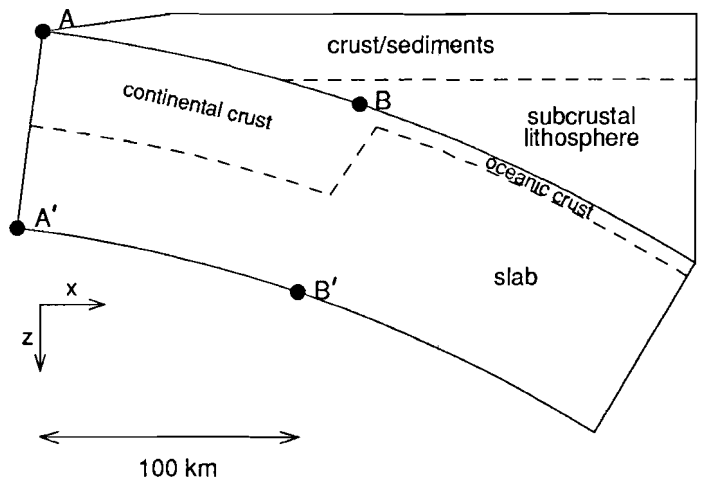

Figure 5.1. Geometry of the thermal model, for a situation that continental lithosphere has been subducted to a depth of a few tens of km. No vertical exaggeration. Point B denotes the leading edge of the subducting continental plate.

perpendicular to the plate contact) is 3 km. It is noted that the thickness of the subducting lithosphere may well be greater than 75 km. Limiting the thickness of the downgoing plate to 75 km does not significantly influence our modelling results, however.

Temperatures at the surface are kept at 0 °C. During model calculations, the slab below the volcanic line (coinciding with the right side of the model) is generally of oceanic origin. Temperatures at the right side of the model, at depths less than 80 km, are those for a geotherm with a surface heat flow of 80 mW m^{-2}. As follows from heat flow data (e.g., Watanabe et al., 1977) and the composition of arc magmas (Tatsumi et al., 1983), temperatures within the upper plate below the volcanic zone and the back-arc region remain high during the subduction of oceanic lithosphere into the mantle. This may be caused by subduction induced mantle flow in the asthenospheric wedge above the slab (Hsui et al., 1983).

For the subduction of oceanic lithosphere, temperatures at the left side of the model are calculated using a boundary layer model for the cooling of oceanic lithosphere from Crough (1975). These temperatures depend on the age of the subducting oceanic lithosphere, which has been taken to be equal to 70 Myr; close to the average age of presently subducting oceanic lithosphere.

For the subduction of a continental plate, temperatures (in °C) within continental lithosphere at the left side of the model are taken to be equal to those of a steady state continental geotherm (e.g., Chapman, 1986). For the upper crust for instance:

$$T(z) = T_s + \frac{Q_s z}{k} - \frac{A_{uc} z^2}{2k} \qquad (1)$$

where T_s is the surface temperature (taken to be 0 °C), Q_s the surface heat flow and k the thermal conductivity. Unless otherwise stated, the thickness of both the upper crust (D_{uc}) and the lower crust (D_{lc}) of the subducting continental plate are taken to be 18 km. Following Pollack and Chapman (1977), it has been assumed that the radiogenic heat production rate A_{uc} within the upper crust accounts for 40 % of the surface heat flow ($A_{uc} = 0.4Q_s/D_{uc}$). The radiogenic heat production rate A_{lc} for lower crustal material is taken to be 0.5 μW m^{-3} (Chapman, 1986). The radiogenic heat production rate for mantle material is taken to be zero. A mantle temperature has been adopted of 1325 °C. The thermal conductivity is taken to be 2.5 W m^{-1} $°C^{-1}$ for crustal material and 3.1 W m^{-1} $°C^{-1}$ for subcrustal material. Densities of upper crustal, lower crustal and mantle material are taken to be 2700, 3000 and 3300 kg m^{-3} respectively. A resulting set of continental geotherms (with Q_s ranging between 40 and 90 mW m^{-2}) is given in Figure 5.2.

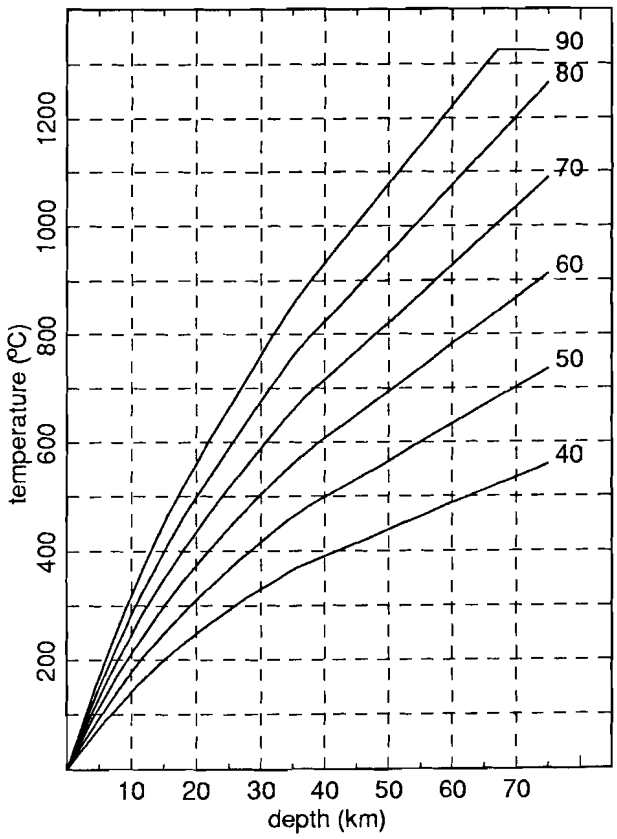

Figure 5.2. Temperatures for continental lithosphere, as a function of depth, for a set of steady state continental geotherms. Surface heat flow ranges between 40 and 90 mW m^{-2}.

It is clear that, for a given depth, large differences in temperature can occur. Temperatures at the Moho range from about 370 to 870 °C. The large differences in temperature, within continental lithosphere just prior to its subduction, are likely to have a profound influence on the mechanical structure of the continental plate during the early phase of its subduction. Rather than assuming that the subducting continental plate has an average thermal structure, calculations have been made for various geotherms of the continental plate, corresponding to a surface heat flow that ranges between 40 and 90 mW m^{-2}. This range encompasses both continental shields (Q_s about 40 to 55 mW m^{-2}) and regions with high heat flow due to relatively recent tectonic or magmatic events (Q_s > 75 mW m^{-2}).

For the subduction of oceanic lithosphere we have shown (van den Beukel and Wortel, 1987; 1988) that, for the upper part of a subduction zone, frictional heating has a large influence on temperatures at and above the plate contact. We inferred shear stresses at the plate contact from heat flow data, rheological arguments and the distribution of interplate thrust earthquakes. Underthrusting of fluid-rich sediments, which causes relatively low shear stresses during brittle deformation, will take place both for the subduction of oceanic and for the subduction of continental lithosphere. We have thus initially assumed that, for brittle deformation, shear stresses at the plate contact for the subduction of continental lithosphere are similar to those inferred for the subduction of oceanic lithosphere. Following van den Beukel and Wortel (1987), it has initially been adopted that:

$$\tau_{br} = \gamma P \quad (\gamma = 0.05) \tag{2}$$

where P is the lithostatic pressure (= ρgz). Calculations have also been made for other values of γ, however. The geometries of fold and thrust belts and accretionary wedges, and observed pore fluid pressures indicate that shear stresses at the base of a fold and thrust belt are of at least similar magnitude as the shear stresses at the base of an accretionary wedge (Davis et al., 1983). For ductile deformation, at greater depths and higher temperatures, we have inferred shear stresses, both for the subduction of oceanic as well as continental lithosphere, from:

$$\tau_{du} = 0.5\,(\dot{\varepsilon}/A)^{1/n} \exp(E/nRT) \tag{3}$$

where values for n, A and the activation energy E are those for a flow law for wet quartzite, as given by Koch et al. (1980). The strain rate $\dot{\varepsilon}$ is assumed to be $v_c/8 \times 10^{-12}$ s^{-1}, v_c being the convergence velocity between the two plates (in cm/yr). The actual shear stress at the plate contact is taken to be the lowest of the two values calculated with equations 2 and 3.

For all modelling results that will be shown hereafter, the subduction of continental lithosphere has been preceded by the subduction of oceanic lithosphere, with an age of 70 Myr and with a convergence velocity of 8 cm/yr, for a duration of 30 Myr. After such a duration of subduction, a steady state thermal structure has been reached almost completely. The resulting thermal structure is given in Figure 5.3a. Temperatures within the downgoing plate are primarily determined by the downward movement of material.

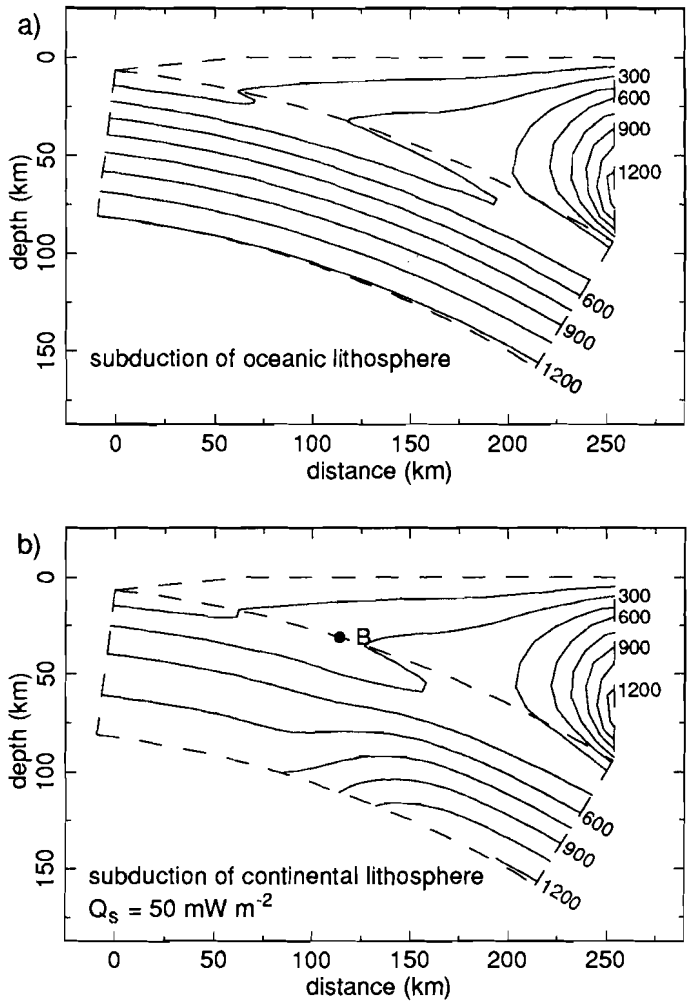

Figure 5.3. Thermal structure of the upper part of a subduction zone. (a) For the subduction of oceanic lithosphere, with an age of 70 Myr and a velocity of 8 cm/yr, prior to the subduction of continental lithosphere. (b-d) For the subsequent subduction of continental lithosphere with a velocity of 4 cm/yr and a surface heat flow, just prior to subduction, of 50 mW m^{-2} (5.3b), 70 mW m^{-2} (5.3c), and 90 mW m^{-2} (5.3d). All parameters are equal to those of the standard parameter set (v_c = 4 cm/yr; $D_{uc} = D_{lc}$ = 18 km; γ = 0.05). Thermal structures are shown at a time 3 Myr after the onset of subduction of continental lithosphere. Point B denotes the leading edge of the subducting continental plate.

Frictional heating has a large influence on temperatures at and above the plate contact. These temperatures are, except for the subduction of very young oceanic lithosphere, influenced less by the age of the subducting oceanic lithosphere or the convergence

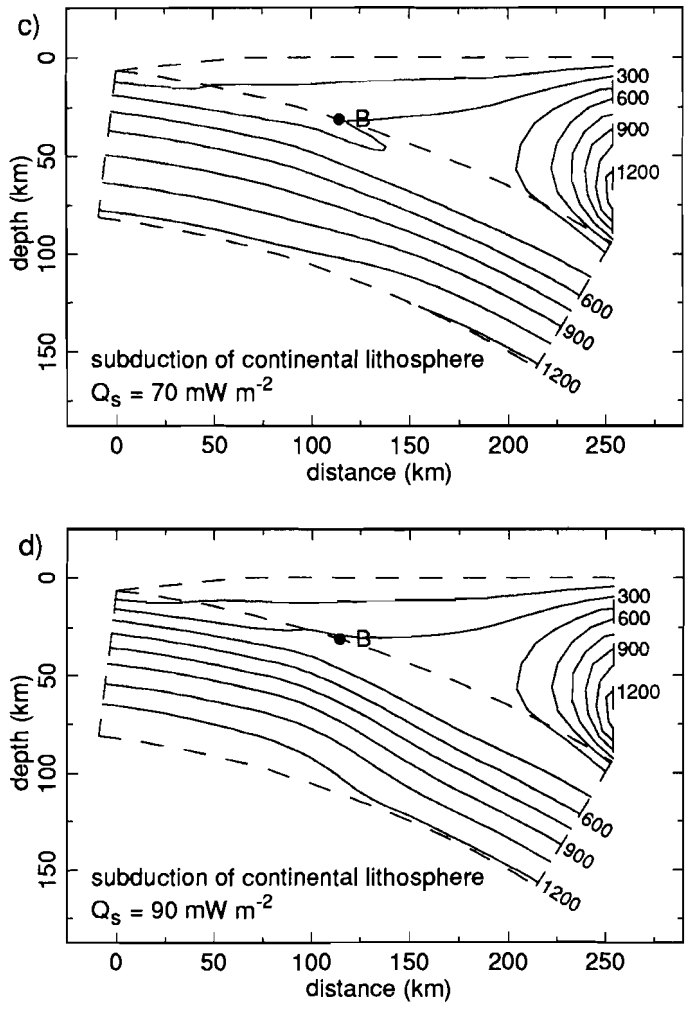

Figure 5.3 (continued).

velocity. Pressure-temperature conditions at the plate contact are in good agreement with those inferred for a high-pressure metamorphic belt such as the Franciscan Complex of California (van den Beukel and Wortel, 1988).

During the thermal modelling it is assumed that, after the closure of the ocean basin, some amount of subduction of continental lithosphere will take place. An increase of resistive forces or a decrease of driving forces will occur gradually, as long as earlier subducted oceanic lithosphere is not detached. In the section on mechanical modelling, estimates will be given of the depth to which continental lithosphere can be subducted, prior to its break-up. In all cases it has been assumed that a transition zone, with a width of

72 km, is situated between the oceanic lithosphere and the leading edge of the continental lithosphere. Prior to its subduction, temperatures within the transition zone change gradually (linearly with distance) from that corresponding to the oceanic plate to that corresponding to the continental plate. All parameters for material within the transition zone (e.g., thermal conductivities) are taken to be equal to those adopted for oceanic lithosphere. This assumption does not significantly influence our thermal modelling results.

Thermal structures during the subduction of continental lithosphere are shown in Figures 5.3b - 5.3d. Parameters for the subduction of continental lithosphere are shown in Table 5.1. We will refer to this parameter set as the standard set of parameters. Results are shown for the subduction of continental lithosphere with a surface heat flow of 50 (Figure 5.3b), 70 (Figure 5.3c) and 90 mW m^{-2} (Figure 5.3d). Thermal structures are shown at a time 3 Myr after the onset of subduction of continental lithosphere. Calculations have been made, however, until the leading edge of the subducting continental lithosphere has reached the right boundary of the model. Temperatures within the subducting plate, except where close to the top of the subducting plate, are primarily determined by the thermal structure of the plate prior to its subduction. Near the plate contact, frictional heating has a large influence on temperatures.

Table 5.1. Parameter values for the standard parameter set

Parameter	Meaning of parameter	Value
v_c	Convergence velocity	4 cm/yr
D_{uc}	Thickness upper crust	18 km
D_{lc}	Thickness lower crust	18 km
γ	see text	0.05

Temperatures and shear stresses at the plate contact (as a function of depth below the surface) for the subduction of continental lithosphere are given in Figure 5.4. This figure gives modelling results at a time that the leading edge of the subducting continental crust has reached the right boundary of the model. Figures 5.4a and 5.4b show modelling results for a case in which shear stresses at the plate contact are determined by the same rheology for both the subduction of continental and oceanic lithosphere. For the subduction of continental lithosphere with low or medium surface heat flow, temperatures at the plate contact are similar to those for the preceding subduction of oceanic lithosphere (dashed line in Figure 5.4a). Average shear stress at the plate contact, for the subduction of continental lithosphere, ranges between about 15 MPa (Q_s = 90 mW m^{-2}) and 25 MPa (Q_s = 40 mW m^{-2}). These values do not exceed an upper limit of about 20 to 30 MPa, inferred by Bird (1978), for the average shear stress at the plate contact for the Himalayas.

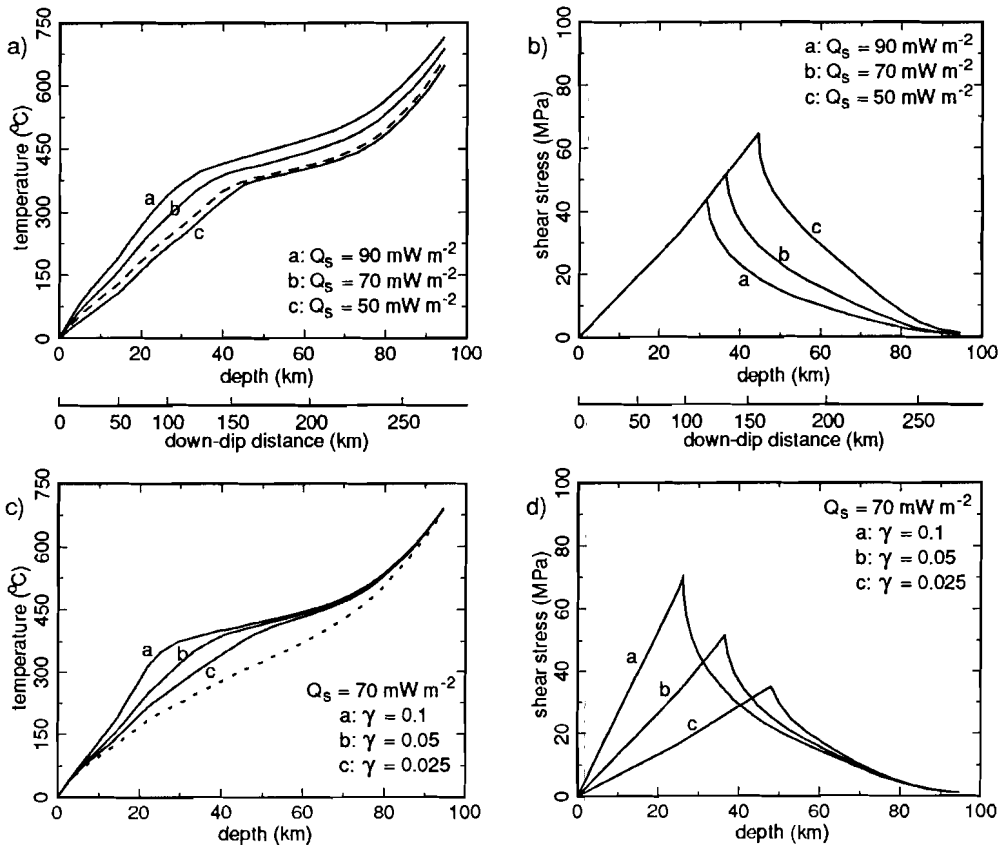

Figure 5.4. Temperatures and shear stresses at the plate contact, as a function of depth below the surface, at a time that the leading edge of the subducting continental plate has reached the right boundary of the model. (a-b) For the subduction of continental lithosphere with a surface heat flow of 50, 70 and 90 mW m^{-2} (all parameters equal to those of standard parameter set). Dashed line denotes temperatures at the plate contact during the subduction of oceanic lithosphere. Lower x-axis gives down-dip distance (along the plate contact) from the left boundary of the model. (c-d) For the subduction of continental lithosphere with a surface heat flow of 70 mW m^{-2} and with γ (which determines shear stresses at the plate contact during brittle deformation) equal to 0.025, 0.05 and 0.1 (all other parameters equal to those of standard parameter set). Dashed line in Figure 5.4c denotes the situation if subduction of continental lithosphere leads to zero shear stresses at the plate contact.

Frictional heating significantly influences temperatures at the plate contact. A higher value for γ leads to higher shear stresses during brittle deformation (see Figure 5.4d) and thus to a greater amount of frictional heating and higher temperatures at the plate contact (see Figure 5.4c). Friction in itself will not lead to melting of material, however. At higher temperatures, during ductile deformation, a small increase in temperatures leads to rapidly

decreasing shear stresses (see Figures 5.4b and 5.4d). Unless the subduction of continental lithosphere leads to a very different amount of frictional heating, temperatures at the plate contact during the subduction of continental lithosphere (at plate tectonic rates) will be similar to those during the subduction of oceanic lithosphere.

It is clear that the thermal modelling results, as given above, are applicable to a situation in which the subducting continental plate has not broken up. In the following section an assessment is made whether continental lithosphere may break up during the early phase of its subduction.

5.3 Mechanical modelling

In this section, we will first infer the strength of material within the downgoing plate from our thermal modelling results. Next, resistive forces due to friction at the plate contact and to buoyancy will be calculated as a function of the depth to which continental crust is subducted. Finally, the depth at which the subducting continental plate will break up will be estimated by comparing resistive forces with the strength of subducting continental crust. An assessment will be made of the influence of various parameters, such as the convergence velocity between the two plates and the surface heat flow of the downgoing continental plate, on the depth to which continental lithosphere can be subducted, prior to its break-up.

Strength of the subducting continental plate. Pressure and temperature dependent rheologies, which incorporate both pressure-dependent brittle deformation and temperature-dependent ductile deformation, have been used to model the strength of material within the subducting continental plate. Differential stresses that cause faulting have been inferred from Sibson (1974). For extensional deformation, for instance, these differential stresses are given by:

$$(\sigma_1 - \sigma_3) = \frac{R' - 1}{R'} (1-\lambda) P \tag{4}$$

with

$$R' = ((1 + \mu^2)^{1/2} - \mu)^{-2} \tag{5}$$

σ_1 and σ_3 are maximum and minimum principal stresses. The coefficient of friction μ has been taken to be 0.75 (Byerlee, 1978). For the pore fluid factor λ, a value has been adopted of 1/3, which implies near-hydrostatic pore fluid pressures. The strength of material for ductile deformation has been inferred from steady state power-law creep flow laws:

$$(\sigma_1 - \sigma_3) = (\dot{\varepsilon}/A)^{1/n} \exp(E/nRT) \tag{6}$$

For material within the upper crust, a flow law for a wet quartzite (from Koch et al., 1980) has been used. The strength for ductile deformation of subcrustal material has been inferred

from a power-law creep flow law for olivine under dry conditions (for differential stresses less than 200 MPa) or from a Dorn-creep flow law (for differential stresses greater than 200 MPa). Parameters of these two flow laws, as well as the constitutive equation for Dorn-creep, are given by Goetze and Evans (1979). The choice of a flow law for the lower crust is less straightforward than that for the upper crust or subcrustal lithosphere. For the strength envelopes, given by the solid lines in Figure 5.5, a flow law for a dry diabase (from Turcotte and Schubert, 1982) has been adopted. Other flow laws have also been used, however, such as that for a relatively weak wet quartzite (from Koch et al., 1980), a wet diorite (from Hansen and Carter, 1982), or a relatively strong orthopyroxenite (from Carter and Tsenn, 1987).

Figure 5.5 shows differential stresses, as a function of depth, for extensional deformation. Strength envelopes for compressional deformation show a very similar pattern. Results are shown for continental lithosphere with a surface heat flow of 50, 70 and 90 mW m^{-2}. It is clear that the thermal structure of the continental lithosphere has a large influence on its strength. For continental lithosphere with an elevated surface heat flow, there are pronounced minima for the strength of material at both the base of the upper crust and the base of the lower crust. The extensional strength T_{lit} of the lithosphere, obtained by integrating the depth dependent strength over the thickness of the plate ranges from about 1.8 x 10^{12} N/m (for Q_s = 90 mW m^{-2}) to about 3.5 x 10^{12} N/m (for Q_s = 50 mW m^{-2}).

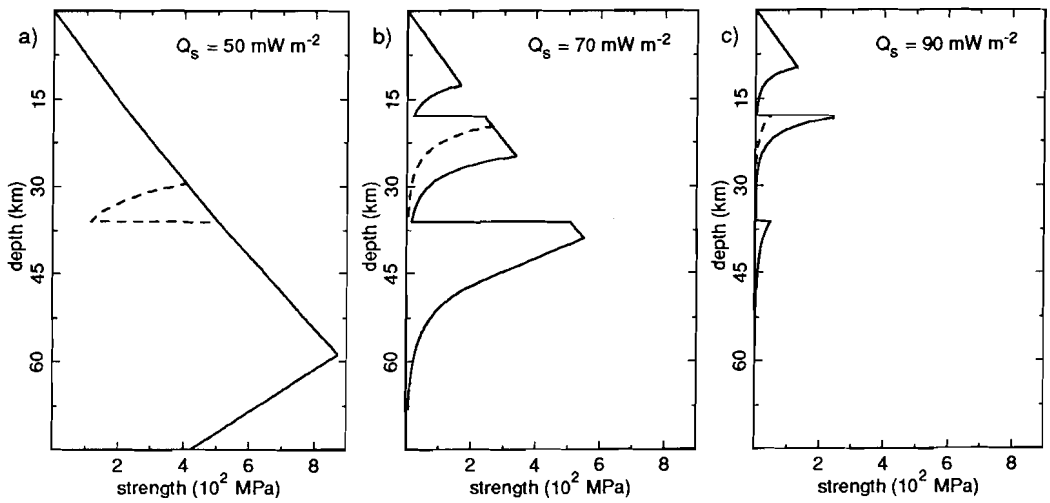

Figure 5.5. Strength envelopes for continental lithosphere with a surface heat flow of 50 mW m^{-2} (5.5a), 70 mW m^{-2} (5.5b), and 90 mW m^{-2} (5.5c). Flow laws for a wet quartzite, dry diabase and dry olivine have been used for upper crustal, lower crustal and mantle material respectively. Dashed line denotes a strength envelope for which a flow law for a wet diorite is used for lower crustal material. $\dot{\varepsilon} = 5 \times 10^{-14}$ s^{-1}.

It should be kept in mind that the strength envelopes given in Figure 5.5 are relatively simple and subject to considerable uncertainty (e.g., Carter and Tsenn, 1987). Several weakening mechanisms (e.g., pressure solution) can lead to a less pronounced maximum in strength near the brittle-ductile transition. Enhanced pore fluid pressures can lead to lower strengths for brittle deformation. Finally, the compositional structure of the continental crust is obviously much more complicated than that in our model, which assumes a simple twofold division into an upper granitic and a lower feldspathic or granulitic crust.

During the early phase of subduction, the increase in pressure will lead to greater strengths for brittle deformation, whereas on the other hand the increase in temperature will lead to smaller strengths for ductile deformation. Figures 5.6a - 5.6c show the strength of the continental lithosphere (T_{lit}) below the leading edge of the subducting continental plate (see Figure 5.1), as a function of the depth to which the leading edge has been subducted. The dashed lines in Figures 5.6a - 5.6c denote the contributions of the upper crust, lower crust and subcrustal lithosphere. It is clear that the thermal structure of the continental plate, just prior to its subduction, has a large influence on the strength of the continental plate during the early phase of its subduction. The strain rate for material within the subducting plate is always taken to be 10 % of the strain rate for material at the plate contact.

During the early phase of subduction, the strength T_{uc} of the upper crust changes rapidly (see Figure 5.6d). Initially the strength of the subducting upper crust increases as a consequence of increasing pressure, leading to greater strengths for brittle deformation. Once that the upper surface of the subducting continental plate has reached a depth of about 20 to 30 km, the strength of the upper crust starts to decrease rapidly, as a result of the increasing temperatures, leading to lower strengths for ductile deformation. The subduction process has a much less pronounced influence on the strength of the lower crust and the subcrustal lithosphere. Here, the amount by which temperatures increase is much smaller, compared to that within the upper crust. In particular, the strength of the subcrustal lithosphere is relatively independent of the depth to which the continental plate has been subducted.

Raising the convergence velocity leads to lower temperatures within the subducting continental plate, in particular within its upper crust. Nevertheless, the strength of the upper crust, as a function of the depth to which its upper surface has been subducted, exhibits a very similar pattern as that for a model with the standard set of parameters (see Figure 5.6e).

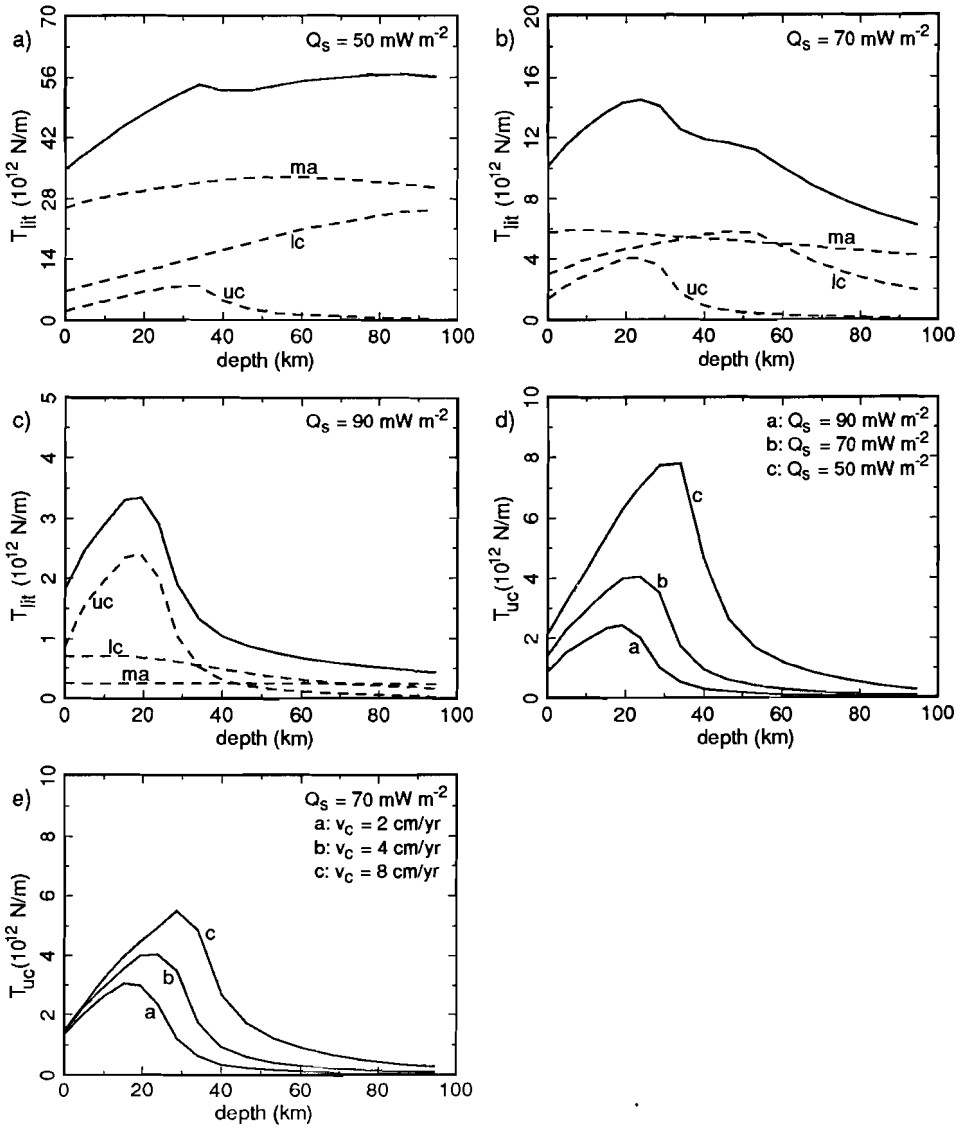

Figure 5.6. (a-c) Strength of the subducting continental lithosphere for extensional deformation (T_{lit}) beneath the leading edge of the subducting continental plate, as a function of the depth to which the leading edge has been subducted. Shown are results for the subduction of continental lithosphere with a surface heat flow of 50 mW m^{-2} (5.6a), 70 mW m^{-2} (5.6b) and 90 mW m^{-2} (5.6c). Dashed lines denote the contributions to the total strength of the plate by the upper crust (uc), the lower crust (lc), and the subcrustal or mantle part of the lithosphere (ma). All parameters are the same as for the standard model (see Table 5.1). Note, that different scales are used for the y-axis. (d-e) Strength of the upper crust for extensional deformation (T_{uc}) beneath the leading edge of the subducting continental plate, as a function of the depth to which the leading edge has been subducted. Figure 5.6d shows modelling results for various surface heat flows of 50, 70 and 90 mW m^{-2} (all parameters equal to those of the standard parameter set). Figure 5.6e shows results for various convergence velocities of 2, 4, and 8 cm/yr (all other parameters equal to those of the standard parameter set).

Resistive forces. Forces opposing the subduction of the continental lithosphere are due to the buoyancy of the continental crust and to friction at the plate contact. The low density of the continental crust leads to an upwards directed buoyancy force. This force is taken to depend linearly upon the difference in density between material within the subducting continental plate and material, situated at the same depth z, within the continental plate prior to its subduction. In agreement with the densities given in the thermal modelling section, a value of 600 kg/m^3 has been adopted for the difference in density between upper crustal and mantle material and a value of 300 kg/m^3 for the difference in density between lower crustal and mantle material. For the subcrustal part of the subducting continental plate, a thermal component of buoyancy forces has been included, which is determined by a difference in density:

$$\Delta\rho_{th} = \rho_m \, \alpha \, (T(x,z) - T'(z)) \tag{7}$$

where T′ is the temperature within a continental plate prior to its subduction. The thermal expansion coefficient α is taken to be 4×10^{-5} °C^{-1}.

The buoyancy of the downgoing continental lithosphere leads to a force (per unit length of trench; note that we only consider the component parallel to the downbending plate):

$$F_{bu} = \int \Delta\rho \; g \sin\delta \; dV \tag{8}$$

where integration takes place over the subducting continental plate between A - A′ and B - B′ (see Figure 5.1), and where δ is the dip of the downgoing plate.

Friction at the upper surface of the subducting continental crust leads to a resistive force F_{fr}, which is obtained by integrating shear stresses at the plate contact between points A and B.

The magnitude of these resistive forces, as a function of the depth to which the leading edge B has been subducted, is shown in Figure 5.7. Shown are results for a model in which the continental plate arriving at the subduction zone has a surface heat flow of 70 mW m^{-2}. Note, however, that buoyancy forces are relatively independent of the thermal structure of the subducting plate. As expected, the crustal component of the total buoyancy force is of opposite sign, and of considerably greater magnitude, than the subcrustal component. For the standard model ($\gamma = 0.05$), the resistive force due to friction is, during the early phase of subduction, approximately equal to that due to buoyancy. Once that low-strength ductile deformation starts to prevail at the plate contact, F_{fr} increases only slowly.

Break-up of subducting continental lithosphere. The magnitude of the resistive forces, acting upon the subducting continental plate, increases as the amount of subducting continental lithosphere increases. In order to continue subduction of the continental part of the subducting plate, these resistive forces must be overcome by forces F_A (acting upon the continental plate just prior to the onset of its subduction) and F_B (acting upon the

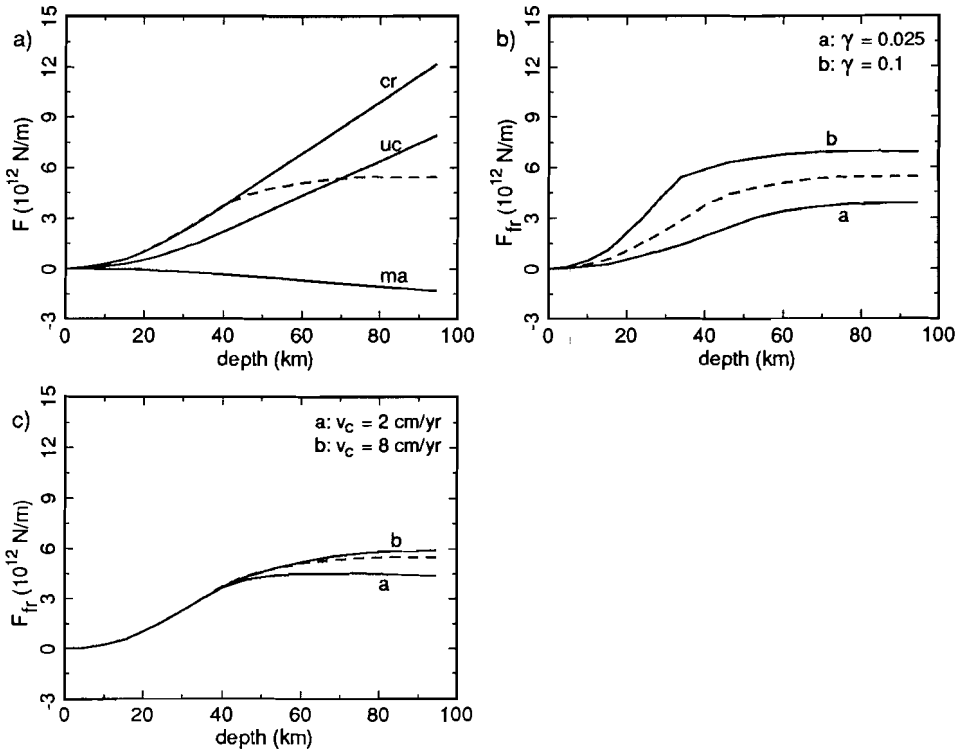

Figure 5.7. (a) Buoyancy forces acting upon subducting continental lithosphere, as a function of the depth to which the leading edge has been subducted. Curves denote the contributions by the upper crust (uc), crust (cr), and subcrustal lithosphere (ma). Dashed line denotes F_{fr}. All parameters are the same as for the standard model. Surface heat flow of the subducting plate is 70 mW m^{-2}. (b-c) The resistive force F_{fr}, caused by friction at the plate contact, as a function of the depth to which the leading edge has been subducted. Heat flow of the subducting continental plate is 70 mW m^{-2}. Shown are results for models with different values for γ of 0.025 and 0.1 (5.7b) and with different values of the convergence velocity v_c of 2 and 8 cm/yr (5.7c). Dashed line denotes modelling results for the standard model.

continental plate beneath the leading edge). Maximum values that these forces can attain are determined by the strength of material. Continuation of subduction of the subducting plate is no longer possible once that sum of the resistive forces becomes greater than the sum of these maximum values of F_A and F_B. This also applies to parts of the subducting plate. For the upper crust between the left side of the model and the leading edge, for instance, we have used the following condition for the detachment of the continental upper crust from the other parts of the subducting plate:

$$F_{res} = C_{A,uc} + T_{B,uc} + F_{base,uc} \qquad (9)$$

where F_{res} is the sum of the resistive forces acting upon the upper crust (due to its buoyancy and to friction at the plate contact). $C_{A,uc}$ is the strength for compressional deformation of the upper crust, just prior to its subduction; $T_{B,uc}$ the strength for extensional deformation (see also Figures 5.6d and 5.6e) of the upper crust beneath the leading edge. $F_{base,uc}$ is obtained by integrating shear stresses (taken to be equal to $0.5(\sigma_1 - \sigma_3)$ over the entire length of the base of the upper crust, where $\sigma_1 - \sigma_3$ is inferred from a flow law for a wet quartzite, using a strain rate equal to that at the plate contact. Similar conditions for detachment have been made for the crust between the left side of the model and the leading edge, as well as for the entire continental lithosphere. In the former case the maximum force $F_{base,cr}$ that can be exerted upon the base of the crust is obtained by integrating shear stresses (inferred from the same flow law that is used for lower crust) over the base of the crust. In the latter case the maximum force F_{base} that can be exerted upon the base of the subducting continental lithosphere is taken to be zero, as the strength of material at the lithosphere-asthenosphere boundary is very low.

The validity of this approach has been investigated by van den Beukel (1989) in a study that focused on the break-up of very young oceanic lithosphere, in the upper part of a subduction zone, during a ridge-trench interaction. The break-up process was studied both with a condition for detachment similar to that given above, and with a finite element model of deformation and stress throughout the subducting plate. The latter model included the effect of bending of the plate. The times at which break-up occurred, as predicted by these two types of models, were found to be in good agreement with each other (see also Figure 6 in van den Beukel, 1989). The use of a relatively simple condition for detachment, as given above, thus seems justified.

Modelling results are shown in Figure 5.8. Shown is the depth to which the leading edge has been subducted at the time at which the condition for detachment for the upper crust (or, alternatively, of both upper and lower crust or the entire continental lithosphere) is reached. Figure 5.8a shows results for models in which a dry diabase rheology has been adopted for the lower crust. It is clear that an increase of the surface heat flow of the subducting continental plate results in a more shallow depth at which the condition for detachment is reached. Subduction of continental lithosphere may here lead to the detachment of the upper crust from the subducting plate (see also Figure 5.9a). This requires subduction of the leading edge of the downgoing plate to a depth of at least 30 km. If, however, a weaker flow law (e.g., a wet diorite or a wet quartzite) is used for lower crustal material, the condition for the detachment of the entire crust is reached at an earlier time than that of the upper crust. In general, we expect the strength of the lower crust to be greater than that inferred from a wet quartzite rheology. Due to the uncertainty of the strength of lower crustal material, it is not clear whether break-up of a subducting continental plate will in general lead to the detachment of the upper crust only (leading to a new plate contact at mid-crustal levels) or to the detachment of both upper and lower crust (leading to a new plate contact at the base of the crust).

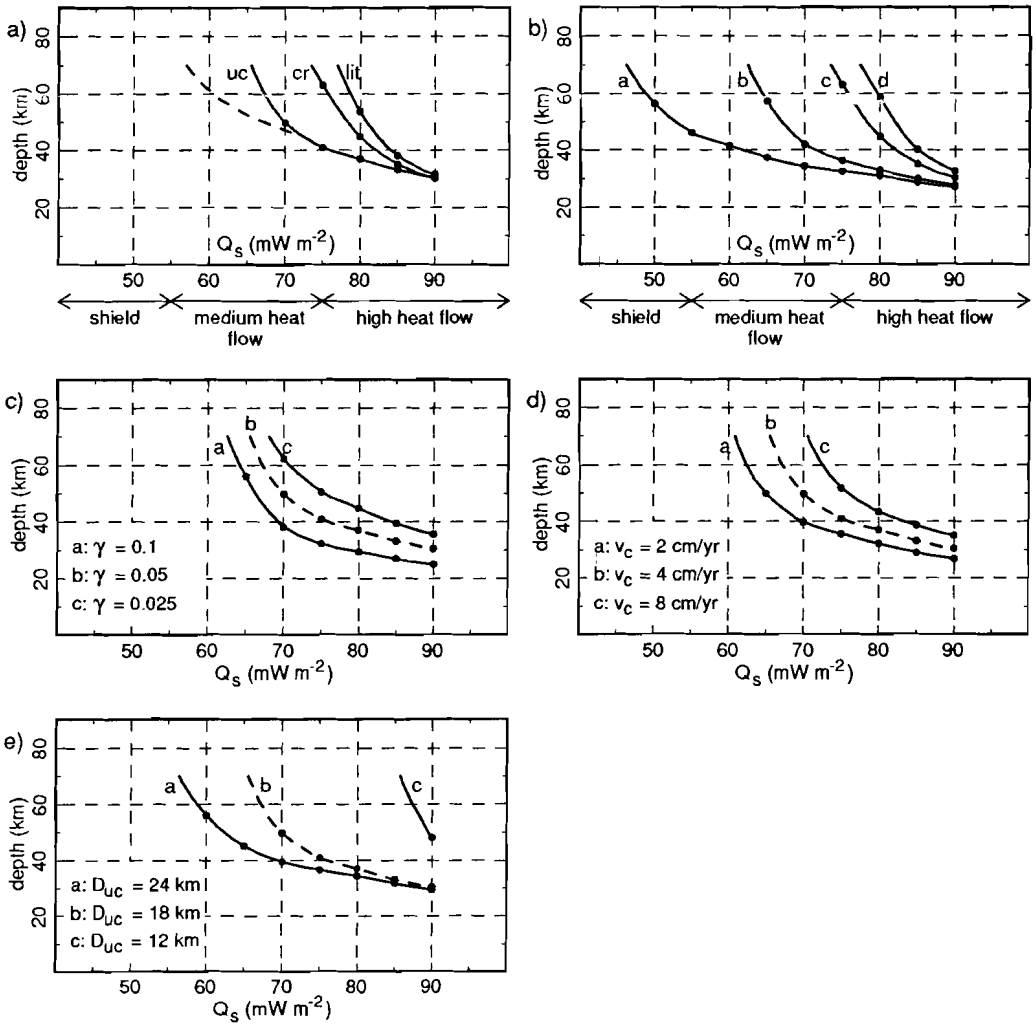

Figure 5.8. Depth to which the leading edge of the continental plate (Point B in Figure 5.1) has been subducted, at the time that the condition for detachment is reached. (a) Modelling results for detachment of the upper crust (uc), crust (cr) and entire continental lithosphere (lit) for the standard model (v_c = 4 cm/yr; $D_{uc} = D_{lc}$ = 18 km; γ = 0.05). Dashed line denotes detachment of a relatively small part of the upper crust near the leading edge (see text). (b) Detachment of the entire crust, for a case in which a flow law for a wet quartzite is used for lower crustal material (curve a), a wet diorite flow law (curve b), a dry diabase flow law (curve c), and a flow law for an orthopyroxenite (curve d). (c) Detachment of the upper crust, for different shear stresses at the plate contact, γ being equal to 0.025 or 0.1. Dashed line denotes standard model. (d) Detachment of the upper crust, for different convergence velocities between the two plates, v_c being equal to 2 or 8 cm/yr. Dashed line denotes standard model. (e) Detachment of the upper crust, for different thicknesses of the upper and lower crust, D_{uc} (= D_{lc}) being equal to 12 or 24 km. Radiogenic heat production rates are taken to be equal to those for the standard model. Dashed line denotes standard model.

For other aspects of the subduction of continental lithosphere, there is less uncertainty. For all model calculations that have been made, the condition for detachment of either upper crust or both upper and lower crust is reached at an earlier time than the condition for break-up of the entire continental lithosphere. We thus do not expect that subduction of continental lithosphere can lead to the transfer of mantle material, originating from the subcrustal part of the subducting continental plate, to the upper plate.

In addition, it is clear that the thermal structure of the subducting plate has a large influence on the depth to which continental crust can be subducted. For high-heat flow continental lithosphere ($Q_s > 75$ mW m^{-2}), detachment of the upper crust, for instance, occurs when the leading edge has reached a depth of about 30 to 40 km, at a depth when the strength of the upper crust has decreased to a relatively low value (see also Figure 5.6). For a typical shield area ($Q_s < 50$ mW m^{-2}), the strength of the subducting upper crust decreases more slowly. In particular, however, it is the absence of a low-strength zone at the base of the upper crust (see also Figure 5.5) that precludes the detachment of upper crustal material from the subducting plate at smaller depths.

Other calculations, for different convergence velocities and thicknesses of the upper crust, are shown in Figures 5.8c - 5.8e. Except otherwise stated, all parameters are equal to those of the standard parameters set (see Table 5.1). A smaller convergence velocity leads to higher temperatures within the subducting plate and thus to smaller strengths. As a result, the condition for detachment is reached at an earlier time. Raising the thickness of the upper crust also leads to break-up at an earlier time, as it decreases the strength the strength of material at the base of the upper crust and increases buoyancy forces forces that act upon upper crustal material. Varying parameters, such as the convergence velocity, has a similar effect on the depth at which the condition for detachment of the crust (or alternatively the entire plate) is reached, but the differences between the various models tend to be smaller.

Up to now, we have only considered the detachment of bodies for which the left boundary coincides with the left boundary of the thermal model and for which the right boundary coincides with (part of) the profile B - B′ in Figure 5.1. In addition the base of these bodies is situated at the base of the upper crust, the lower crust or the lithosphere. This is an obvious choice as the base of the upper crust or lower crust coincides with a strength minimum. Further, after an initial increase in strength, the strength of the upper crust or lower crust is generally lowest beneath the leading edge of the subducting continental lithosphere. Numerous other calculations have been made, however, for other geometries. In general, we have found that the condition for detachment is reached first for bodies with a geometry as described above. To this, there is one exception which concerns bodies of upper crustal material with the base situated at the base of the upper crust, the right boundary beneath the leading edge and the left boundary at only at a relatively small distance (less than about 50 km) from the leading edge. The left boundary of such a body may thus fall within a region where the strength of the subducting upper crust has already

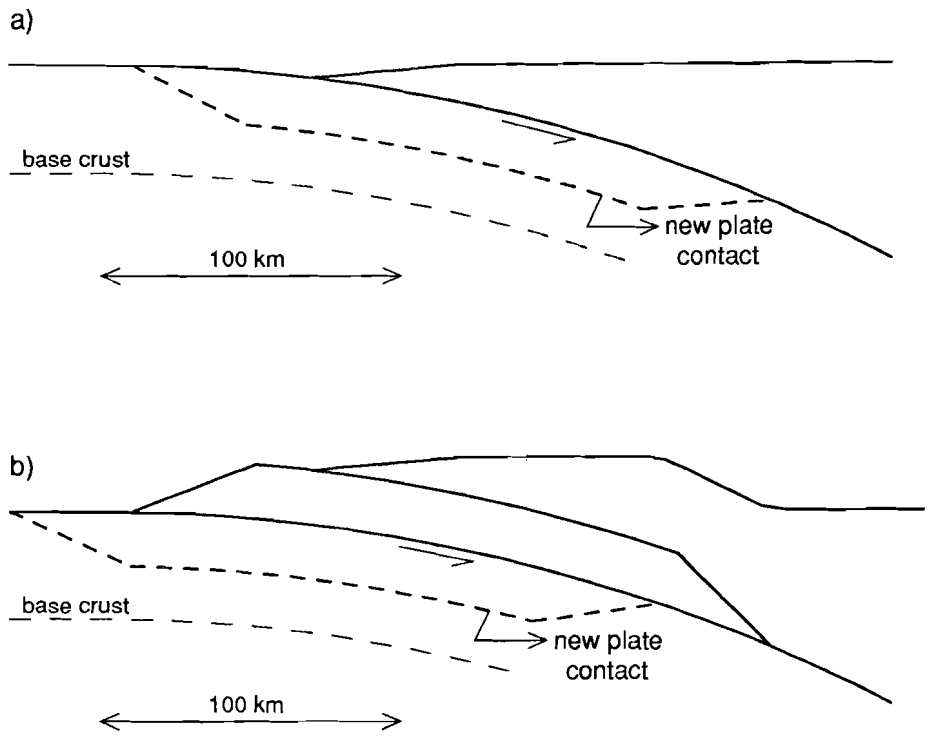

Figure 5.9. (a) Schematic representation of the detachment of the upper crust. (b) Schematic representation of the stacking of thrust sheets.

decreased to a very low value (see Figure 5.6). The depth to which the leading edge has been subducted at the time when the condition for detachment for such a body is reached is given by the dashed line in Figure 5.8a. The relatively small length of such a body may preclude the transfer of all of the upper crustal material to the upper plate. Nevertheless, 'underplating' of such low-strength material, at depths greater than about 50 km, can be an alternative mechanism for the transfer of material to the upper plate, compared to the detachment of relatively large and elongated sheets as described above.

The condition for detachment, as given above, does not take into account the transition zone between the subducting continental and oceanic lithosphere. Rather than making a more detailed study on the subduction of a continental margin, we here want to focus on the subduction of continental lithosphere in general. We expect the influence of the transition zone to be relatively small, however, as the depth to which continental crust can be subducted increases rapidly, if the crustal thickness of the subducting plate is decreased (see Figure 5.8).

The influence of phase changes has not been included in the models. At increasing depths, it becomes increasingly more likely that phase changes will lead to a reduction in the density difference between crustal and mantle material (Richardson and England, 1979). We have thus in Figure 5.8 refrained from giving model results if the depth of the leading edge becomes greater than 70 km. There is considerable uncertainty on the depth at which phase changes to eclogite will take place, which is in particular due to the role of reaction rates (Ahrens and Schubert, 1975). Our modelling results may give a relatively low estimate of the depth of the leading edge at which the condition for detachment is reached, if the depth of the leading edge becomes greater than about 40 km.

Concluding remarks. In summary, it is concluded that a continental plate may break up during the early phase of its subduction, leading to the detachment of (part of) the continental crust from the subducting plate.

If break-up occurs, this is due to the resistive forces (friction, buoyancy) that act upon subducting continental crust, in combination with the relatively low strength of the subducting continental crust. The buoyancy of continental crust in itself is not sufficient to preclude its subduction to mantle depths. Young oceanic lithosphere, less than about 40 Myr old, will also be relatively buoyant during the early phase of its subduction (prior to the basalt-eclogite phase change). Nevertheless, the greater strength of oceanic lithosphere, and in particular the absence of zones with very low strength within the oceanic plate, in general precludes the break-up of such young oceanic lithosphere during the early phase of its subduction, except during the interaction between a relatively fast spreading ridge and a subduction zone (van den Beukel, 1989). In the latter case, detachment was found to involve both the crustal and the subcrustal part of a very young, subducting oceanic plate.

The depth to which continental lithosphere can be subducted coherently will be primarily determined by the thermal and compositional structure of the subducting plate (represented in our modelling by parameters such as the surface heat flow Q_s and the thickness of the upper and lower crust) and the convergence velocity between the two plates. Our modelling predicts for instance that the upper crust of a cold continental shield can be subducted to a much greater depth than the upper crust of a continental plate with relatively high surface heat flow (see Figure 5.8). The modelling results as shown in Figure 5.8 are subject to considerable uncertainty (e.g., as a result of the uncertainty in the strength of the lower crust). Based on our modelling results, we can not predict whether break-up leads to the detachment of the upper crust only or, alternatively, of both the upper and the lower crust. The near-absence of lower crustal material in orogenic belts suggests, however, that the former situation is more likely.

It should be kept in mind that the remarks made on the uncertainty of the strength envelopes as given in Figure 5.5 (see above and Carter and Tsenn, 1987) apply just as well on the results of our mechanical modelling (given in Figure 5.8). It is difficult to quantify this uncertainty. Nevertheless, two aspects of our mechanical modelling results seem

relatively robust. First, the detachment of (part of) the continental crust, once that the leading edge of the subducting crust has reached a depth of about 30 to 50 km, for continental lithosphere with a relatively high surface heat flow ($> \pm 75$ mW m^{-2}). This because the actual strength of continental material is likely to be smaller than the strength of material as given in a strength envelope such as Figure 5.5. Secondly, the subduction of both upper and lower crust to depths of about 70 km or more, for the subduction of continental lithosphere with a low surface heat flow ($< \pm 50$ mW m^{-2} for the situation modelled in Figure 5.8a). This because detachment requires the existence of a very low strength zone within the continental crust, which is absent in a continental plate with very low heat flow or, alternatively, with a very thin crust.

Our modelling indicates that in some cases, continental crust (both upper crust and lower crust) can be subducted to mantle depths. In particular this may be the case for the subduction of continental lithosphere with a low surface heat flow, as well as for the early phase of subduction of continental lithosphere. The latter situation is likely to involve the subduction of continental lithosphere with a relatively small crustal thickness, at a relatively high rate.

5.4 Discussion

Continuation of subduction of continental lithosphere. The force opposing the subduction of continental lithosphere, caused by processes within the upper part of a subduction zone (the region encompassed in our thermal model), is determined by friction at the plate contact and by buoyancy forces. An upper limit for this resistive force is the force exerted upon the subducting plate for the subduction of a cold continental plate. At the time that the leading edge reaches the right boundary of the thermal model, this force may range up to about 1.8×10^{13} N/m. This is an upper limit as phase changes are likely to increase the density of the continental crust, prior to the moment that it reaches the right boundary of the model. A lower limit is given by the resistive force, exerted upon a relatively hot subducting continental plate, at the time that it breaks up. For a subducting plate with a surface heat flow greater than 80 mW m^{-2} this force amounts to about 0.4×10^{13} N/m. This value is even somewhat lower than the resistive force of about 0.6×10^{13} N/m, due to friction at the plate contact, during the preceding subduction of oceanic lithosphere.

Gravitational forces exerted upon subcrustal continental lithosphere, which is subducted into the mantle, may in part compensate the resistive forces within the upper part of the subduction zone. Thus the net resistive force exerted upon the subducting plate is likely to be smaller than the total resistive force due to processes within the upper part of the subduction zone.

The continuation of subduction of continental lithosphere at a segment of a subduction

zone will be determined by the forces exerted on all the boundaries of the plate. Thus no generally applicable rules can be given and the total amount of convergence at continental collision zones may vary widely. In all cases that the subduction of continental lithosphere has been preceded by the subduction of oceanic lithosphere, however, a certain amount of continental lithosphere will be subducted as a consequence of the slab pull exerted by the earlier subducted oceanic lithosphere.

After the detachment or thermal assimilation of earlier subducted oceanic lithosphere, subduction of continental lithosphere will lead to a net resistive force. Continuation of subduction of continental lithosphere now requires that this net resistive force is overcome by net driving forces that are exerted upon other parts of the plate. This seems to be the case for the Indo-Australian plate, where the net resistive force at the Himalayas is compensated by ridge push forces (up to about 3×10^{12} N/m) and net driving forces due to slab pull, which may range up to about 1×10^{13} N/m for the subduction of relatively old oceanic lithosphere (England and Wortel, 1980; Wortel, 1980). For such a situation there is no theoretical upper limit for the amount of convergence that can take place at a continental collision zone.

Stacking of thrust sheets. Subduction of continental lithosphere may well continue after that (part of) the continental crust has been detached, leading to the emplacement of a relatively large thrust sheet (see also Figure 5.9). If this thrust sheet consists of upper crustal material, most of the new plate contact will initially have a temperature of about 350 - 500 °C. For the detachment of the entire crust, these temperatures may range from about 450 - 850 °C. Some simple modelling results are shown in Figure 5.10. Here, it is assumed that the upper crust is detached. After its detachment, velocities within the upper crust are taken to be zero. At this time the upper surface of the subducted continental crust is situated at the line A - B. For simplicity, it is assumed that the location of the plate boundary is changed throughout the modelled region, the new plate boundary being situated at the line AA - CC. Further it has been assumed during the thermal modelling that continental lithosphere, now arriving at the subduction zone, is instantaneously subducted to a depth of about 20 km (the depth of point AA at the base of the detached upper crust), which is obviously a gross simplification. Temperatures at a given section of the new plate contact will start to decrease rapidly once that underthrusting of relatively cold material is occurring. Eventually, continuation of subduction can lead to a similar situation as described above, which may again lead to break-up and detachment of (part of) the crust. The thermal structures, given in Figure 5.10, represent the situation at the time that a condition for the detachment of the upper crust, similar to that given above in the section on mechanical modelling, is reached. The depth to which the leading edge (denoted by point BB in Figure 5.10) has been subducted at this moment may differ from that at the time of the first break-up, (e.g., as a result of the different initial thermal structure of the material above the plate contact). Shear stresses at the new plate contact may also differ, although it seems likely that subduction of sediments and fluids will again lead to relatively

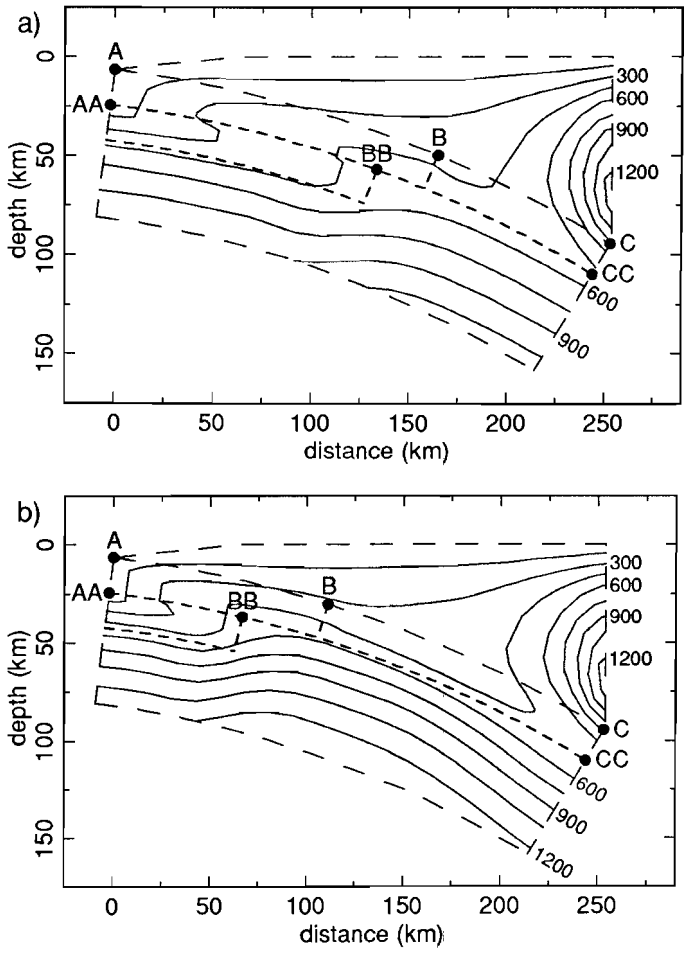

Figure 5.10. Thermal structure at the moment that the condition for detachment is reached for the second time. Heat flow of the subducting continental plate is 70 mW m^{-2} (5.10a) or 90 mW m^{-2} (5.10b). All parameters are equal to those of the standard parameter set.

low shear stresses at the plate contact during brittle deformation. For the modelling results shown in Figure 5.10, shear stresses at the new plate contact are determined by the same rheology that was used for the old plate contact.

Continuation of subduction of continental lithosphere may thus lead to stacking of thrust sheets. A schematic representation of this process is given in Figure 5.9b. Over a period of time of a few tens of Myr, the upper part of the structure of stacked thrust sheets will slowly be eroded. Continental material that is detached, after having been subducted to

a depth of a few tens of km, will only reach its peak metamorphic temperatures during the relatively slow, subsequent uplift phase. Pressure-temperature paths, inferred for material such as that currently exposed in the Tauern Window in the Alps (Droop, 1985; Selverstone, 1985), primarily constrain conditions during the uplift phase, but are not in disagreement with an early subduction phase of relatively low-T high-P blueschist facies conditions, similar to that in our thermal models.

Comparison with the structure of orogenic belts. In our models, we have only considered deformation within the subducting lower plate. Part of the convergence between the two plates may be accommodated by deformation in the upper plate, however. Subduction and deformation of the Indian plate may have accounted for about 700 (± 300) km of convergence during the early phase of the India-Eurasia continental collision (Patriat and Achache, 1984). At later stages, however, most of the convergence between the two plates has been accommodated by lateral expulsion and thrusting in a broad zone within the Eurasian plate (Chengfa et al., 1986; Tapponier et al., 1986). At present, underthrusting of the Indian plate at the Himalayas occurs at a rate of about 1 - 2 cm/yr, the total convergence rate between India and Eurasia being about 5 cm/yr (Molnar, 1984). For the Alps most convergence has been accommodated by subduction and deformation of the European plate (e.g., Butler, 1986).

Thrust faults bounding large crystalline basement segments are a common feature of orogenic belts (e.g., Brewer et al., 1981). Displacements of at least 100 km have been inferred for the Main Central Thrust and the still active Main Boundary Fault in the Himalayas (Molnar, 1984). For the Alps, large displacements are thought to have occurred at the Austroalpine and Frontal Pennine thrusts. Significant amounts of continental crust have been subducted on such dominant thrust faults. The stacking of large crystalline thrust sheets has been shown to be of prime importance for the structure of a number of orogenic belts (e.g., Bradbury and Nolen-Hoeksema (1985) and Butler et al. (1986) for the Alps; Molnar (1984) and Mattauer (1986) for the Himalayas, and Norton (1986) for the Norwegian Caledonides). Apparently, the structure of these orogenic belts has been largely determined by the development of two duplex structures; one that consists of crystalline basement and one that consists of its sedimentary cover. The length of such large scale crystalline thrust sheets in orogenic belts is typically about 100 - 200 km; the thickness about 10 - 20 km (Hatcher and Williams, 1986). These dimensions suggest that detachment of the upper crust, leading to a new plate contact at mid-crustal levels, is more likely than the detachment of both upper and lower crust.

During the initial phase of subduction, the strength of the upper crust increases significantly as a result of an increase in pressure, leading to greater strengths for brittle deformation. For a strength envelope based on a quartzite rheology, as given in Figure 5.5, an increase of the pressure at the top of the plate of 1 kbar (corresponding to subduction of continental lithosphere below a column of foreland basin sediments with a thickness of

about 4 km) leads to an increase in the strength of the upper crust, for compressional deformation, of about 40 % (Q_s = 40 mW m^{-2}) to 65 % (Q_s = 100 mW m^{-2}). It thus may well be that imbrication and thrusting within the upper crust of the downbending plate is initiated in the region where the plate starts to downbend, near the edge of the foreland basin, and thus at some distance from the orogenic belt itself. For the Alpine region, such a situation may have occurred beneath the Jura Mountains, where reflection seismic data indicate that the southern margin of the Jura Mountains is associated with a major basement imbrication (Ziegler, 1982).

A quantitative comparison between model results and the structure of orogenic belts is difficult, since it requires an estimate of the depth to which continental crust has been subducted in orogenic belts as well as estimates of properties of the subducted continental plate. These properties can only be estimated for continental lithosphere close to the orogenic belt, that has not yet been subducted, and may thus be considerably in error. The following discussion should thus be regarded as tentative.

The structure of the Alps is compatible with stacking of thrust sheets and subduction of the upper surface of the continental crust to a maximum depth of about 30 - 45 km (e.g., Menard and Thouvenot, 1984). The heat flow of European continental lithosphere, just North and West of the Alps is about 70 - 90 mW m^{-2} (Cermak, 1979). Subduction of such continental lithosphere is likely to lead to detachment of (part of) the crust, provided that the thickness of the subducting crust is not relatively small.

For the central part of the Himalayas (near 85 to 90 °E), thrusting at a number of major faults (Main Boundary thrust, Main Central thrust, Kangmar thrust) has resulted in stacking of thrust sheets (Allègre et al., 1984; Molnar, 1984). The crustal thickness of the resulting structure is about 75 km. For the western part of the Himalayas, seismicity extends to a depth of about 300 km in the Pamir-Hindu Kush region (Chatelain et al., 1980). Based on inversions of the 3-D velocity structure of this region, Roecker (1982) has proposed that continental lithosphere (possibly including the entire continental crust) has here been subducted to mantle depths. Although the amount of convergence has been similar, the extent of the crustal-stacking wedge seems to be much greater for the central part of the Himalayas than for the western part (Mattauer, 1986). Sparse heat flow data for the Indian shield, South of the central part of the Himalayas range between about 60 and 80 mW m^{-2} (Gupta, 1982; Negi et al., 1986). Heat flow data in the northern part of the Indian shield, West of approximately 80 °E are considerably lower (about 40 - 55 mW m^{-2}; Gupta, 1982).

Evidence for the subduction of continental crust to mantle depths may be most conclusive for the subduction of Australian continental lithosphere at the Banda arc. Here, seismicity studies indicate the subduction of continental crust to a depth of about 150 km (McCaffrey et al., 1985). At least part of this crust will have been of relatively small thickness as it belonged to the now subducted continental margin. The geochemical

composition of the Banda arc rocks also points to derivation (at least in part) of subducting continental crust (e.g., Poreda and Craig, 1989). Our modelling indicates that the subduction of a relatively thin continental crust, with a relatively high velocity, may well lead to the subduction of both upper and lower crust to mantle depths.

Acknowledgements. I thank Rinus Wortel, Sierd Cloetingh and N. J. Vlaar for their support, and for many discussions, over the last four years. I thank Royal Dutch/Shell for a research grant which enabled me to complete a PhD thesis, of which the present paper is part.

References

Ahrens, T. J., and G. Schubert, Gabbro-eclogite reaction rate and its geophysical significance, *Rev. Geophys. Space Phys., 13,* 383-400, 1975.

Allègre, C. J., and 34 others, Structure and evolution of the Himalaya-Tibet orogenic belt, *Nature, 307,* 17-22, 1984.

Bally, A. W., Thoughts on the tectonics of folded belts, in *Thrust and nappe tectonics, Geol. Soc. London, Spec. Publ., 9,* edited by K. R. McClay and N. J. Price, pp. 13-32, Oxford, 1981.

Bird, P., Initiation of intracontinental subduction in the Himalaya, *J. Geophys. Res., 83,* 4975-4987, 1978.

Boyer, S. E., and D. Elliot, Thrust systems, *Bull. Am. Assoc. Petrol. Geol., 66* 1196-1230, 1982.

Bradbury, H. J., and R. C. Nolen-Hoeksema, The Lepontine Alps as an evolving metamorphic core complex during A-type subduction: evidence from heat flow data, mineral cooling ages, and tectonic modeling, *Tectonics, 4,* 187-211, 1985.

Brewer, J. A., F. A. Cook, L. D. Brown, J. E. Oliver, S. Kaufman, and D. S. Albaugh, COCORP seismic reflection profiling across thrust faults, in *Thrust and nappe tectonics, Geol. Soc. London, Spec. Publ., 9,* edited by K. R. McClay and N. J. Price, pp. 501-511, Oxford, 1981.

Burchfiel, B. C., Eastern European Alpine system and the Carpathian orocline as an example of collision tectonics, *Tectonophysics, 63,* 31-61, 1980.

Butler, R. W. H., Thrust tectonics, deep structure and crustal subduction in the Alps and Himalayas, *J. Geol. Soc. London, 143,* 857-873, 1986.

Butler, R. W. H., S. J. Matthews, and M. Parish, The NW external Alpine Thrust Belt and its implications for the geometry of the western Alpine Orogen, in *Collision tectonics, Geol. Soc. London, Spec. Publ., 19,* edited by M. P. Coward and A. C. Ries, pp. 245-260, Oxford, 1986.

Byerlee, J. D., Friction of rocks, *Pure Appl. Geophys., 116,* 615-626, 1978.

Carter, N. L., and M. C. Tsenn, Flow properties of continental lithosphere, *Tectonophysics, 136,* 27-63, 1987.

Cermak, V., Heat flow map of Europe, in *Terrestrial heat flow in Europe,* edited by V. Cermak and L. Rybach, pp. 3-40, Springer, Berlin, 1979.

Chapman, D. S., Thermal gradients in the continental crust, in *The nature of the lower continental crust, Geol. Soc. London, Spec. Publ., 24,* edited by J. B.. Dawson et al., pp. 63-70, 1986.

Chatelain, J. L., S. W. Roecker, D. Hatzfeld, and P. Molnar, Microearthquake seismicity and fault plane solutions in the Hindu Kush region and their tectonic implications, *J. Geophys. Res., 85,* 1365-1387, 1980.

Chengfa, C. and 26 others, Preliminary conclusions of the Royal Society and Academia Sinica 1985 geotraverse of Tibet, *Nature, 323,* 501-507, 1986.

Crough, S. T., Thermal model of oceanic lithosphere, *Nature, 256,* 388-390, 1975.

Davis, D., J. Suppe, and F. A. Dahlen, Mechanics of fold-and-thrust belts and accretionary wedges, *J. Geophys. Res., 88,* 1153-1172, 1983.

Droop, G. T. R., Alpine metamorphism in the south-east Tauern Window, Austria: 1. P-T variations in space and time, *J. Metamorphic Geol., 3,* 371-402, 1985.

England, P., and R. Wortel, Some consequences of the subduction of young slabs, *Earth Planet. Sci. Lett., 47,* 403-415, 1980.

Gillet, P., P. Choukroune, M. Ballèvre, and P. Davy, Thickening history of the western Alps, *Earth Planet. Sci. Lett., 78,* 44-52, 1986.

Goetze, C., and B. Evans, Stress and temperature in the bending lithosphere as constrained by experimental rock mechanics, *Geophys. J. R. Astron. Soc., 59,* 463-478, 1979.

Gupta, M. L., Heat flow in the Indian Peninsula - Its geological and geophysical implications, *Tectonophysics, 83,* 71-90, 1982.

Hansen, F. D.., and N. L. Carter, Creep of selected rocks at 1000 MPa (abstract), *Eos Trans. AGU, 63,* 437, 1982.

Hatcher, R. D.., and R. T. Williams, Mechanical model for single thrust sheets. Part I: Taxonomy of crystalline thrust sheets and their relationships to the mechanical behavior of orogenic belts, *Geol. Soc. Am. Bull., 97,* 975-985, 1986.

Hsui, A. T., B. D. Marsh, and M. N. Toksöz, On melting of the subducted oceanic crust: effects of subduction induced mantle flow, *Tectonophysics, 99,* 207-220, 1983.

Koch, P. S., J. M. Christie, and R. P. George, Flow law of "wet" quartzite in the alpha quartz field (abstract), *Eos Trans. AGU, 61,* 376, 1980.

Mattauer, M., Intracrustal subduction, crust-mantle decollement and crustal-stacking wedge in the Himalayas and other collision belts, in *Collision tectonics, Geol. Soc. London, Spec. Publ., 19,* edited by M. P.. Coward and A. C.. Ries, pp. 37-50, Oxford, 1986.

McCaffrey, R., P. Molnar, S. W. Roecker, and Y. S. Joyodiwiryo, Microearthquake seismicity and fault plane solutions related to arc-continent collision in the eastern Sunda arc, Indonesia, *J. Geophys. Res., 90,* 4511-4528, 1985.

McKenzie, D. P., Speculations on the consequences and causes of plate motion, *Geophys. J. R. Astr. Soc., 18,* 1-18, 1969.

Meissner, R., *The continental crust,* 426 pp., Academic Press, Orlando, 1986.

Ménard, G. and F. Thouvenot, Ecaillage de la lithosphère européene sous les Alpes Occidentales: arguments gravimétriques et sismiques liés à l'anomalie d'Ivrea, *Bull Soc. Géol. France, 26,* 875-884, 1984.

Molnar, P., Structure and tectonics of the Himalaya, *Ann. Rev. Earth Planet. Sci., 12,* 489-518, 1984.

Molnar, P., and D. Gray, Subduction of continental lithosphere, some constraints and uncertainties, *Geology, 7,* 58-62, 1979.

Negi, J. G., O. P. Pandey, and P. K. Agrawal, Super-mobility of hot Indian lithosphere, *Tectonophysics, 131,* 147-156, 1986.

Norton, M. G., Late Caledonide extension in western Norway: a response to crustal thickening, *Tectonics, 5,* 195-204, 1986.

Patriat, P. and J. Achache, India-Eurasia collision chronology has implications for crustal shortening and driving mechanism of plates, *Nature, 311,* 615-621, 1984.

Pollack, H. N., and D. S. Chapman, On the regional variation of heat flow, geotherms, and lithospheric thickness, *Tectonophysics, 38,* 279-296, 1977.

Poreda, R. and H. Craig, Helium isotope ratios in circum-Pacific volcanic arcs, *Nature, 338,* 473-478, 1989.

Richardson, S. W., and P. C. England, Metamorphic consequences of crustal eclogite production in overthrust orogenic zones, *Earth Planet. Sci. Lett., 42,* 183-190, 1979.

Roecker, S. W., Velocity structure of the Pamir-Hindu Kush region: Possible evidence of subducted

crust, *J. Geophys. Res., 87,* 945-959, 1982.

Selverstone, J., Petrologic constraints on imbrication, metamorphism, and uplift in the SW Tauern Window, Eastern Alps, *Tectonics, 4,* 687-704, 1985.

Sibson, R. H., Frictional constraints on thrust, wrench and normal faults, *Nature, 249,* 542-544, 1974.

Tapponier, P., G. Peltzer, and R. Armijo, On the mechanics of the collision between India and Asia, in *Collision tectonics, Geol. Soc. London, Spec. Publ., 19,* edited by M. P.. Coward and A. C.. Ries, pp. 115-157, Oxford, 1986.

Tatsumi, Y., M. Sakuyama, H. Fukuyama, and I. Kushiro, Generation of arc basalt magmas and thermal structure of the mantle wedge in subduction zones, *J. Geophys. Res., 88,* 5815-5825, 1983.

Turcotte, D. L. and G. Schubert, *Geodynamics,* 450 pp., Wiley, New York, 1982.

van den Beukel, J., and R. Wortel, Temperatures and shear stresses in the upper part of a subduction zone, *Geophys. Res. Lett., 14,* 1057-1060, 1987.

van den Beukel, J., and R. Wortel, Thermo-mechanical modelling of arc-trench regions, *Tectonophysics, 154,* 177-193, 1988 (Chapter 2 of this thesis).

van den Beukel, J., Break-up of young oceanic lithosphere in the upper part of a subduction zone: Implications for the emplacement of ophiolites, *Tectonics,* in press, 1989 (Chapter 4 of this thesis).

Watanabe, T., M. G. Langseth, and R. N. Anderson, Heat flow in back-arc basins of the western Pacific, in *Island arcs, deep sea trenches and back-arc basins,* edited by M. Talwani and W. C.. Pitman, pp. 137-160, AGU, Washington D.C., 1977.

Williams, G. D., Thrust tectonics in the south central Pyrenees, *J. Struct. Geol., 7,* 11-17, 1985.

Wortel, M. J. R., Age-dependent subduction of oceanic lithosphere, Ph. D. Thesis, 147 pp., Univ. of Utrecht, Utrecht, 1980.

Ziegler, P. A., *Geological atlas of Western and Central Europe,* 130 pp., Shell Int. Petrol. Maatschappy, Den Haag, 1982.

Samenvatting

In het plaattektonisch model wordt het buitenste gedeelte van de aarde, de lithosfeer, gezien als een mozaïek van relatief sterke platen die ten opzichte van elkaar bewegen. Het merendeel van de tektonische en vulkanische activiteit op aarde speelt zich af bij de plaatgrenzen. Met name de divergente plaatgrenzen zoals mid-oceanische ruggen (waar nieuwe oceanische lithosfeer wordt gecreëerd) en de convergente plaatgrenzen (waar oceanische lithosfeer wordt gesubduceerd in de mantel) spelen hierbij een belangrijke rol. Voorbeelden van convergente plaatgrenzen zijn de subductiezones rondom de Pacifische Oceaan, zoals die bij Peru-Chili, Japan en de Filippijnen.

In dit proefschrift wordt de thermische en mechanische structuur van het bovenste gedeelte van convergente plaatgrenzen onderzocht met behulp van numerieke modelmethoden. Het zijn met name de processen in het bovenste gedeelte van subductiezones die grote consequenties hebben voor geologische structuren. Hierbij dient te worden opgemerkt dat het subductieproces, naast de subductie van een plaat, ook leidt tot de vorming van nieuwe continentale korst in de overschuivende plaat (hetzij door vulkanische processen, hetzij door de overdracht van materiaal van de onderschuivende plaat naar de bovenste plaat).

Over het algemeen leidt het subductieproces tot de subductie van een plaat, over de gehele dikte, tot in de mantel. Dit basismodel van coherente subductie van de gehele plaat is als uitgangspunt gebruikt bij de verschillende numerieke modellen. Dit geldt met name voor de thermische modellen voor de subductie van oceanische lithosfeer die worden gegeven in de eerste helft van dit proefschrift (hoofdstukken 2 en 3). In de tweede helft van dit proefschrift (hoofdstukken 4 en 5) wordt vervolgens nagegaan of een plaat kan opbreken gedurende de eerste fase van het subductieproces. Bij deze mechanische modellen wordt de sterkte van materiaal afgeleid uit de temperatuur (volgend uit thermische modellen) en de compositie van het materiaal. De aandacht is hierbij eerst gericht op de subductie van oudere oceanische lithosfeer (die niet blijkt op te breken), vervolgens op de subductie van jonge oceanische lithosfeer (die alleen onder speciale omstandigheden blijkt te kunnen opbreken) en tenslotte op de subductie van continentale lithosfeer (waarvoor het opbreken eerder regel dan uitzondering blijkt te zijn).

In hoofdstuk 2 worden thermische modellen van convergente plaatgrenzen gepresenteerd voor de subductie van oceanische lithosfeer. Temperaturen en schuifspanningen op het plaatcontact worden onderzocht met behulp van warmtestroomdata, rheologische argumenten en de verdeling van aardbevingen op het plaatcontact. Temperaturen blijken vooral te worden bepaald door de naar beneden gerichte beweging van materiaal, inherent aan het subductieproces, en door wrijving op het plaatcontact. Behalve voor de subductie van jonge oceanische lithosfeer (met een ouderdom die kleiner is dan 30 miljoen jaar) blijken temperaturen op en boven het plaatcontact slechts in geringe mate afhankelijk te zijn van de ouderdom van de subducerende plaat en de convergentiesnelheid tussen de twee platen. Deze temperaturen worden vergeleken met temperaturen die kunnen worden afgeleid uit het voorkomen van bepaalde mineralen in hoge-druk metamorfe gebieden. Een gedetailleerde studie van de Cascadia subductiezone bij Z.W. Canada wordt gegeven in hoofdstuk 3.

In hoofdstuk 4 wordt met behulp van numerieke methoden onderzocht of oceanische lithosfeer kan opbreken in of nabij het bovenste gedeelte van een subductiezone. Voor oudere oceanische lithosfeer blijkt dit niet het geval te zijn. Jonge oceanische lithosfeer blijkt alleen te kunnen opbreken gedurende de interactie tussen een relatief snel spreidende rug en een subductiezone. Ten gevolge van dit opbreken kan een plak relatief jonge oceanische lithosfeer (met een maximum dikte van 10 tot 20 km) deel uit gaan maken van de overschuivende plaat in het gebied tussen de trog en de vulkanische zone. Uiteindelijk, na het sluiten van het oceanische bekken, kan deze van oorsprong oceanische lithosfeer geïncorporeerd worden in een gebergte. Voorgesteld wordt dat ophiolieten met een door harzburgiet gedomineerde mantelsectie een dergelijke plaatsingsgeschiedenis hebben meegemaakt.

Sluiting van een oceanisch bekken, gevolgd door de botsing tussen twee continentale platen, leidt tot gebergtevorming zoals die nu plaatsvindt bij de Himalaya's. In hoofdstuk 5 wordt ingegaan op de thermische en mechanische gevolgen van de subductie van continentale lithosfeer. Uit de modelberekeningen volgt dat, in tegenstelling tot oceanische lithosfeer, continentale lithosfeer over het algemeen wel zal opbreken gedurende de eerste fase van het subductieproces. Ook wordt aangetoond dat het opbreken van continentale lithosfeer waarschijnlijk alleen zal leiden tot de overdracht van korstmateriaal naar de bovenste, overschuivende plaat. Dit proces leidt tot een aanmerkelijke verdikking van de korst in deze bovenste plaat. Het meer frequente opbreken van continentale lithosfeer is het gevolg van de relatief lage dichtheid en de relatief geringe sterkte van continentale korst.

Acknowledgements

Ik wil graag iedereen bedanken die mij de afgelopen jaren behulpzaam is geweest bij het tot stand komen van dit proefschrift.
In de eerste plaats Prof. N. J. Vlaar, voor zijn grote inzet voor geofysica in Utrecht en voor zijn adequate begeleiding van mijn onderzoek op een aantal essentiële momenten. Ik heb veel geleerd van de uitgebreide kennis van Prof. Rinus Wortel op het gebied van tektonofysica. Zijn grondige en nauwgezette manier van onderzoek doen zijn een voorbeeld voor mij geweest.
Ik zal Prof. Sierd Cloetingh's enthousiasme en nieuwe ideeën missen. Ik wil hem speciaal bedanken voor zijn hulp en adviezen op finite element gebied.
Ik wil graag alle collega's van de afdeling geofysica bedanken voor de samenwerking gedurende de afgelopen jaren. Ik hoop dat het jullie allen goed gaat.

I thank Royal Dutch/Shell for the financial support that they gave me over a period of three years. In particular I would like to thank P. Featherstone and W. Horsfield, from the Koninklijke Shell Exploratie en Productie Laboratorium at Rijswijk, for the interest that they showed in my research.

De vriendschap en hulp van Ruud en Marijke Eskes en van Wim Nieuwenboom zijn voor mij van groot belang geweest.
Willy, bedankt dat je altijd naast me hebt gestaan.

Curriculum vitae

De schrijver van dit proefschrift behaalde in 1976 het diploma Atheneum-B aan het St. Gertrudis Lyceum te Roosendaal. In 1977 werd begonnen met de studies filosofie en natuurkunde aan de Rijksuniversiteit Utrecht. Nadat in 1981 het kandidaatsexamen N3 werd afgelegd, werd in 1985 het doctoraal examen geofysica met hoofdrichting fysica van de vaste aarde en bijvakken medische fysica en signaalverwerking behaald. Vervolgens was hij, gedurende een periode van vier jaar, als wetenschappelijk assistent verbonden aan de afdeling theoretische geofysica van het instituut voor aardwetenschappen aan de Rijksuniversiteit Utrecht. Sinds Augustus 1989 is hij werkzaam bij de Shell Internationale Petroleum Maatschappij B.V. te Den Haag.